COMPLEXES FORMED BY ZINC AND CYANIDE IONS AT ELEVATED pH

by

Christian Monberg

Submitted in partial fulfilment of the
requirements for the degree of
Master of Science,
in the
Department of Chemistry and Applied Chemistry,
University of Natal

Durban
1990

TO MY PARENTS

PREFACE

The experimental work described in this thesis was carried out in the Department of Chemistry and Applied Chemistry, University of Natal, Durban, under the supervision of Professor F. Marsicano.

These studies represent original work by the author and have not been submitted in any form to another University. Where use was made of the work of others it has been duly acknowledged in the text.

ACKNOWLEDGMENTS

I am indebted to many people and organisations for their assistance during the course of this work.

Firstly, I must thank my supervisor, Prof. F. Marsicano, for his assistance, advice and encouragement during the course of this work and his never ending enthusiasm for my project, as well as his comments on all parts of the thesis.

I must also thank Prof. J.W. Bayles for his support and assistance in the supervision of this work.

I wish to thank my parents, my wife, Wendy and my sons, Carl and Neil, for all their help, support and encouragement over the years. I also wish to thank various friends for their help and support, in particular the Furnivalls.

I am grateful to the technical staff of the Department for all their help and cooperation.

I also wish to thank my laboratory colleagues Bice Martincigh and Faizel Mulla, not only for providing a convivial working environment, but also for their assistance and many stimulating discussions on technical and other matters.

I am grateful to Lorraine Meredith for the splendid job of typing this thesis.

Finally, I wish to acknowledge, with gratitude, the financial support of the Council for Mineral Technology (MINTEK).

ABSTRACT

The experimental work described in this thesis is aimed primarily towards elucidation of the speciation of zinc–cyanide systems at elevated pH. In this study the formation and stability of H^+–CN^-, binary Zn^{2+}–CN^- and ternary Zn^{2+}–CN^-–OH^- complexes were studied by glass electrode potentiometry in aqueous solutions at 25.0^0C and in a medium of ionic strength of 0.1 moℓ dm^{-3}. The solution pH was varied to cover the range 4 to 11. The study was undertaken with a view to establishing whether and under what conditions soluble binary zinc–cyanide complexes and ternary zinc–cyanide–hydroxide complexes form, and to determine formation constants for any such species that are found. This information would be useful in defining more precisely the speciation of solutions containing zinc and cyanide ions at elevated pH values.

A titration method was used, in which hydrogen ion concentration was monitored by means of a glass indicating electrode. The cell was calibrated to allow measurements of hydrogen ion concentration rather than hydrogen ion activity. Owing to precipitation difficulties, the reagents were used at sub–millimolar concentration levels. The potentiometric data was interpreted with the aid of various formation function plots together with the use of various computer programs, such as HALTAFALL and ESTA.

The results show that the ternary complex $Zn(CN)_3(OH)^{2-}$ is formed in significant amounts in solutions of pH > 8.5. Some evidence was also obtained for the existence of the five coordinated species $Zn(CN)_3(OH)_2^{3-}$ and $Zn(CN)_3^{3-}$ in these solutions, but existence of the latter two species cannot yet be regarded as firmly established. No polynuclear complexes were detected at the sub–millimolar concentrations used. Formation constants are reported for H^+–CN^- and both binary Zn^{2+}–CN^- and ternary Zn^{2+}–CN^-–OH^- species.

CONTENTS

GLOSSARY OF SYMBOLS AND ABBREVIATIONS

Zn_T : total (analytical) concentration of zinc (complexed and uncomplexed) in solution.

CN_T : total (analytical) concentration of cyanide (complexed and uncomplexed) in solution.

H_T : total (analytical) concentration of hydrogen ions (complexed and uncomplexed) in solution.

M_T : total (analytical) concentration of metal ion M (complexed and uncomplexed) in solution.

L_T : total (analytical) concentration of ligand L (complexed and uncomplexed) in solution.

E^{01}_{cell} : a calibration constant (independent of $[H^+]$) appearing in a modified Nernst type equation $E_{cell} = E^{01}_{cell} + E_j + k \log[H^+]$ used for relating measured cell EMF to hydrogen ion concentration.

E_j : sum of liquid junction potentials generated across the liquid junctions present in the cell.

k : a calibration constant termed the "electrode calibration slope", which has a value close to (but not necessarily identical to) the Nernstian value 2.3026 RT/F.

[X] : represents the concentration (in moℓ dm^{-3}) of any species X in solution in free (uncomplexed/non–coordinated) form.

E^0_{cell} : $E^0_{cell} = E^{01}_{cell} + E_j$ (see above).

β_{pqr} : represents the cumulative formation constant for formation of the species $Zn_p\ CN_q\ H_r^{(2p+r-q)+}$ and is defined as $[Zn_p\ CN_q\ H_r]/[Zn]^p[CN]^q[H]^r$ (charges omitted). Negative values for r represent hydroxide ions rather than hydrogen ions.

$\bar{Z}_H$: represents the hydrogen formation function, defined as $(H_T - [H] + [OH])/L_T$.

$\bar{Z}_M$: represents the metal formation function, defined as $(L_T - A \sum_{r=1}^{R} \beta_{01r}[H]^r)/M_T$.

A : represents the "apparent" free ligand concentration, defined as $(H_T - [H] + [OH])/\sum_{r=1}^{R} n\beta_{01r}[H]^r$.

$\bar{Q}$: represents the "deprotonation function", defined as $(H_T^* - H_T)/M_T$.

H_T^* : represents a fictitious total hydrogen ion concentration in the system at the observed pH calculated from a hydrogen mass–balance equation ignoring all metal complex formation, i.e. $H_T^* = [H] - [OH] + \sum_{r=1}^{R} r\beta_{01r}[L]^*[H]^r$.

$[L]^*$: represents a fictitious concentration of free (uncomplexed) ligand, calculated at the observed pH from a ligand mass–balance equation ignoring all metal complex formation, i.e. $[L]^* = L_T/(1 + \sum_{r=1}^{R} \beta_{01r}[H]^r)$.

p[H] : defined as $-\log_{10}[H^+]$.

pA : defined as $-\log_{10}A$.

$\bar{Z}_H^*$: represents a hydrogen formation function for the ligand–hydrogen subsystem in a ligand–hydrogen–metal ion containing system, defined as $(H_T^* - [H] + [OH])/L_T$.

OBJE : an objective function used in the computer program ESTA for optimising values of formation constants from potentiometric cell EMF data. Can be regarded as a measure of "goodness of fit".

CHAPTER ONE

INTRODUCTION

For over a century, cyanide has been used in the recovery of precious metals, such as gold and silver from ores (1–3).

Zinc, has been almost universally used as a reductant for precious metals dissolved in cyanide solutions, although for specific reasons aluminium has been used (1–3).

The process by which metallic gold is precipitated by zinc from aurocyanide solutions has been termed "zinc cementation".

Despite the age of the zinc cementation process, it is only recently that fundamental studies have been carried out to determine the details of the mechanisms of the reactions involved in the cementation of gold onto zinc in aurocyanide solutions (1,4).

In a recent paper, R.L. Paul (4) describes the unit operations involved in the recovery of gold from an ore. The flow sheet for a "conventional" gold recovery plant consists of crushing and milling of the ore, followed by cyanidation, filtration, and recovery of gold by cementation onto zinc dust. In some plants, gravity separation is used to recover larger particles of gold liberated by milling before the pulp is cyanided. A schematic flow sheet for the recovery of gold is shown in Figure 1.1.

In recent times many gold producers have introduced additional processing steps or replaced existing unit operations by newly developed techniques, in order to reduce operating costs while increasing overall recovery of gold (4). Flotation is commonly used in the recovery of the pyritic (FeS_2) content of an ore. Microscopic particles of gold occluded within the pyrite can be liberated by roasting of the pyrite to hematite (Fe_2O_3). The carbon–in–pulp (CIP) process, which uses

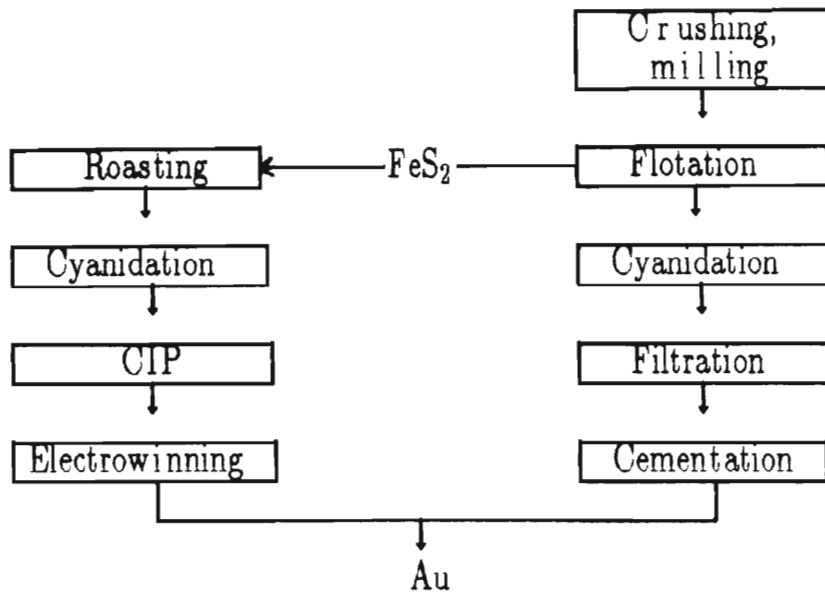

Figure 1.1 A schematic flow sheet for the recovery of gold from some pyritic feed material. (Taken from reference 4).

activated charcoal, permits the recovery of dissolved gold from the leached pulp without the need for filtration (2,4,5). The CIP process has had a major impact on the processing of pulps, such as calcines and slimes from the treatment of dump material, which are not easily filtered (4). Figure 1.1 shows schematically, how some of the recent developments fit into the flow sheet for the extraction of gold from some pyritic feed material.

R.L. Paul (4), concludes that the recovery of gold from an ore is predominantly an electrochemical process. The cyanidation, cementation and electrowinning unit operations have a very clear electrochemical basis, as do flotation and CIP unit operations.

The overall stoichiometry of the zinc cementation process is as follows (1,4):

$$Zn + 2Au(CN)_2^- \rightarrow Zn(CN)_4^{2-} + 2Au \quad . \qquad (1.1)$$

Since the introduction of the use of zinc for the recovery of gold from cyanide solutions in 1890, various improvements, such as the use of zinc dust instead

of zinc shavings, the addition of lead nitrate, the de–aeration of the pregnant solutions have resulted in precipitation recoveries of more than 99 percent (1). The efficiency of the zinc cementation process is generally very high, barren solutions with a gold content lower than 0.01 $mg.\ell^{-1}$ usually being obtained (4), but occasionally problems are experienced in reduction plants in the gold industry (1,2,4,5).

The electrochemical study by Nicol *et al.* (1) of the kinetics and mechanism of the cementation of gold by metallic zinc in cyanide–containing aqueous solutions has shown that the rate of anodic dissolution of zinc increases markedly with cyanide concentration at constant pH, and also with pH value at constant total (analytical) cyanide concentration. It was suggested that hydroxyl ions, through formation of soluble binary zinc–hydroxy complexes of the type $Zn(OH)_4^{2-}$ or ternary zinc–hydroxyl–cyanide complexes participate in the rate determining step of the dissolution reaction.

A survey of the literature shows that the zinc–cyanide system has been studied quite extensively since 1903, with a view to determining the species present in solution, and associated formation constants.

Previous publications (6–23) dealing with this activity are listed in Table 1.1.

Inspection of Table 1.1 indicates that:

(i) uncertainty exists concerning the species thought to be present in solution, particularly with regard to the species $Zn(CN)^+$, $Zn(CN)_5^{3-}$ and $Zn(CN)_6^{4-}$. There have been no reports of ternary Zn–CN–OH species or polynuclear complexes, and

(ii) the values of formation constants quoted for the various species vary over a range of 1 to 2 log units, i.e. by more than would be expected even when account is taken of the effect of ionic strength on the formation constants concerned.

ABLE 1.1 Results of previous studies of formation of complexes of Zn(II) with the cyanide ion in aqueous solution

ıte udy	Temp. /°C	Ionic Strength /mol dm^{-3}	Logarithm to base 10 of the cumulative formation constant, log β (unless otherwise indicated)						Method Used	References
			$ZnCN^+$	$Zn(CN)_2$	$Zn(CN)_3^-$	$Zn(CN)_4^{2-}$	$Zn(CN)_5^{3-}$	$Zn(CN)_6^{4-}$		
)3	21	variable				16.9			Zn metal electrode	Euler[6]
)4	18	variable			17.52	evidence			Zn metal electrode	Kunschert[7]
29	room temp.	variable				16.0	20.17	evidence	Polarography	Pines[8]
31	18	variable			20.25	or 17.3			Zn metal electrode	Masaki[9]
32	12.5	variable				18.5→20			Zn amalgam electrode	Britton and Dodd[10]
50	12.5	variable				19			Re–interpretation	Bjerrum[11]
50	12.5	variable				evidence	evidence	evidence	Polarography	ϕsterud and Prytz[12]
51	18	variable				12.60(?)			Zn metal electrode	Stabrovskii[13]
53	25	Corr.→0				16.76			Zn amalgam electrode	Suzuki[14]
58	32	Sat.Na_2SO_4				evidence			Freezing point	Kordes and Langenhoff[15]
59	25	Corr.→0				16.72			Zn amalgam electrode	Blackie and Gold[16]
61	25	variable				evidence			Infrared spectra	Penneman and Jones[17]
61	25	dil. $K_2Zn(CN)_4$ (?)				log $K_4 = 5$			pH Method	Penneman and Jones[17]
65	25	Corr.→0	no evidence	11.07	16.05	19.62			Glass electrode and polarography	Izatt *et al.*[18]
69	25	0.1	no evidence	10.64	15.74	19.98			Glass electrode	Martin and Blanc[19]
71	40	Corr.→0		10.70	15.20	18.30			Glass electrode	Izatt *et al.*[20]
71	25	3	5.3	11.0	16.7	21.6			Glass electrode and zinc amalgam	Persson[21]
71	25	variable high concs.					no evidence	no evidence	Spectrophotometry	Ashurst *et al.*[22]
72	25	0.5	4.94	9.7	14.7	18.44			Zn amalgam electrode	Collier *et al.*[23]

Kunschert (7) and Ferrel *et al.* (24) report that both zinc and zinc amalgam electrodes are attacked by aqueous cyanide solutions and thus, as pointed out by Izatt *et al.* (18) results obtained using these electrodes should be considered questionable. Persson (21), found that the dissolution of zinc from zinc amalgam electrodes increased rapidly with cyanide concentration, however he showed that a zinc amalgam electrode can be used provided that oxygen is carefully excluded from the solutions and the cyanide concentration kept low.

Izatt *et al.* (18), using the potentiometric titration method with a glass membrane indicating electrode to measure the pH of the zinc–cyanide system, found no evidence for the existence of the $Zn(CN)^+$ complex. They used polarography to support their potentiometric findings. The values of the analytical (total) concentration of zinc (Zn_T) and cyanide (CN_T) in solution at the beginning of each potentiometric titration, carried out by Izatt *et al.* (18), as well as the ligand: metal ratios ($^{CN}T/Zn_T$) and the pH ranges covered are given in Table 1.2.

Persson (21), studied the zinc–cyanide system at an ionic strength of 3.0 moℓ dm^{-3}. He used the potentiometric titration method with a glass membrane indicating electrode to record the cell EMF. The values of the analytical concentrations of zinc (Zn_T) and cyanide (CN_T) in solution at the beginning of each potentiometric titration, carried out by Persson (21), as well as the ligand: metal ratios ($^{CN}T/Zn_T$) and the pH ranges covered are given in Table 1.2. Persson found that the $Zn(CN)^+$ complex only exists in a very narrow range, and claimed that Izatt *et al.* did not detect the existence of the complex, because they worked outside this range. The experimental conditions used by Izatt *et al.* (18) and Persson (21) are compared in Table 1.2

There has been some apparent disagreement in the literature over the question of whether or not complexes of the form $Zn(CN)_n^{(2-n)+}$ with n>4 exist in solutions containing sufficiently high concentrations of the cyanide ion. Both Pines (8) and Østerud and Prytz (12) deduced the presence of the species $Zn(CN)_5^{3-}$ and

TABLE 1.2 Initial values of Zn_T and CN_T, the ligand: metal ratios, as well as the pH ranges covered in the potentiometric titrations considered in the studies by Izatt *et al.* (18) and Persson (21).

Titration	Zn_T/mol dm^{-3}	CN_T/mol dm^{-3}	CN_T/Zn_T	pH range
Izatt *et al.*				
1	8.496×10^{-4}	6.741×10^{-3}	7.93	10.310 → 5.277
2	8.492×10^{-4}	6.777×10^{-3}	7.98	10.322 → 5.299
3	8.492×10^{-4}	6.777×10^{-3}	7.98	10.284 → 5.316
4	4.244×10^{-4}	3.367×10^{-3}	7.93	10.185 → 5.509
5	4.242×10^{-4}	3.850×10^{-3}	9.08	10.142 → 5.277
Persson				
1	3.00×10^{-4}	1.530×10^{-3}	5.10	8.52 → 6.78
2	5.00×10^{-4}	3.066×10^{-3}	6.13	8.48 → 6.64
3	3.04×10^{-4}	1.238×10^{-3}	4.07	8.29 → 6.74

$Zn(CN)_6^{4-}$ from polarographic evidence. The latter authors worked with total zinc concentrations in the range 10^{-4} to 10^{-3} mol dm^{-3} and cyanide concentrations from zero up to about 0.6 mol dm^{-3}. They reported four distinct polarographic waves, denoted W_{c_0}, W_{c_1}, W_{c_2} and W_{c_3} in their publication, for species other than the zinc aquo ion. The wave W_{c_1} was found at a CN_T:Zn_T ratio of 4:1 upwards, through 24:1 i.e. $[CN^-]_{free}$ = 0.02 mol dm^{-3}, but had disappeared by CN_T:Zn_T = 120:1, i.e. $[CN^-]_{free}$ = 0.12 mol dm^{-3}. This wave was assigned to $Zn(CN)_4^{2-}$. The wave W_{c_2}, assigned to $Zn(CN)_5^{3-}$, was found to appear at CN_T:Zn_T = 8:1, i.e. $[CN^-]_{free}$ = 0.004 mol dm^{-3}. It was still present at CN_T:Zn_T = 120:1, i.e. $[CN^-]_{free}$ = 0.12 mol dm^{-3}, but had disappeared by $[CN^-]_{free}$ = 0.6 mol dm^{-3}. The wave W_{c_3}, assigned to $Zn(CN)_6^{4-}$, was distinct at $[CN^-]_{free}$ = 0.12 mol dm^{-3}, but had also disappeared at $[CN^-]_{free}$ = 0.6 mol dm^{-3}. An interesting and unexplained feature of the polarographic results was that the waves assigned to $Zn(CN)_5^{3-}$ and $Zn(CN)_6^{4-}$ apparently both disappeared when the cyanide concentration was raised from about 0.12 mol dm^{-3} to about 0.6 mol dm^{-3}.

Of particular interest in this connection is the elegant infrared study of this system by Ashurst, Finkelstein and Goold (22) in 1971. In keeping with the requirements of the infrared technique, they worked with zinc concentrations of the order of 0.25 mol dm^{-3} and total cyanide concentrations of 1.7 to 2.5 mol dm^{-3}. Measurements of the absorbance of free (uncoordinated) cyanide ions were consistent with CN:Zn binding in the ratio 4:1 and not 5:1 or 6:1. It should be noted that, in these measurements, the free cyanide concentrations in the two solutions studied were, respectively, 0.56 and 1.50 mol dm^{-3}.

The results of Ashurst *et al.* do not appear to necessarily conflict with those of Østerud and Prytz when the absence of polarographic waves for $Zn(CN)_5^{3-}$ and $Zn(CN)_6^{4-}$ at comparable free cyanide concentrations is considered. The metal ion concentrations were also very different in the two studies, which presents the possibility of polynuclearity at higher concentrations.

Izatt *et al.* (18) did not take into consideration the possible existence of ternary Zn–CN–OH complexes in the manipulation of their potentiometric data, despite the fact that they reached moderately high pH values (see Table 1.2).

Nevertheless, the speciation of zinc in zinc–cyanide solutions, particularly at high cyanide concentrations (above about 0.01 moℓ dm^{-3}), cannot be regarded as well understood. Since increasing cyanide concentrations also implies an increase in solution pH, the possibility exists that at least some of these anomalies may be explicable in terms of the formation of ternary Zn–CN–OH complexes in solution at high pH.

This study was directed primarily towards elucidation of the speciation of zinc–cyanide systems at moderately high pH values. This report describes a potentiometric study of the H–CN and the Zn–CN–OH systems, undertaken with a view to establishing whether and under what conditions soluble binary zinc–cyanide complexes of the type $Zn(CN)_4^{2-}$ and ternary zinc–cyanide–hydroxyl complexes form, and to determine formation constants for any such species that are found. This information would be useful in defining more precisely the speciation of solutions containing zinc and cyanide ions at high pH values.

This potentiometric study was carried out at an ionic strength of 0.10 moℓ dm^{-3} and a temperature of 25.0^{o}C, because the gold cementation process occurs at roughly these conditions.

The study was carried out in two stages. The first stage involved the potentiometric determination of the formation constant for HCN, under the experimental conditions of this study. Table 1.3 shows values for the formation constant of HCN from previous studies (21,25–30). As no HCN formation constant value was available at an ionic strength of 0.1 moℓ dm^{-3} and a temperature of 25^{o}C,

an estimated value of 9.01 was obtained using equation (1.2).

$$\ln \frac{K(T_1)}{K(T_2)} = -\frac{\Delta H^\circ}{R}\left(\frac{1}{T_1} - \frac{1}{T_2}\right) \quad , \tag{1.2}$$

$$\ln K\,(25) = \ln K\,(20) - \frac{\Delta H^\circ}{R}\left(\frac{1}{298} - \frac{1}{293}\right) \quad , \tag{1.3}$$

using $\Delta H = -10.43$ K cal. mol^{-1} at 25°C (31),
and log K (20) = 9.14, at an ionic strength of
0.1 mol dm^{-3} (26,29)

log K (25) = 9.01 .

The second stage involved the study of the zinc–cyanide system at moderately high pH values.

There are a large number of references (32 – 36), which deal with the study of chemical equilibria and the determination of stability constants.

In the study of ionic equilibria various types of complexes can be formed and various quantities are used to describe and discuss complex equilibria. The various types of complexes and quantities will be described below, prior to discussing the various methods available for the determination of stability constants.

In this study the symbol β_{pqr} represents the cumulative formation constant of the species $M_pL_qH_r$, where M, L and H represented the metal ion, ligand and hydrogen ions respectively. p and q are non–negative integers. r is an integer which when positive indicates hydrogen ions and when negative indicates hydroxide ions. The use and meanings of these symbols are elaborated on in the following pages.

TABLE 1.3 Results of previous studies of the formation of HCN in aqueous solutions

Date of Study	Temperature /°C	Ionic Strength /mol dm^{-3}	Logarithm to base 10 of formation constant, log β	Method used	Reference
1932	18	Variable	9.32	Glass electrode	Britton *et al.*[25]
1957	20	0.1 ($NaNO_3$)	9.14 ± 0.01	Glass electrode	Anderegg[26]
1959	25	Corr. → 0	9.216	Spectrophotometric	Ang[27]
1962	10	Corr. → 0	9.63 ± 0.01	Glass electrode	Izatt *et al.*[28]
	15	Corr. → 0	9.49 ± 0.01		
	20	Corr. → 0	9.36 ± 0.01		
	25	Corr. → 0	9.21 ± 0.01		
	30	Corr. → 0	9.11 ± 0.01		
	35	Corr. → 0	8.99 ± 0.01		
	40	Corr. → 0	8.88 ± 0.02		
	45	Corr. → 0	8.78 ± 0.02		
1965	20	0.1 (KNO_3)	9.14		Schwarzenbach *et al.*[29]
1966	20	Corr. → 0	9.36 ± 0.01	Glass electrode	Boughton *et al.*[30]
	26	Corr. → 0	9.19 ± 0.02		
	33	Corr. → 0	9.05 ± 0.03		
1971	25	3.0 ($NaClO_4$)	9.484 ± 0.01	Glass electrode	Persson[21]

Various types of complex species are known. The simplest systems of complexes are the mononuclear complexes, in which only one series of complexes is formed. These can include,

(i) oligomers, M_p, which form by self association, such as Hg_2^{2+},
(ii) acids, H_rL_q, in solutions which contain no complexing metal ions i.e. p = 0, and
(iii) complexes, ML_q.

Another system of complexes are the polynuclear complexes, in which the complexes contain more than one central metal ion, (M_pL_q, p>1). Polynuclear complexes may be homo– or hetero–nuclear, depending on whether the central metal ions are the same or different.

A system of complexes exists, in which more than one type of ligand is attached to the metal ion, ($M_pL_qX_r$). These are called "mixed ligand or ternary" complexes. X may be the hydrogen ion (a "protonated" complex), the hydroxyl ion (in which case the complexes are usually described as "hydrolysed"), or a second type of ligand.

The reactions which lead to the formation of metal complexes are substitution reactions, in which one or more solvent molecules are substituted by a ligand molecule. Interaction between the species of interest and the bulk electrolyte may also occur, but for simplicity it is assumed that the concentrations of the solvent and bulk electrolyte remain constant and their contributions are ignored.

When considering the formation of mononuclear metal complexes, ML_q, in aqueous solutions, a metal ion M (or more generally any Lewis acid i.e. an electron acceptor) can react with a ligand L (or Lewis base i.e. an electron donor) to form a series of complexes generally represented by the following reversible reaction:

$$M(aq) + qL(aq) \rightleftharpoons MLq(aq);\ q>0 \quad . \qquad (1.4)$$

For the sake of simplicity charges have been omitted. The resulting complexes of the above reaction can be cations, anions or uncharged molecules.

The activites (a) of the species present at equilibrium are related to the thermodynamic (activity) equilibrium constant ${}_a\beta_{1q}$ at a given temperature as follows:

$$ {}_a\beta_{1q} = \frac{{}^aML_q}{{}^a_M \cdot {}^a_L{}^q} \quad . \tag{1.5} $$

However the activity of a species Z is simply related to its concentration ([Z]) by the activity coefficient, γ_z:

$$ a_z = \gamma_z[Z] \quad . \tag{1.6} $$

Thus equation (1.5) can be rewritten as

$$ {}_a\beta_{1q} = \frac{\gamma_{ML_q}[ML_q]}{\gamma_M[M] \cdot \gamma_L^q[L]^q} $$

$$ = \frac{\gamma_{ML_q}}{\gamma_M\gamma_L^q} \cdot \frac{[ML_q]}{[M][L]^q} $$

$$ = \frac{\gamma_{ML_q}}{\gamma_M\gamma_L^q} \cdot \beta_{1q} \quad . \tag{1.7} $$

If reaction (1.4) is carried out in a medium of constant ionic strength, I, the activity coefficients of the various species present in solution will remain approximately constant. Thus, ${}_a\beta_{1q}$ will be proportional to β_{1q}, since the activity coefficient quotient is constant.

Hence the concentration quotient

$$ \beta_{1q} = \frac{[ML_q]}{[M][L]^q} \quad . \tag{1.8} $$

will also be constant. β_{1q} is known as the (cumulative) stability constant and is a constant for a given reaction at a given temperature and ionic strength.

Reaction (1.4) can also be expressed as a series of q steps:

$$\begin{aligned} M + L &\rightleftharpoons ML \quad , \\ ML + L &\rightleftharpoons ML_2 \quad , \\ &\vdots \\ ML_{q-1} + L &\rightleftharpoons ML_q \quad , \end{aligned}$$

and equilibrium constants or stepwise stability constants for each of these steps can be written as follows:

$$\begin{aligned} K_{11} &= \frac{[ML]}{[M][L]} \quad , \\ K_{12} &= \frac{[ML_2]}{[ML][L]} \quad , \\ &\vdots \\ K_{1q} &= \frac{[ML_q]}{[ML_{q-1}][L]} \quad . \end{aligned}$$

Thus it follows that the cumulative stability constants are obtained from the product of the stepwise stability constants:

$$\begin{aligned} \beta_{11} &= K_{11} \\ \beta_{12} &= K_{11} \cdot K_{12} \\ &\vdots \\ \beta_{1q} &= K_{11} \cdot K_{12} \cdots K_{1q} \\ &= \prod_{i=1}^{q} K_{1i} \quad . \end{aligned}$$

In this study the hydrogen ion was considered as the third species, besides M and L. Hence the reaction analogous to reaction (1.4) is

$$pM(aq) + qL(aq) + rH(aq) \rightleftharpoons M_pL_qH_r(aq) \quad . \tag{1.9}$$

The corresponding cumulative stability constant is defined as

$$\beta_{pqr} = \frac{[M_pL_qH_r]}{[M]^p[L]^q[H]^r} \quad , \tag{1.10}$$

where [M], [L] and [H] represent the free (uncomplexed) concentrations of metal ions, ligand and hydrogen ions respectively.

In this study, of the zinc–cyanide system, the symbol β_{pqr} represents the cumulative formation constant of the species $Zn_pCN_qH_r^{(2p+r-q)+}$ and is defined as

$$\beta_{pqr} = \frac{[Zn_pCN_qH_r]}{[Zn]^p[CN]^q[H]^r} \quad , \tag{1.11}$$

where charges are omitted for simplicity.

The formation constant for the protonation of the ligand may be written as

$$\beta_{0qr} = \frac{[H_rL_q]}{[H]^r[L]^q} \quad . \tag{1.12}$$

Various techniques, such as potentiometry, polarography, spectrophotometry, ion exchange and others are available and have been employed in the study of chemical equilibria and for the determination of stability constants.

The ideal method of studying equilibria in solution should give accurate

and precise values of the free concentrations of all species present in any conceivable system without disturbing the position of equilibrium, and should be quick. No technique is without its problems, but "of the methods available, potentiometry is the most versatile, most precise and most popular" (37).

Spectrophotometric measurements of solutions in which several species absorb are often difficult to interpret, since the absorbance of the solution depends on the concentrations and molar absorptivities of the species which absorb radiation of the wavelength used. Each chromophore contributes to the measured absorbance to a different extent, so the expression for the absorbance of a solution involves the molar absorptivities of all chromophores in addition to stability constants and concentration variables.

The stability constants obtained from polarograms are usually less precise than those obtained from potentiometric measurements. Polarography is generally restricted to systems in which the metal ions can be reversibly reduced at a dropping mercury electrode.

Potentiometry can be used to study equilibria in non–aqueous organic solvents, and in fused salts as well as in aqueous systems.

It is seldom if ever possible to obtain direct measurements of the equilibrium concentrations of all the species which are present in a solution in which complexes are formed. Using potentiometry, it is possible to measure the equilibrium concentration of one species and relate it to the reactions occurring and the associated stability constants (see Section 4.1.1), since the concentration changes caused by complex formation are reflected in the potential of a sensing electrode.

In potentiometry a large variety of sensing probes, such as quinhydrone electrodes, glass electrodes, ion–selective electrodes and metal amalgam electrodes, are available for the study of equilibria.

In this work, a potentiometric titration method was used, in which a glass–membrane electrode was used to measure the concentration of the free (uncomplexed) hydrogen ion. This was possible because the reactions being studied involved competition between the hydrogen ion and the zinc metal ion for the ligand. Low sodium error glass electrodes were used in this study, so that measurements could be obtained at high pH values, without the electrode membrane being affected by the hydroxide ions. Other electrodes such as zinc–amalgam and cyanide ion–selective electrodes were considered for use in this work, but were not used due to limitations. It has been shown that the presence of cyanide complexes of metal ions causes interference with the cyanide ion–selective electrode measurement of free (uncomplexed) cyanide (38). As mentioned earlier in this chapter, the use of zinc and zinc–amalgam electrodes is considered questionable (7,18,21,24).

A typical potentiometric cell, suitable for following the hydrogen ion concentration is given below:

reference electrode	test solution in which equilibrium takes place	glass electrode

A description of the cell used in this study, as well as the various methods used to calibrate it are given in Chapter 5.

The composition of the test solution can be varied by addition of titrants from burettes. The experimental titrations should be designed, so that as much information as possible can be obtained from a single titration. The actual titration experiments can be designed in a number of ways (32). Chapter 6 describes the design of the experimental titrations carried out in this work.

In the study of equilibria in solutions, a neutral or background electrolyte, such as $NaCl O_4$ or KNO_3, is often used in large excess over the reacting species. The neutral electrolytes are used in such concentrations that the

activity coefficient for any particular ion is supposed to be constant in all solutions. Sometimes the ionic strength is kept constant, or the total concentration of all ions is kept constant, or the concentration of inert cations or anions is kept constant.

If the activity coefficients are kept constant, the concentration of various reacting ions may be calculated directly from EMF measurements and in applying the law of mass action, one may use concentrations instead of activities.

M.T. Beck (35), states that the inert electrolyte used in the studies of solution equilibria should meet the following criteria:

(i) it must be a strong electrolyte;
(ii) its cations must not associate with the ligand or with the various complexes formed;
(iii) its anions must not associate with the central metal ion or with the complexes;
(iv) redox reactions must not occur between the constituents of the inert electrolyte and the central ion or ligand;
(v) it must have an adequate solubility;
(vi) its contribution to the measured physical or chemical property must be negligible.

$NaClO_4$ and KNO_3 are the most frequently used of the few salts that satisfy these criteria.

In this work, the ionic strength of all solutions was adjusted to 0.10 mol dm^{-3} using $NaClO_4$.

The quantity of inert background electrolyte required to make up a solution to the required ionic strength is obtained with the aid of the following

equation:

$$I = \tfrac{1}{2} \sum_i c_i z_i^2 \quad , \tag{1.13}$$

where

I is the ionic strength,
c_i is the concentration of the i^{th} species,
z_i is the charge number of the i^{th} species.

The applicability of the constant ionic medium is based on the Lewis–Randall principle (39), which was later theoretically corroborated by the Debye–Hückel theory (40).

Once the data has been collected from the potentiometric titrations, they have to be processed. A large number of methods have been described for obtaining stability data from potentiometric titration data. Graphical representation of the numerical data in the form of formation curves is often the first step in the treatment of potentiometric data. Graphical methods allow "dud" experimental points and systematic errors to be detected, as well as indicating the presence of complicated species, such as mixed ligand or polynuclear complexes. Having obtained sufficient good data the next step in the processing of the data is to deduce the nature of the species present, and to calculate the corresponding stability constants. For systems which can be described by only one or two parameters, graphical methods involving either linear, non–logarithmic plots or curve fitting methods can be used to determine the stability constants. The processing of more complicated systems requires the use of computer programs such as MINIQUAD (41,42) and ESTA (43,44).

In this study, graphical methods were not used to determine the stability constants from the potentiometric data.

Amongst the advantages that this study has over previous studies of the

zinc cyanide system are:

the large amount of potentiometric data, which was collected over a wide range of Zn_T, CN_T, CN_T/Zn_T and pH values (see Tables 1.2 and 7.2); the experimental techniques employed in this study, such as cell calibration and the use of low sodium error glass electrodes; and the use of up–to–date computer programs for model selection, such as ESTA, which reduce the element of subjectivity involved in proposing a model.

CHAPTER TWO

MATERIALS

This chapter deals with the materials used in this study and the way in which solutions were prepared and standardised. Freshly boiled doubly deionized water was used throughout this work in analytical tests and to make up all solutions, in an attempt to avoid contamination by carbonate. All solutions used in the experiments were prepared by dilution of the relevant standardised stock solutions, described below, and were made up to an ionic strength (I) of 0.10 mol dm^{-3}, by using calculated amounts of the sodium perchlorate ($NaClO_4$) stock solution. All volumetric glassware used in this study was "A" grade.

2.1 PREPARATION AND STANDARDISATION OF STOCK SOLUTIONS OF STRONG ACID AND STRONG BASE

Stock solutions of strong acid and strong base were prepared using analytical reagent grade perchloric acid ($HClO_4$) and sodium hydroxide (NaOH) respectively.

2.1.1 Preparation and standardisation of perchloric acid stock solution

The perchloric acid ($HClO_4$) stock solution ($\approx$ 3.0 mol dm^{-3}) was prepared by dilution of $HClO_4$ (BDH 72% Analar sp. gr. 1.70).

The $HClO_4$ stock solution was standardised by titration against freshly recrystallised borax (BDH Analar) (45).

2.1.2 Preparation and standardisation of sodium hydroxide solution

Initially, the sodium hydroxide (NaOH) solution ($\approx$ 1.0 mol dm^{-3}) was freshly prepared for each experiment, using 1.0 mol dm^{-3} NaOH ampoules (MERCK Titrisol or BDH CVS). The use of ampoules was stopped, because it was found that many contained unacceptable levels of dissolved carbonate in the hydroxide.

When ampoules of NaOH were no longer used, the NaOH stock solution ($\approx$ 1.0 moℓ dm^{-3}) was freshly prepared for each experiment by dissolving about 20 g of NaOH pellets (BDH Analar) in a 500 cm^3 volumetric flask. The flask was flushed with nitrogen gas, while it was being made up to the mark. The stock solution was stored under nitrogen in a polyethylene bottle.

The NaOH solutions were standardised against $HC\ell O_4$, either by use of methyl orange as indicator or for the more dilute NaOH solutions, potentiometrically, using Gran plot techniques (see Section 4.1.3.2).

2.2 PREPARATION AND STANDARDISATION OF STOCK SOLUTION OF BACKGROUND ELECTROLYTE

Owing to the low concentration of reactants used in this study, the background electrolyte, sodium perchlorate ($NaC\ell O_4$) had to be as pure as possible, so a method of preparation described by Sjöberg (46) was used.

The $NaC\ell O_4$ stock solution ($\approx$ 4.5 moℓ dm^{-3}) was prepared by neutralising 35% $HC\ell O_4$ (MERCK GR) with solid anhydrous sodium carbonate (Na_2CO_3) (MERCK GR) or solid sodium carbonate decahydrate ($Na_2CO_3 \cdot 10H_2O$) (MERCK GR). After the $HC\ell O_4$ had been neutralised a slight excess of Na_2CO_3 was added. This slightly alkaline solution (pH $\approx$ 8.0) was allowed to stand for a week. If Fe–, Aℓ– and Si– impurities are present they usually precipitate during this period as silicates or hydroxides (46–49). The solid impurities were filtered off using a G4 sintered glass filter. The filtrate was acidified to a pH value of approximately 1.0, using $HC\ell O_4$, and then boiled to expel the carbonate, as CO_2. After boiling, the solution was neutralised to a pH value of approximately 6.0, with freshly prepared NaOH solution. Neither $C\ell^-$, nor CO_3^{2-}, could be detected using the silver nitrate ($AgNO_3$) test (50,51). Fe^{2+} could not be detected using the potassium ferrocyanide ($[Fe(CN)_6]^{4-}$) test (52). Fe^{3+} could not be detected using the potassium ferricyanide ($[Fe(CN)_6]^{3-}$) test (53).

The $NaC\ell O_4$ stock solution was standardised, by passing 5 cm^3 aliquots

of the $NaC\ell O_4$ stock solution through a cation–exchange column, prepared by weighing out approximately 70.0 g cation–exchange resin (BDH Amberlite IR–120 (H)). Just prior to use, the cation–exchange resin column was eluted with 500 cm^3 of a 10% $NaC\ell$ (MERCK GR) solution, rinsed with water, eluted with 600 cm^3 of a 6% $HC\ell$ solution, and then again rinsed with water. The above procedure was used to ensure that the resin had undergone a complete cycle of charging and discharging before it was used.

Each 5 cm^3 aliquot of the $NaC\ell O_4$ stock solution was eluted through the resin using 150 cm^3 of water. After each elution the resin was rinsed with water.

The resultant $HC\ell O_4$ solution was titrated against a freshly prepared and standardised NaOH solution. The cation–exchange method was used in preference to drying the material to constant mass and then analysing it, because it was more rapid. The results were reproducible to within about 1%.

2.3 PREPARATION AND STANDARDISATION OF ZINC PERCHLORATE STOCK SOLUTION

A typical zinc perchlorate ($Zn(C\ell O_4)_2$) stock solution ($\approx$ 0.1 moℓ dm^{-3}) was prepared by dissolving 8.1388 g zinc oxide (ZnO) (BDH Analar) in approximately 70.0 cm^3 $HC\ell O_4$ (3.2153 moℓ dm^{-3}) in a beaker. The solution was filtered to remove solid impurities, before being transferred into a one dm^3 volumetric flask and made up to the mark.

The $Zn(C\ell O_4)_2$ stock solution was standardised for Zn^{2+}, using a standard 0.1 moℓ dm^{-3} ethylenediaminetetra–acetic acid (EDTA) solution (54), which was made up from EDTA (MERCK Titriplex III) dried at 80°C for 24 hours (55). Eriochrome Black T was used as indicator (54).

The excess acid in the $Zn(C\ell O_4)_2$ stock solution was determined potentiometrically by a Gran plot method (see Section 4.1.3.1), in which a known amount of $HC\ell O_4$ was added to a known volume of the $Zn(C\ell O_4)_2$ stock solution and

this was titrated with a freshly prepared and standardised NaOH solution.

2.4 PREPARATION AND STANDARDISATION OF SODIUM CYANIDE SOLUTIONS

The sodium cyanide (NaCN) solutions were freshly prepared for each experiment, since it has been reported that sodium cyanide solutions decompose on standing (12,20,28,56). This was confirmed in this study, by observing the movement of peaks on UV–visible spectra. Marsh *et al.* (56) reported that the decomposition products of the reaction between CN^- and H_2O were CO and NH_3.

The NaCN solution ($\approx$ 0.1 moℓ dm^{-3}) was prepared by dissolving a known mass of NaCN (MERCK GR) in water.

The NaCN solution was standardised for CN^- using the Leibig–Dénigès method (57), in which aliquots of the NaCN solution were titrated with a standardised silver nitrate ($AgNO_3$) (BDH Analar) solution. The $AgNO_3$ solution was standardised against a standard Na$C\ell$ (MERCK GR) solution using the Mohr titration method (58).

Any excess base that may have been present in the NaCN solution was determined by potentiometric titration, in which a known amount of NaOH of known concentration was added to a known volume of the NaCN solution, and this was titrated with an $HC\ell O_4$ solution of known concentration. Gran plots were used to determine the end points of titrations of mixtures of bases with strong acids (see Section 4.1.3.3).

CHAPTER THREE

APPARATUS

This project consisted of two sections, firstly the potentiometric determination of protonation and stability constants in the zinc–cyanide–hydrogen ion system, under acidic and basic conditions at 25.0°C and an ionic strength of 0.10 mol dm^{-3}. The second section consisted of an examination of solutions containing mixtures of CN^- and HCN by ultraviolet–visible spectrophotometry.

Grade "A" glassware was used for all volumetric work.

3.1 POTENTIOMETRIC APPARATUS

Stability constants were determined by means of a competition reaction involving competition of H^+ and Zn^{2+} for the ligand species. The concentration of the uncomplexed hydrogen ion or hydroxide ion was measured using an electrochemical cell, comprising a reference electrode/salt bridge assembly and an indicating glass electrode. RADIOMETER G202B (low sodium error) glass electrodes were used. The glass electrodes were conditioned before use and stored according to the manufacturer's instructions. Usually only one glass electrode was used, but in some experiments a second electrode was used as a check. The reference electrode and salt bridge were assembled using two INGOLD liquid junction tubes type 303–95–T–NS, which had been modified, so that they could be thermostatted. Figure 3.1 shows a diagram of the reference electrode/salt bridge assembly used in this study. The solution in the salt bridge was 0.10 mol dm^{-3} sodium perchlorate, while that in the reference electrode was 0.01 mol dm^{-3} sodium chloride + 0.09 mol dm^{-3} sodium perchlorate. A drop of silver perchlorate ($AgClO_4$) solution was added to the reference electrode solution, before inserting the METROHM silver–silver chloride (Ag/AgCl) reference electrode, type EA–275, to ensure that the reference electrode solution was saturated with AgCl, thus preventing dissolution of the AgCl coating on the electrode.

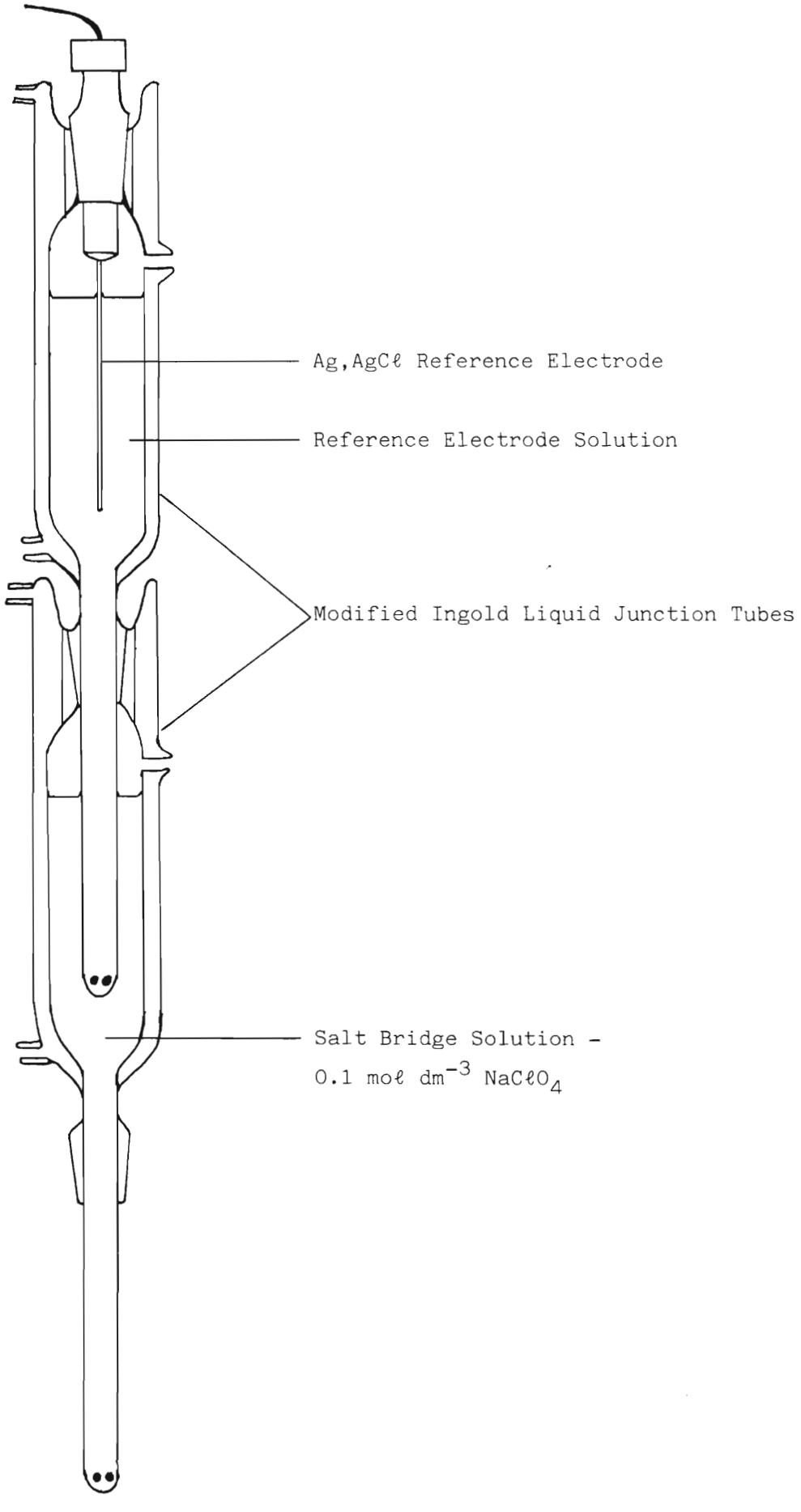

Figure 3.1: Diagram of Reference Electrode/Salt Bridge Assembly.

The indicating glass electrode, the reference electrode/salt bridge assembly, a thermometer or a second glass electrode, a METROHM EA 649 gas bubbler and a burette were introduced into the METROHM jacketted glass reaction vessel, type EA 880–T–50. Figure 3.2 shows a diagram of the cell arrangement.

A JULABO P12 Paratherm III water bath unit was used to thermostat the system at 25.0 ± 0.05^{o}C. The water was circulated through the jacketted glass reaction vessel and the jackets of the junction tubes.

Potentiometric measurements were performed using a RADIOMETER PHM 64 Research pH meter reading to 0.1 mV.

The working solution, in the reaction vessel, was maintained under a carbon dioxide free atmosphere of high purity nitrogen, which had been scrubbed of acid and alkaline impurities by passing the nitrogen through a 10% sodium hydroxide and a 10% sulphuric acid solution. Before the nitrogen gas came into contact with the working solution it was presaturated by passage through a 0.1 mol dm^{-3} sodium perchlorate solution. The working solution, in the reaction vessel, was continuously agitated by the nitrogen gas bubbling through it and/or by the magnetic stirrer used.

Titrant solutions were added to the reaction vessel using a METTLER DV 10 automatic titrator with a METTLER DV 210 automatic burette assembly. Sodium hydroxide titrant solutions were kept in a modified solution reservoir under a continuous flow of high purity nitrogen, which had been passed through a U–tube containing soda–lime and anhydrous calcium sulphate to remove any carbon dioxide and water, which may have come through the acid and alkaline scrubbing solutions. Figure 3.3 shows a diagram of the solution reservoir assembly used for sodium hydroxide titrant solutions.

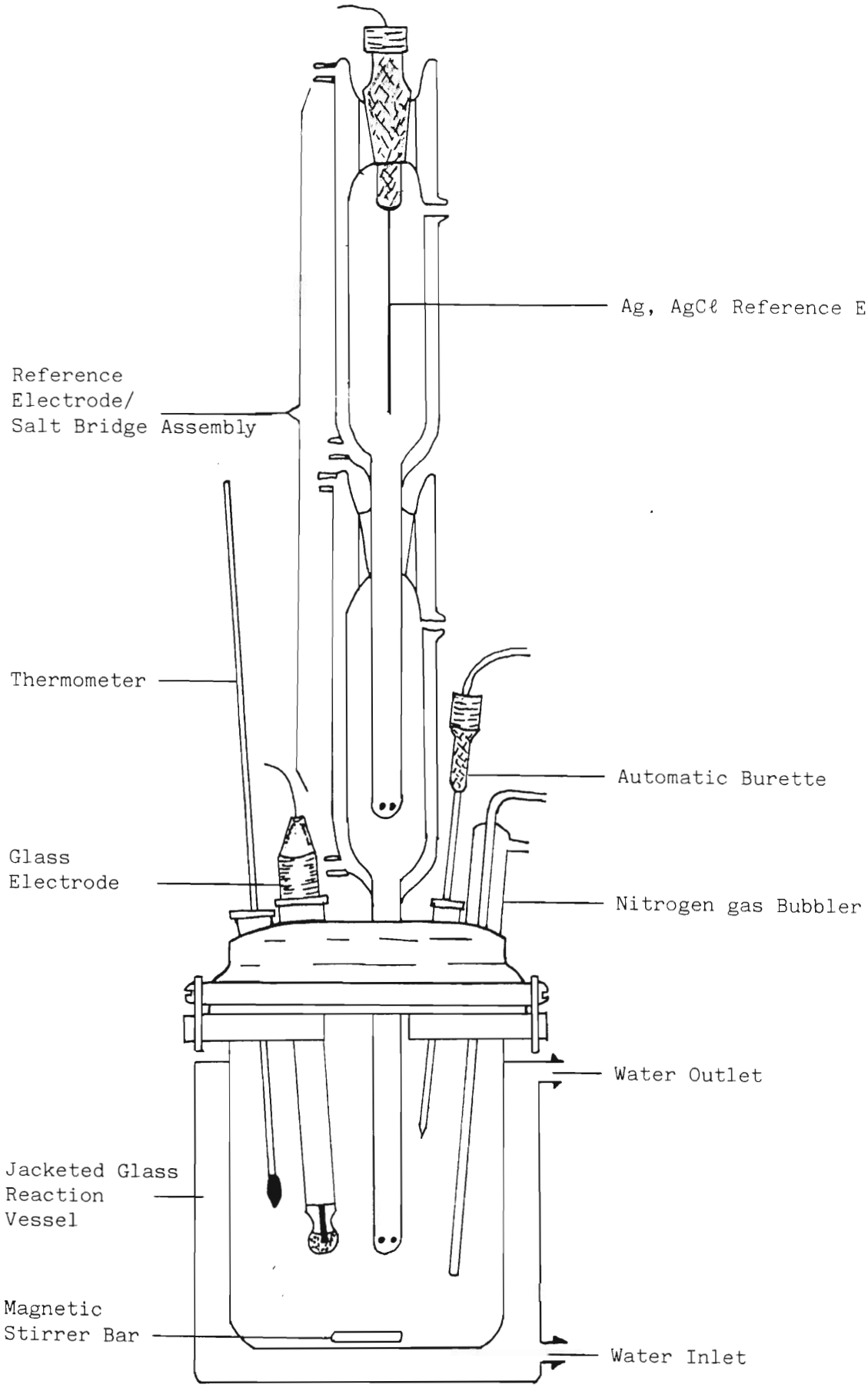

Figure 3.2: Diagram of Potentiometric Cell Assembly.

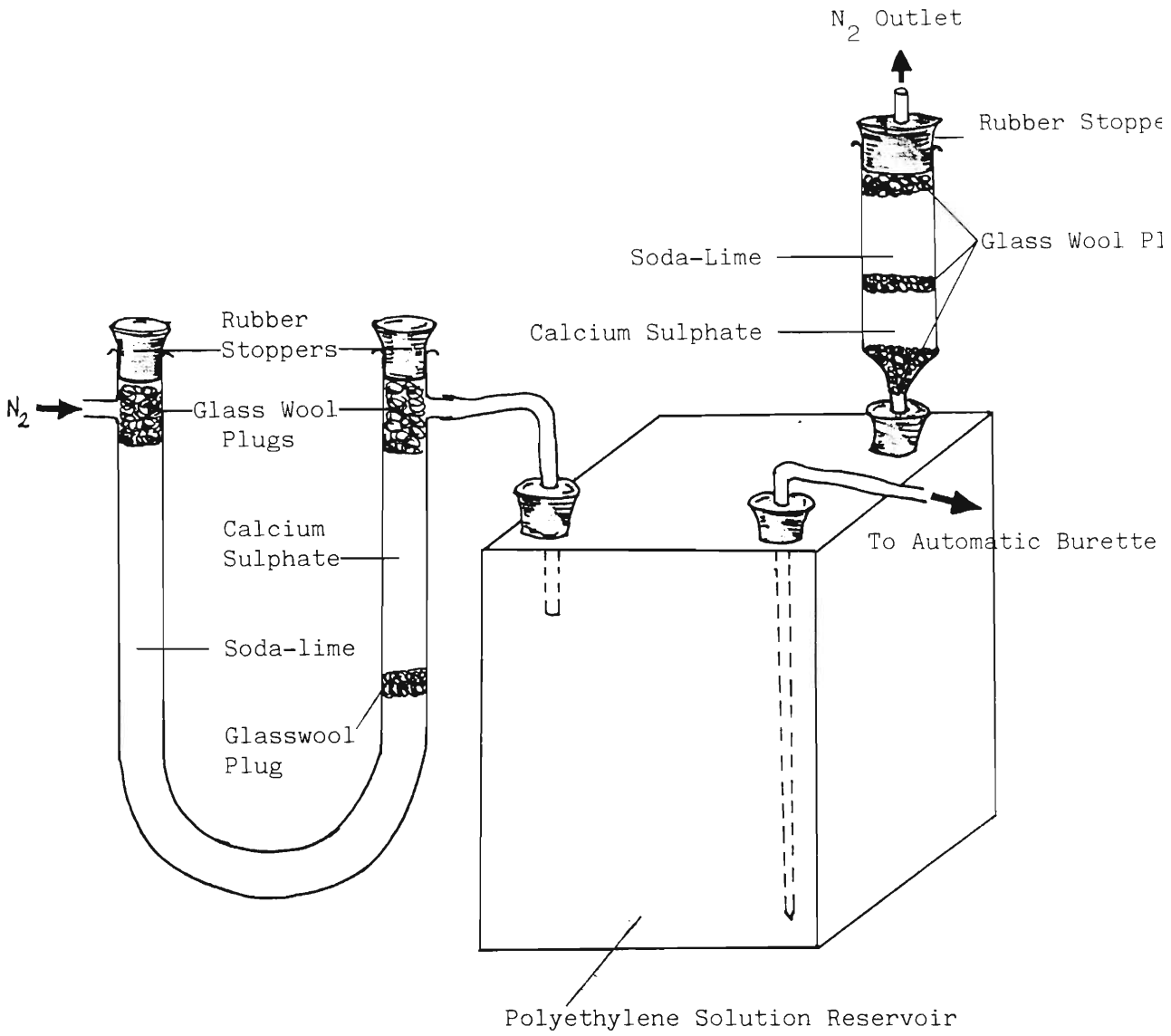

Figure 3.3 Modified Solution Reservoir used for NaOH Solutions.

3.2 ULTRAVIOLET–VISIBLE SPECTROPHOTOMETRIC APPARATUS

A PYE UNICAM SP 1800 UV–visible spectrophotometer in combination with a PYE UNICAM AR 25 recorder was used to examine solutions containing mixtures of CN^- and HCN. The solutions were studied in the 190 to 350 nm range. Quartz silica cells having a path length of 1.0 cm were used.

CHAPTER FOUR

CALCULATION TECHNIQUES

This chapter describes the various mathematical techniques used in this study for the analysis of potentiometric titration data. The two main techniques used were graphical and computational. The techniques were often used simultaneously.

Data of high precision can generally be satisfactorily processed by computer, although data described by not more than two parameters can be treated equally well using graphical methods. The essence of either approach is the comparison of an experimental function, obtained from experimental data, with theoretical functions, calculated by substituting values of the parameters into the appropriate equations. For example, an experimental function such as a formation curve, $\bar{Z}_M$(obs)vs log [L], derived from the measurements of M_T, L_T and [L] may be compared with a number of theoretical formation curves, $\bar{Z}_M$(calc)vs log [L], which are obtained by substituting different values of β_{pqr} into equations of the type shown below

$$\bar{Z}_M = \frac{\sum_{o}^{N} n\beta_n [L]^n}{\sum_{o}^{N} \beta_n [L]^n} \qquad (4.1)$$

The most acceptable values of the stability constants are those used to calculate the function, which best reproduces the experimental formation curve.

For a method to be acceptable it must make full use of the experimental data, give a good indication as to which complexes are present in solution, give the best values of the parameters treated as unknowns in the calculation, and should be flexible enough to allow the weighting of measurements. A good method should

show up systematic errors. In the case of a computer technique the limits of error in the values of the parameters obtained should be given.

The calculation techniques used in this study are given below.

4.1 GRAPHICAL METHODS

Graphical methods have the advantage that they visually display gross errors, show up "outliers" and systematic errors in the data obtained.

The shapes of curves provide information about the nature of the systems being investigated.

The disadvantage of graphical methods is that stability constants of complicated systems cannot be evaluated simultaneously, but have to be evaluated in several stepwise calculations. An accumulation of error is associated with each step.

Generally, graphical methods are used in conjunction with computer techniques when potentiometric titration data are being analysed.

Apart from the graphical techniques used in this study for the presentation of potentiometric titration data, a graphical technique called "the Gran plot" method (59–63) was used (see Section 4.1.3). The Gran plot technique was used to determine the concentrations of acid and base solutions.

The graphical techniques used in this study for the presentation of potentiometric titration data are described below.

4.1.1 Formation and deprotonation functions

The hydrogen formation function, is defined as

$$\bar{Z}_H = \frac{H_T - [H^+] + [OH^-]}{L_T} \quad , \tag{4.2}$$

where $\bar{Z}_H$ represents the hydrogen formation function,

H_T is the total (analytical) concentration of hydrogen ions in solution,

$[H^+]$ represents the concentration (in moℓ dm^{-3}) of free hydrogen ions in solution,

$[OH^-]$ represents the concentration (in moℓ dm^{-3}) of free hydroxide ions in solution,

and L_T represents the total (analytical) concentration of ligand L in solution.

Equation (4.2) can be further rearranged to give a general equation for $\bar{Z}_H$, which is shown below (64).

$$\bar{Z}_H = \frac{\sum_{r=0}^{\mathbb{R}} r\beta_{oqr}[H^+]^r}{\sum_{r=0}^{\mathbb{R}} \beta_{oqr}[H^+]^r} \quad , \tag{4.3}$$

where $\mathbb{R}$ is the maximum number of protons that can be associated with the ligand molecule.

The function $\bar{Z}_H$ (also denoted as $\bar{j}$ by some authors) is usually plotted versus $-\log[H^+]$ or p[H], where p[H] represents $-\log[H^+]$. The resultant curve is called a "formation curve". The formation curves often give an insight into the type of system being analysed i.e. number of protonation steps involved.

In simple systems, the formation constants can be determined using graphical methods (65). In more complicated systems such as those involving two step protonation, equation (4.3) can be rearranged such that for low values of $[H^+]$

and hence $\bar{Z}_H$, the values of the formation constants may be refined by successive approximation (66).

Graphical methods for obtaining values of β_{01r} from $\bar{Z}_H$ and $[H^+]$ data become much more involved when $r \geq 3$, because formation curves which represent more than two overlapping equilibria have no symmetry properties which can be exploited (67); and due to the accumulation of error associated with each step of the successive approximation refinement process, such complex systems are best evaluated using computer methods.

The metal formation function, defined as

$$\bar{Z}_M = \frac{L_T - A(1 + \sum_{r=1}^{R} \beta_{01r}[H^+]^r)}{M_T} \quad , \tag{4.4}$$

$$\text{where } A = \frac{H_T - [H^+] + [OH^-]}{\sum_{r=1}^{R} r\,\beta_{01r}[H^+]^r} \quad , \tag{4.5}$$

and M_T represents total (analytical) concentration of metal ion M (complexed and uncomplexed) in solution.

The function $\bar{Z}_M$ is usually plotted versus pA = –log A, where A represents the "apparent" free ligand concentration.

Under certain circumstances the functions $\bar{Z}_H$, $\bar{Z}_M$ and A have simple physical interpretations. For systems consisting of hydrogen ions and ligand only (apart from spectator ions) $\bar{Z}_H$ represents the average number of hydrogen ions coordinated to the ligand species L. When metal ions are present as well, $\bar{Z}_H$ continues to represent the average number of hydrogen ions coordinated to the

ligand, irrespective of the nature of the complexes formed between metal ion and ligand, provided that hydrolysis of metal–containing species to form $M_p(OH)_r$ and $M_pL_q(OH)_r$ does not occur, and that protonated complex species of the type $M_pL_qH_r$ do not form. When hydrolysis or complex protonation occurs $\bar{Z}_H$ is still well defined mathematically, but no longer has the same physical interpretation. The function $\bar{Z}_M$ is only defined for solutions containing hydrogen ions, ligand and metal ions. For systems or conditions in which no hydrolysis of the metal aquo ion or any of the complexes takes place, and no protonated complex species are formed, $\bar{Z}_M$ represents the average number of ligand molecules coordinated to the metal ion, and A = [L], the concentration of free (uncomplexed and unprotonated) ligand. Under these conditions, the function $\bar{Z}_M$ is identical to the function $\bar{n}$ used by numerous authors in the field. With some experience, the nature of the dominant species can often be deduced from the shapes of $\bar{Z}_M$ versus pA plots, and conclusions can be drawn, for example, concerning the presence or absence of polynuclear complexes (68), and the onset of hydrolysis.

When hydrolysis or protonation of complexes does occur, both $\bar{Z}_M$ and A lose the simple interpretations given above. When extensive hydrolysis occurs, the function $\bar{Z}_M$ becomes ill–conditioned and very sensitive to small uncertainties in the analytical quantity H_T, for example. Also A can take on negative values, making pA undefined. In general, $\bar{Z}_M$ versus pA plots are not useful for graphical presentation of potentiometric data in circumstances where extensive hydrolysis occurs.

A "deprotonation function", $\bar{Q}$, has recently been defined by Murray and May (44,69,70) as:

$$\bar{Q} = \frac{H_T^* - H_T}{M_T} \quad , \tag{4.6}$$

where H_T^* is the total hydrogen ion concentration in the system at the observed p[H], calculated from a mass–balance equation ignoring all metal complex formation. When metal containing species are ignored, the mass–balance equation for ligand reads:

$$L_T = [L]^* + \sum_{r=1}^{R} \beta_{01r}[L]^*[H^+]^r \quad , \tag{4.7}$$

$$\text{therefore } [L]^* = \frac{L_T}{1 + \sum_{r=1}^{R} \beta_{01r}[H^+]^r} \quad , \tag{4.8}$$

where $[L]^*$ is a fictitious concentration of free (uncomplexed) ligand – since metal containing species are ignored. Under the same fictitious circumstances, the mass–balance equation for hydrogen ions reads:

$$H_T^* = [H^+] - [OH^-] + \sum_{r=1}^{R} r\beta_{01r}[L]^*[H^+]^r \quad . \tag{4.9}$$

Substituting into equation (4.6) gives,

$$\bar{Q} = \frac{[H^+] - [OH^-] + L_T[\sum_{r=1}^{R} r\beta_{01r}[H^+]^r/(1+\sum_{r=1}^{R} \beta_{01r}[H^+]^r)] - H_T}{M_T} \quad .(4.10)$$

The function $\bar{Q}$ can be interpreted as follows. If metal ions M are added to a solution containing hydrogen ions and ligand, the metal ions will complex with a certain amount of the ligand present, and in so doing, will liberate hydrogen ions, thus lowering the solution p[H]. Some hydrolysis might also occur, also lowering the solution p[H]. A certain amount of mineral acid, given by $(H_T^* - H_T)$ would have to be removed from the solution (e.g. by addition of strong alkali) in order to raise the p[H] back to its original value. $\bar{Q}$ represents the number of moles of acid liberated in the solution per mole of M, by virtue of the complexing power of the metal ion – hence the term "deprotonation function", since the hydrogen ions are thought of as liberated from protonated ligand.

The function $\bar{Q}$ is plotted as a function of solution p[H]. It is particularly valuable in those regions of titrations (usually at high p[H]) where $\bar{Z}_M$ and pA functions become ill conditioned. It has been suggested (69) that plots of $\bar{Q}$ versus p[H] may be less sensitive to experimental error than plots of $\bar{Z}_M$ versus pA, and may therefore be preferable for purposes of comparison between observed and calculated data.

It is useful to define a hydrogen formation function $\bar{Z}_H^*$ (denoted $\bar{n}$ by Murray and May (69)) for the ligand–hydrogen subsystem in a ligand–hydrogen–metal system, such that,

$$\bar{Z}_H^* = \frac{H_T^* - [H^+] + [OH^-]}{L_T} \qquad (4.11)$$

$\bar{Z}_H^*$ is the value of $\bar{Z}_H$ calculated ignoring the formation of metal complexes. It can be shown that if a solution contains only one predominant complex of formula $M_pL_qH_r$, then the hydrogen stoichiometry of the complex, r, is given by

$$r = q\bar{Z}_H^* - p\bar{Q}$$

Negative values of r denote hydroxide groups on (or deprotonation of) the complex. This property of the formation function $\bar{Z}_H^*$ and deprotonation function $\bar{Q}$ can be useful in identifying the major species present in the system when there is reason to believe that one complex predominates over a given region of a titration (e.g. when a plateau is observed in the metal formation function).

4.1.2 System modelling

System modelling is the graphical comparison of curves obtained from the experimental data with theoretical curves obtained using values computed from

optimised stability constants for proposed complexes in the system being studied, in order to postulate a set of equilibria which describe the reactions occurring in the system.

The graphical method shows up random errors such as scattered points, while systematic errors, such as an incorrect theoretical model, causes the theoretical curve to deviate from the experimental curve.

In simple systems, such as instances where the maximum number of ligands bound to a metal ion is one or two, values of parameters may often be obtained very satisfactorily by "non–linear curve fitting" (71). For systems which consist of a single complex, ML, the experimental plots of $\bar{Z}_M$ against –log[A] are of unique shapes (71).

4.1.3 Gran plots

In potentiometric titrations the equivalence point is often taken as the point of inflexion on a titration curve, obtained by plotting the cell EMF, (E), as a function of the volume, (V), of reagent added. Often these curves show only a small potential change near the equivalence point and it has been customary to plot the "differential curve", $\Delta E/\Delta V$ as a fuction of the volume of reagent added. The peak of this curve is then taken as the equivalence point. Alternatively the point where the "second derivative curve", $\Delta^2E/\Delta V^2$ plotted as a function of the volume of reagent added, has a zero value, may be used.

Gran (59,60) devised a method of treating potentiometric titration data, so that the plots did not require a large number of readings corresponding to small changes in volume in the region of the equivalence point, but also made use of readings obtained in regions far from the equivalence point.

The Gran (59–63) method consists of linearising the titration curve by computing from the titration data a function which when plotted against the volume of titrant gives a straight line, which can be extrapolated to the equivalence point.

Gran's graphical method can be applied to potentiometric titrations involving acids, bases, ionic precipitations, complex formation and oxidation–reduction reactions.

In this study Gran's method was used in the standardisation of strong base solutions, the determination of carbonate concentrations in base solutions, the determination of excess base in sodium cyanide stock solutions and the excess acid in zinc perchlorate stock solutions.

The methods used are described below. All titrations were carried out at a temperature of 25.0^{0}C and at an ionic strength of 0.10 moℓ dm^{-3}.

4.1.3.1 Titration of a strong acid with a strong base

If V_o cm^3 of a strong acid, with an original concentration, in moℓ dm^{-3}, of C_A, is titrated with a strong base, of concentration C_B, the concentration of hydrogen ions, C_H, after the addition of V cm^3 of base will be:

$$C_H = C_A \frac{V_o}{V_o+V} - C_B \frac{V}{V_o+V} \quad . \tag{4.12}$$

At the equivalence point

$$C_A V_o = C_B V_e \quad , \tag{4.13}$$

where V_e is the volume of base added when the equivanence point is reached.

Substituting equation (4.13) into equation (4.12) leads to

$$C_H = C_B \frac{V_e - V}{V_o+V} \quad . \tag{4.14}$$

Now,

$$\text{antilog}\,(-\text{pH}) = 10^{-\text{pH}} = a_H = \gamma_H \times C_H \quad , \tag{4.15}$$

where a_H and γ_H represent the activity and activity coefficient of the hydrogen ion, respectively.

Equation (4.14) and (4.15) together give

$$10^{-pH} = \gamma_H \frac{C_B}{V_o+V}(V_e-V) \quad , \tag{4.16}$$

which can be transformed to

$$(V_o+V)\ 10^{-pH} = \gamma_H \times C_B (V_e-V) \quad , \tag{4.17}$$

or more generally to

$$(V_o+V)\ 10^{-pH} = k_1 (V_e-V) \quad , \tag{4.18}$$

where k_1 is a constant, including the activity coefficient, which in appropriate instances, can be considered constant during a titration. This is normally achieved by holding the ionic strength constant.

Similarly it can be shown that when the equivalence point has been passed, the concentration of hydroxide ions, C_{OH}, is given by

$$C_{OH} = C_B \frac{V}{V_o+V} - C_A \frac{V_o}{V_o+V} \tag{4.19}$$

$$= \frac{C_B}{V_o+V}(V-V_e) \tag{4.20}$$

Now,

$$C_H = \frac{K_w}{C_{OH}} \quad , \tag{4.21}$$

which together with equation (4.15) gives

$$\text{antilog pH} = 10^{pH} = \frac{C_B}{\gamma_H \times K_w(V_o+V)}(V-V_e) \quad , \tag{4.22}$$

which can be more generally transformed to

$$(V_o+V)\ 10^{pH} = k_2(V-V_e) \quad , \tag{4.23}$$

where k_2 is a constant, including the activity coefficient, which in appropriate instances can be considered constant during a titration.

If the cell potential, E, of the galvanic cell

$$(+) \quad \begin{matrix}\text{electrode reversible} \\ \text{to hydrogen ions}\end{matrix} \quad \Big| \quad \begin{matrix}\text{titration} \\ \text{solution}\end{matrix} \quad \Big\| \quad \begin{matrix}\text{reference} \\ \text{half cell}\end{matrix} \quad (-)$$

is measured, then, assuming ideal electrode behaviour, E is related to the free hydrogen ion concentration, $[H^+]$, by the Nernst equation –

$$E = E^0 + \frac{2.303RT}{nF} \log [H^+] \quad . \tag{4.24}$$

Since it is assumed that the cell behaves reversibly and that the activity coefficients are constant, the value of E^0 is constant. Rearranging equation (4.24) leads to

$$\frac{nEF}{2.303RT} = \frac{nE^0F}{2.303RT} + \log[H^+] \quad . \tag{4.25}$$

The first term on the right hand side of equation (4.25) is a constant so that

$$pH \propto \frac{-EF}{2.303RT} \quad . \tag{4.26}$$

Equations (4.18) and (4.23) may therefore be written as

$$(V_o+V)\ 10^{EF/2.303RT} = k_1(V_e-V) \tag{4.27}$$

and

$$(V_o+V)\ 10^{-EF/2.303RT} = k_2(V-V_e) \quad . \tag{4.28}$$

Two quantities ϕ and ϕ' can now be defined as

$$\phi = (V_o+V)\ 10^{EF/2.303RT} \tag{4.29}$$

and

$$\phi' = (V_o+V)\ 10^{-EF/2.303RT} \quad . \tag{4.30}$$

From equations (4.27) and (4.28) it is clear that the quantities ϕ and ϕ' are linear functions of V, such that $\phi(V)$ and $\phi'(V)$ both intersect on the abscissa at the point (V_e,O).

Figure 4.1 shows an example in which a Gran plot for the titration of a strong acid with a strong base was used to standardise the base solution. The solutions were made up to an ionic strength of 0.10 moℓ dm^{-3} using $NaC\ell O_4$. Representative data for this plot is given in Table 4.1.

From Figure 4.1 one obtains V_e = 7.05 cm^3, from which the concentration of hydroxide can be calculated to be 0.0107 moℓ dm^{-3}.

Deviations of the Gran functions from linearity were observed for some of the titrations of strong acid with strong base, used to standardise the base.

Examples of these deviations are shown in Figures 4.2 and 4.3.

Figure 4.2 shows that curvature occurs at values of V remote from V_e and corresponding to high values of hydrogen ion concentration.

TABLE 4.1

Titration of a mixture of 7.00 cm^3 of 0.0107 moℓ dm^{-3} $HC\ell O_4$ plus 50.00 cm^3 of 0.10 moℓ dm^{-3} $NaC\ell O_4$ with a solution containing approximately 0.01 moℓ dm^{-3} NaOH. (V_o =57.00 cm^3).

V/cm^3	$(V_o+V)/cm^3$	E_{cell}/mV	$\phi \times 10^3/cm^3$
0.00	57.00	85.9	16.13
2.00	59.00	76.7	11.67
3.00	60.00	70.7	9.40
4.00	61.00	63.0	7.08
4.50	61.50	58.1	5.90
5.00	62.00	52.2	4.73
5.50	62.50	44.4	3.52
6.00	63.00	33.3	2.30
6.50	63.50	13.7	1.08
			$\phi' \times 10^7/cm^3$
8.00	65.00	−314.5	1.34
9.00	66.00	−333.7	2.88
9.50	66.50	−338.6	3.51
10.00	67.00	−342.8	4.16
11.00	68.00	−350.5	5.70
12.00	69.00	−355.8	7.11

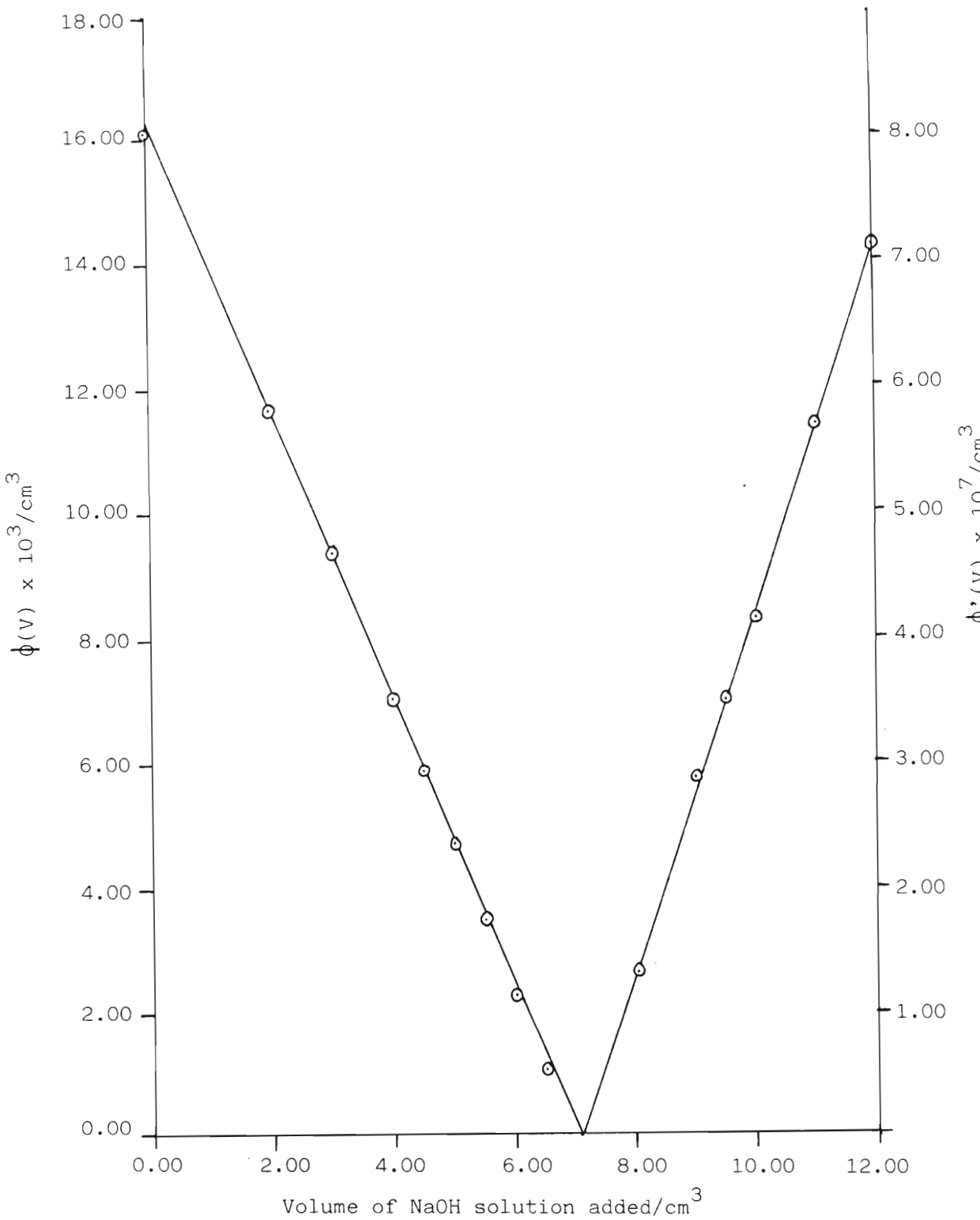

Figure 4.1: Gran plot of the functions $\phi(V)$ and $\phi'(V)$ for the titration of a strong acid with a strong base.

This type of deviation from linearity can be explained in terms of the activity coefficient and/or the junction potentials not being negligible at the extreme values of the hydrogen ion concentration (61.63). Rossotti amd Rossotti (61) state that "if the plots are linear near the equivalence point, the values of V_e must be obtained from this region alone". Representative data for this plot is given in Table 4.2. The solutions were made up to an ionic strength of 0.10 mol dm^{-3} using $NaCl O_4$.

TABLE 4.2

Titration of a mixture of 20.00 cm^3 of 0.0103 mol dm^{-3} $HCl O_4$ plus 50.00 cm^3 of 0.10 mol dm^{-3} $NaCl O_4$ with a solution containing approximately 0.01 mol dm^{-3} NaOH. (V_o = 90.00 cm^3).

V/cm^3	$(V_o+V)/cm^3$	E_{cell}/mV	$\phi \times 10^3/cm^3$
0.00	90.00	104.3	5.21
2.00	92.00	101.9	4.85
4.00	94.00	99.3	4.48
6.00	96.00	96.5	4.10
8.00	98.00	93.3	3.70
10.00	100.00	89.9	3.31
12.00	102.00	86.0	2.90
14.00	104.00	81.5	2.48
16.00	106.00	76.3	2.06
17.00	107.00	73.3	1.85
18.00	108.00	70.0	1.65
19.00	109.00	66.2	1.43
20.00	110.00	61.8	1.22
21.00	111.00	56.7	1.01
22.00	112.00	50.1	0.79
24.00	114.00	29.1	0.35

From Figure 4.2, V_e = 25.74 cm^3 from which the concentration of hydroxide is calculated to be 0.0080 mol dm^{-3}.

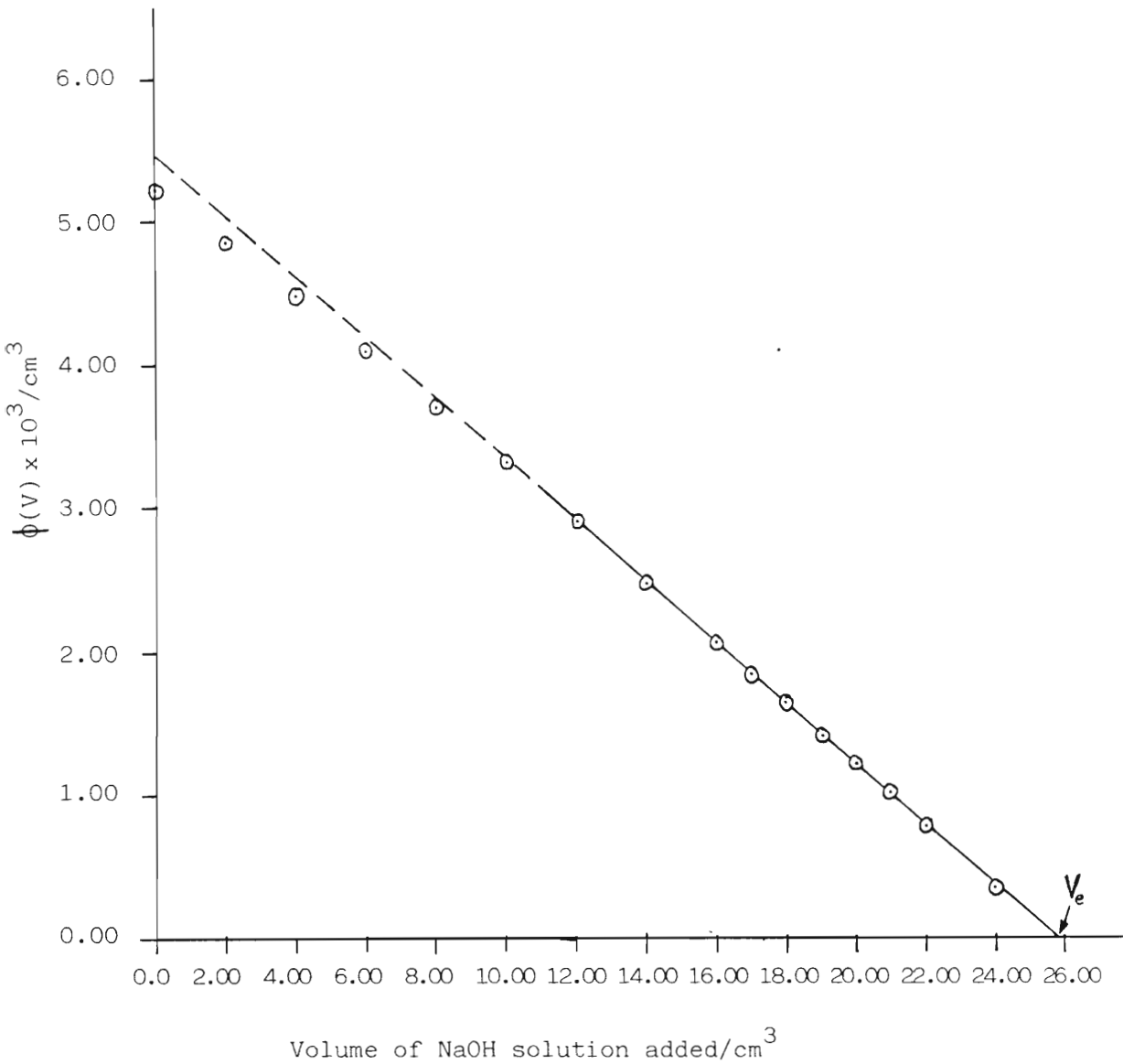

Figure 4.2: Gran plot of the function $\phi(V)$ for the titration of a strong acid with a strong base, demonstrating deviation of $\phi(V)$ from linearity at high $[H^+]$.

Figure 4.3 shows a Gran plot, in which the basic Gran function, $\phi'(V)$, is curved in the region of V_e. Rossotti and Rossotti (61) explained this type of deviation as being due to the strong base solution being contaminated with carbonate (63). Rossotti and Rossotti (61) state that if the function, $\phi'(V)$ is linear over an appreciable range of V, then the function may be extrapolated to cut the abscissa at the point V_e', resulting in the two functions $\phi(V)$ and $\phi'(V)$ intersecting below the abscissa.

From the equivalence point (V_e) obtained from the acid Gran function, the total base concentration, which is equal to sum of the hydroxide ion concentration and twice the carbonate ion concentration, is obtained (63,72). The equivalence point (V_e') obtained from the base Gran function is equal to the concentration of hydroxide ions in the basic titrant solution. Thus from the two equivalence points the hydroxide ion concentration and an estimate of the carbonate ion concentration of the basic solution can be determined.

Representative data for Figure 4.3 is given in Table 4.3. The solutions were made up to an ionic strength of 0.10 mol dm^{-3} using $NaClO_4$.

From Figure 4.3, V_e = 6.97 cm^3 and V_e' = 7.45 cm^3, from which the concentration of the hydroxide and carbonate in the base solution can be calculated as follows:

$$[OH^-] + 2[CO_3^{=}] = [\text{Total Base}] = \frac{10.00 \times 0.0010}{6.97} = 1.43 \times 10^{-3} \text{ mol dm}^{-3}$$

$$[OH^-] = \frac{10.00 \times 0.0010}{7.45} = 1.34 \times 10^{-3} \text{ mol dm}^{-3}$$

and $[CO_3^{=}] = 4.5 \times 10^{-5}$ mol dm^{-3} .

TABLE 4.3

Titration of a mixture of 10.00 cm^3 of 0.0010 mol dm^{-3} $HCl O_4$ plus 50.00 cm^3 of 0.10 mol dm^{-3} $NaCl O_4$ with a solution containing approximately 0.0010 mol dm^{-3} NaOH. (V_o = 60.00 cm^3).

V/cm^3	$(V_o+V)/cm^3$	E_{cell}/mV	$\phi \times 10^1/cm^3$
0.00	60.00	26.3	16.70
2.00	62.00	16.8	11.92
3.00	63.00	10.6	9.52
3.50	63.50	7.0	8.34
4.00	64.00	2.5	7.06
5.00	65.00	−7.9	4.78
5.50	65.50	−15.6	3.57
6.00	66.00	−27.3	2.28
			$\phi' \times 10^6/cm^3$
7.50	67.50	−211.2	0.25
8.00	68.00	−231.2	0.55
8.50	68.50	−243.7	0.90
9.00	69.00	−254.1	1.36
10.00	70.00	−266.4	2.22
11.00	71.00	−274.6	3.10
12.00	72.00	−280.3	3.93

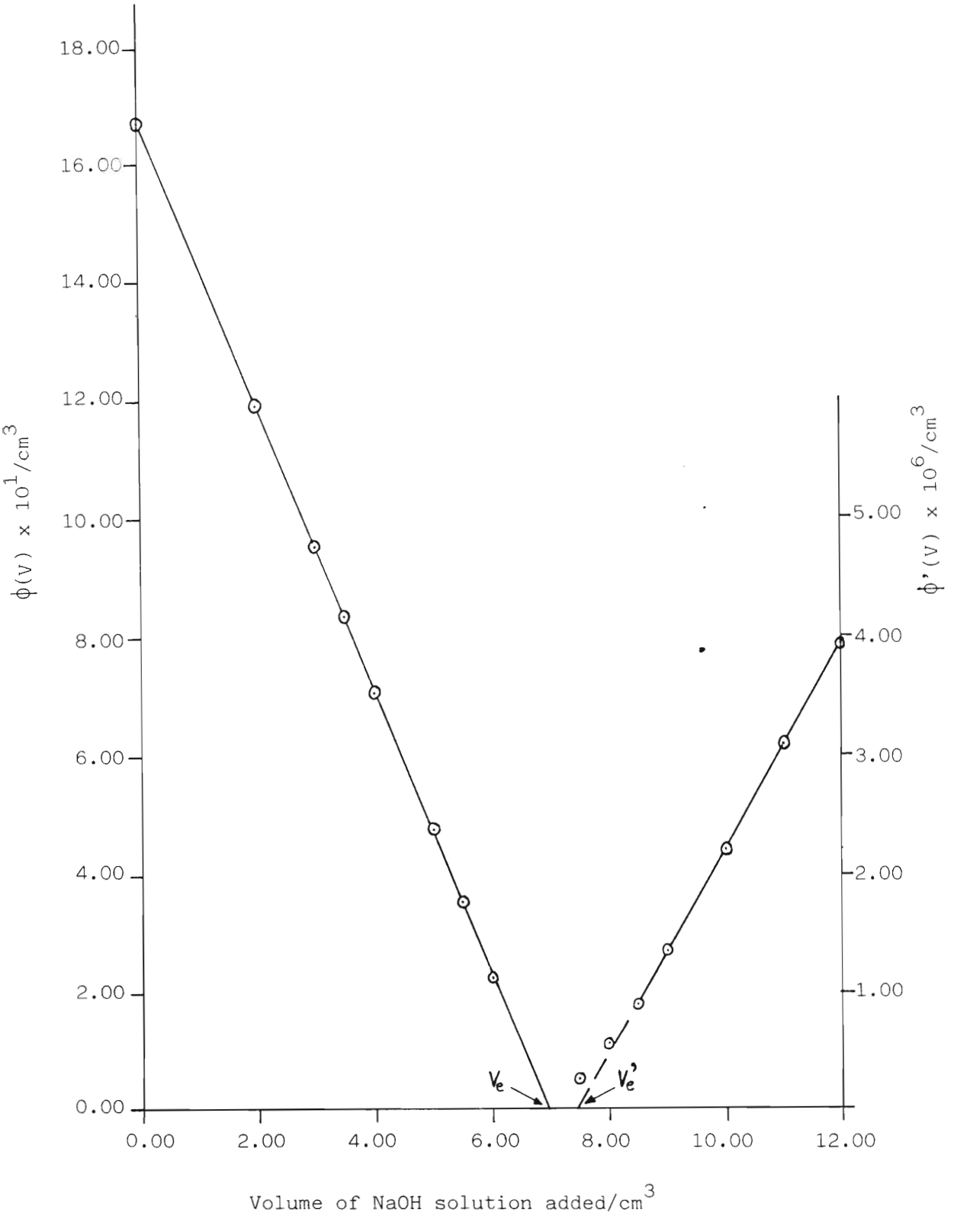

Figure 4.3: Gran plot of the functions $\phi(V)$ and $\phi'(V)$ for the titration of a strong acid with a solution containing both carbonate and hydroxide.

4.1.3.2 Titration of a strong base with a strong acid

When V_o cm^3 of a strong base, with a concentration in mol dm^{-3} of C_B, is titrated with a strong acid of concentration C_A, the concentration of hydroxide ions C_{OH} after the addition of V cm^3 of acid will be:

$$C_{OH} = C_B \frac{V_o}{V_o+V} - C_A \frac{V}{V_o+V} \quad . \tag{4.31}$$

At the equivalence point

$$C_B V_o = C_A V_e \quad , \tag{4.32}$$

where V_e is the volume of acid added when the equivalence point is reached. Substitution of equation (4.32) into equation (4.31) leads to

$$C_{OH} = C_A \frac{V_e - V}{V_o+V} \quad . \tag{4.33}$$

Now

$$\text{antilog}\,(-\text{pOH}) = 10^{-\text{pOH}} = a_{OH} = \gamma_{OH} \times C_{OH} \quad , \tag{4.34}$$

where a_{OH} and γ_{OH} represent the activity and activity coefficient of the hydroxide ion, respectively, equation (4.33) and (4.34) together give:

$$10^{-\text{pOH}} = \gamma_{OH} \frac{C_A}{V_o+V} (V_e - V) \quad , \tag{4.35}$$

which can be transformed to

$$(V_o+V)\, 10^{-\text{pOH}} = \gamma_{OH} C_A (V_e - V) \quad . \tag{4.36}$$

Substituting $pOH = pK_w - pH$ in equation (4.36) leads to

$$(V_o+V)\ 10^{pH-pK_w} = \gamma_{OH}C_A(V_e-V) \quad . \tag{4.37}$$

Rearranging, one obtains

$$(V_o+V)\ 10^{pH} = \frac{\gamma_{OH}C_A}{10^{-pK_w}}(V_e-V) \quad , \tag{4.38}$$

$$\text{therefore } (V_o+V)\ 10^{pH} = k_3(V_e-V) \quad , \tag{4.39}$$

where k_3 is a constant, provided that γ_{OH} is constant. As mentioned previously this is normally achieved by holding the ionic strength constant. Similarly it can be shown that when the equivalence point has been passed

$$(V_o+V)\ 10^{-pH} = k_4(V-V_e) \quad , \tag{4.40}$$

where k_4 is a constant. If the cell potential E is measured, where E is related to the free hydrogen ion concentration by the Nernst equation (see 4.24) and it is assumed that the cell behaves reversibly and that the activity coefficients are constant, the value of E^0 is a constant. Rearranging equation (4.24) gives the equation (4.26).

Equations (4.39) and (4.40) may therefore be written as

$$(V_o+V)\ 10^{-EF/2.303RT} = k_3(V_e-V) \tag{4.41}$$

and

$$(V_o+V)\ 10^{EF/2.303RT} = k_4(V-V_e) \quad . \tag{4.42}$$

Two quantities Φ' and Φ can now be defined as

$$\Phi' = (V_o+V)\ 10^{-EF/2.303RT} \qquad (4.43)$$

and

$$\Phi = (V_o+V)\ 10^{EF/2.303RT} \qquad (4.44)$$

Comparison of equations (4.43) and (4.44) with equations (4.30) and (4.29) respectively, indicates that corresponding Gran functions can be used for the alkaline and acid regions of the titrations considered.

The titration of strong base solutions with strong acid solutions was used to standardise base solutions. Deviations of the Gran functions from linearity, similar to those which occurred in the titration of a strong acid with a strong base (see Section 4.1.3.1) were observed.

An example of the deviation due to carbonate contamination is shown in Figure 4.4. Representative data for this plot is given in Table 4.4.

From Figure 4.4 one obtains V_e = 6.24 cm^3 and V_e' = 6.09 cm^3 from which the concentration of the hydroxide and carbonate in the base solution can be calculated as follows:

$$[OH^-] + 2[CO_3^{=}] = [\text{Total base}] = \frac{6.24 \times 0.0100}{6.60} = 9.45 \times 10^{-3}\ \text{mol dm}^{-3}$$

$$[OH^-] = \frac{6.09 \times 0.0100}{6.60} = 9.23 \times 10^{-3}\ \text{mol dm}^{-3}$$

$$[CO_3^{=}] = 1.1 \times 10^{-4}\ \text{mol dm}^{-3}.$$

TABLE 4.4

Titration of a mixture of 6.60 cm^3 of a basic solution, containing approximately 0.0093 moℓ dm^{-3} NaOH with approximately 0.0001 moℓ dm^{-3} carbonate plus 50.00 cm^3 of 0.10 moℓ dm^{-3} $NaC\ell O_4$, with a solution containing 0.0100 moℓ dm^{-3} $HC\ell O_4$. (V_o = 56.60 cm^3).

V/cm^3	$(V_o+V)/cm^3$	E_{cell}/mV	$\Phi' \times 10^7/cm^3$
0.00	56.60	−379.5	14.67
1.00	57.60	−374.3	12.19
2.00	58.60	−368.3	9.82
3.00	59.60	−360.5	7.37
4.00	60.60	−350.5	5.08
5.00	61.60	−334.8	2.80
6.00	62.60	−298.8	0.70
			$\Phi \times 10^3/cm^3$
8.00	64.60	41.6	0.33
9.00	65.60	53.6	0.53
10.00	66.60	62.2	0.75
11.00	67.60	67.1	0.92
12.00	68.60	71.6	1.11
13.10	69.70	75.6	1.32

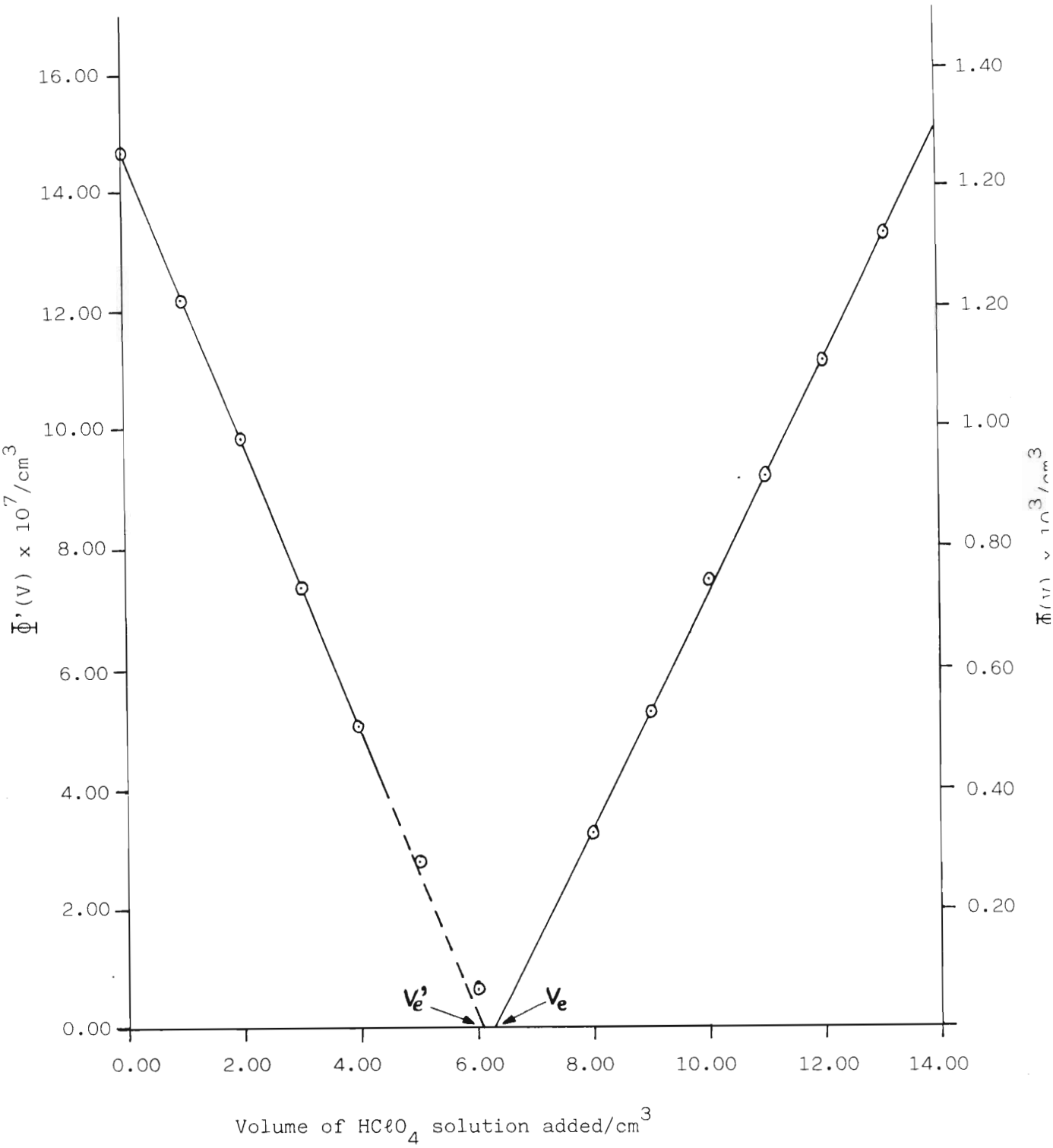

Figure 4.4: Gran plot of the functions $\Phi'(V)$ and $\Phi(V)$ for the titration of a solution containing both carbonate and hydroxide with a strong acid.

4.1.3.3 Titration of a weak base with a strong acid

If V_o cm^3 of a weak base, B, which is not fully dissociated in solution, with an initial concentration in moℓ dm^{-3} of C_{WB} is titrated with a strong acid of concentration in moℓ dm^{-3} of C_A, the equation for the weak monoprotic base can be represented as:

$$B + H_2O \overset{K_b}{\rightleftharpoons} BH^+ + OH^- \quad , \tag{4.45}$$

where K_b is the stoichiometric base dissociation constant of B.

Then

$$K_b = \frac{[BH^+][OH^-]}{[B]} \tag{4.46}$$

and

$$[OH^-] = \frac{K_b[B]}{[BH^+]} \tag{4.47}$$

After the addition of V cm^3 of acid the concentration of BH^+ and B in solution can be expressed as:

$$[BH^+] = \frac{VC_A}{V_o+V} \tag{4.48}$$

and

$$[B] = \frac{C_{WB}V_o - C_AV}{V_o+V} \tag{4.49}$$

The Gran method ignores the effect of the reversible reaction (72).

At the equivalence point, V_e,

$$C_{WB}V_o = C_A V_e \quad . \tag{4.50}$$

Substituting equations (4.48), (4.49) and (4.50) into equation (4.46), gives,

$$K_b = \frac{VC_A[OH^-]}{C_A(V_e - V)} \quad , \tag{4.51}$$

thus,

$$V[OH^-] = K_b(V_e - V) \quad . \tag{4.52}$$

Since,

$$[OH^-] = \frac{K_W}{[H^+]} \quad , \tag{4.53}$$

thus,

$$p[OH^-] = pK_W - p[H^+] \quad . \tag{4.54}$$

Substituting equation (4.54) into equation (4.52), gives,

$$V\,10^{pH} = \frac{K_b(V_e - V)}{10^{-pK_w}\gamma_H} \quad . \tag{4.55}$$

The cell potential, E, is given by equation (4.24). E^0 is constant, as it is assumed that the cell behaves reversibly and that the activity coefficients are constant, since the ionic strength was kept constant during a titration. Therefore

$$V \times 10^{pH} = k_5(V_e - V) \quad , \tag{4.56}$$

where k_5 is a constant, provided that γ_H is constant. This is normally achieved by holding the ionic strength constant. Similarly it can be shown that when the equivalence point has been passed:

$$(V_o+V)\ 10^{-pH} = k_6(V-V_e) \quad , \tag{4.57}$$

where k_6 is also a constant.

If the cell potential, E, is measured, where E is related to the free hydrogen ion concentration by the Nernst equation and it is assumed that the cell behaves reversibly and that the activity coefficients are constant, then the value of E^0 is a constant. Equation (4.56) and (4.57) may be written as:

$$V \times 10^{-EF/2.303RT} = k_5(V_e-V) \tag{4.58}$$

and

$$(V_o+V)\ 10^{EF/2.303RT} = k_6(V-V_e) \quad . \tag{4.59}$$

Two quantities ψ' and ψ can now be defined as

$$\psi' = V \times 10^{-EF/2.303RT} \tag{4.60}$$

and

$$\psi = (V_o+V)\ 10^{EF/2.303RT} \quad . \tag{4.61}$$

From equations (4.58) and (4.59) it is clear that the quantities ψ' and ψ are linear functions of V, such that $\psi'(V)$ and $\psi(V)$ both intersect on the abscissa at the point $(V_e,0)$.

In this work the excess amount of base in the sodium cyanide stock solution was determined by adding a known quantity of sodium hydroxide of known concentration, to a known quantity of the sodium cyanide stock solution and titrating this solution with a strong acid. Thus the total base in the solution was made up of the added sodium hydroxide, and the excess sodium hydroxide from the sodium cyanide stock solution. The neutralization of this alkaline solution was treated as two cases:–

(i) titration of a strong base with a strong acid (see Section 4.1.3.2) and,

(ii) the titration of a weak base with a strong acid.

The solutions titrated were never allowed to become acidic.

Figure 4.5 shows an example of a plot of E_{cell} against the volume of strong acid titrated into an alkaline solution containing sodium cyanide with an unknown quantity of excess sodium hydroxide, to which a known amount of sodium hydroxide had been added.

Representative data for Figure 4.5 is given in Table 4.5.

The first equivalence point in Figure 4.5 corresponds to the situation when the total concentration of hydroxide ions in the alkaline solution was neutralised by the hydrogen ions added at that point. The exact equivalence point was obtained by treating the data between 7.0 cm^3 and 19.0 cm^3 of $HClO_4$ added, as that of a strong base titrated with a strong acid, as described in Section 4.1.3.2. From the Gran plot of this data the equivalence point is obtained as 19.8 cm^3 $HClO_4$. The excess concentration of hydroxide ions in the sodium cyanide stock solution can thus be determined.

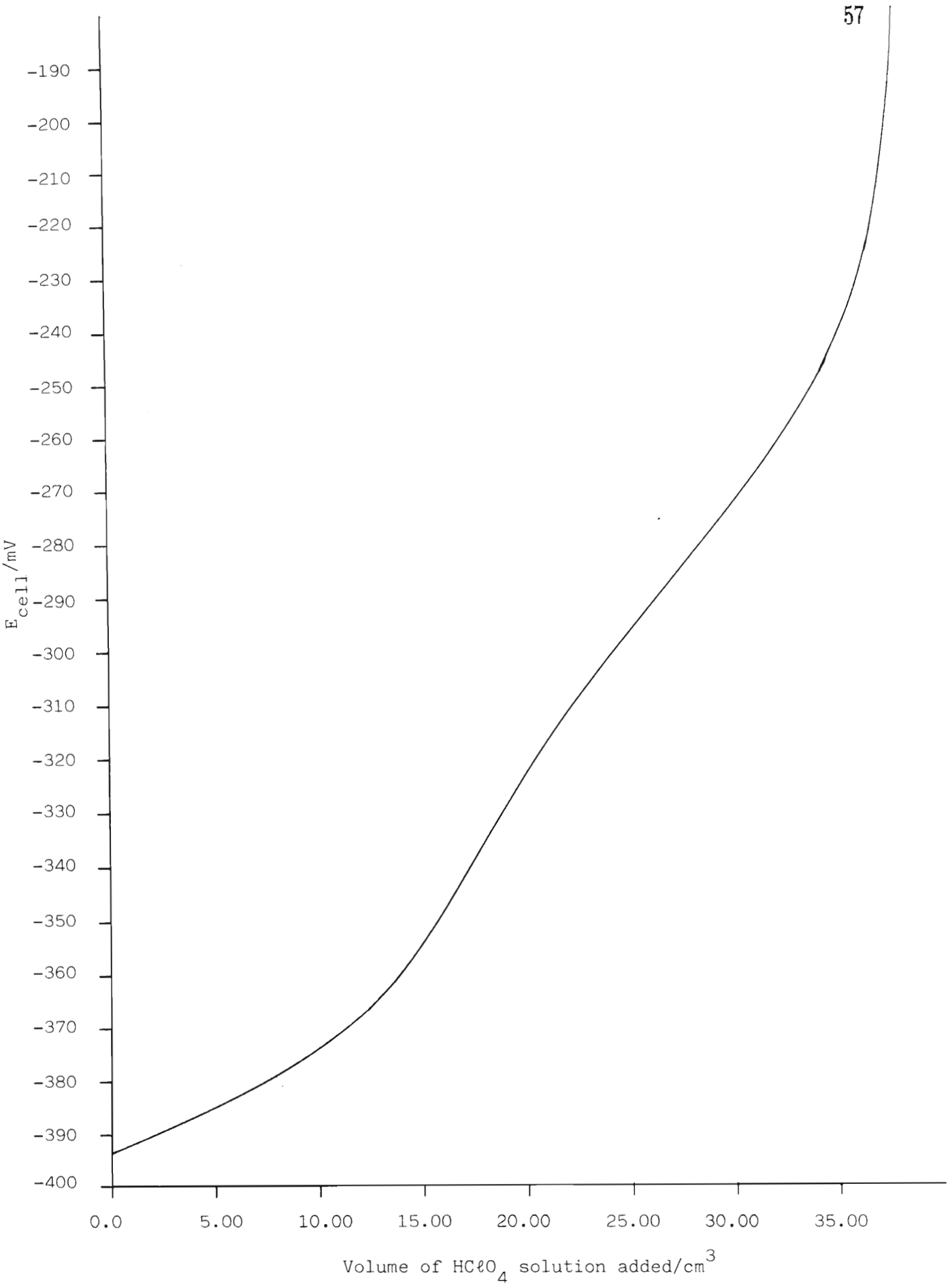

Figure 4.5: Titration curve for the titration of a solution containing sodium hydroxide and sodium cyanide with perchloric acid.

TABLE 4.5

Titration of an alkaline solution containing 50.0 cm^3 $NaCl O_4$ (0.10 mol dm^{-3}), 20.0 cm^3 NaCN (0.0099 mol dm^{-3}) with excess NaOH of unknown concentration and 20.0 cm^3 NaOH (0.0100 mol dm^{-3}) with a solution containing $HCl O_4$ (0.0100 mol dm^{-3}). (V_o = 90.00 cm^3).

The ionic strength of all solutions was make up to 0.10 mol dm^{-3} using $NaCl O_4$.

V/cm^3	$(V_o+V)/cm^3$	E_{cell}/mV	$\Phi' x\ 10^7/cm^3$
0.0	90.0	−393.9	40.85
1.0	91.0	−392.3	38.88
3.0	93.0	−388.8	35.35
5.0	95.0	−385.1	30.61
7.0	97.0	−381.0	26.65
8.5	98.5	−377.8	23.89
10.0	100.0	−374.1	21.00
11.5	101.5	−369.9	18.10
13.0	103.0	−364.2	14.72
14.0	104.0	−359.7	12.47
15.0	105.0	−354.5	10.27
16.0	106.0	−348.7	8.29
17.0	107.0	−342.3	6.52
18.0	108.0	−335.5	5.05
19.0	109.0	−329.0	3.00
20.0	110.0	−322.7	3.87
21.0	111.0	−316.9	4.89
23.0	113.0	−306.2	7.55
24.0	114.0	−301.1	9.29
25.0	115.0	−296.3	11.30

Cont./.....

Table 4.5 continued/

V/cm^3	$(V_o+V)/cm^3$	E_{cell}/mV	$\Phi' x\ 10^7/cm^3$
26.0	116.0	−291.6	13.69
27.0	117.0	−287.0	16.52
28.0	118.0	−282.4	19.92
29.0	119.0	−277.9	23.94
30.0	120.0	−273.1	29.09
			$\psi' x\ 10^5/cm^3$
31.0	121.0	−268.3	10.61
32.0	122.0	−262.8	8.84
32.5	122.5	−260.0	8.05
33.0	123.0	−256.8	7.22
33.5	123.5	−253.8	6.52
34.0	124.0	−250.0	5.71
34.5	124.5	−246.8	5.11
35.0	125.0	−242.0	4.30
35.5	125.5	−237.5	3.66
36.0	126.0	−231.6	2.95
36.5	126.5	−225.0	2.32
37.0	127.0	−216.5	1.69
37.5	127.5	−206.8	1.17
38.0	128.0	−186.5	0.54

The second equivalence point is that of the weak base, and the exact point can be determined using the Gran plot method for the titration of a weak base with a strong acid for the points from 31.0 cm^3 to 38.0 cm^3 $HCl O_4$ added. Figure 4.6 shows the Gran plot for the data given in Table 5.4 for the titration of a weak base with a strong acid. The information concerning the concentration of the cyanide stock solution was used as a check on the Liebig–Déniges method (see Section 2.4).

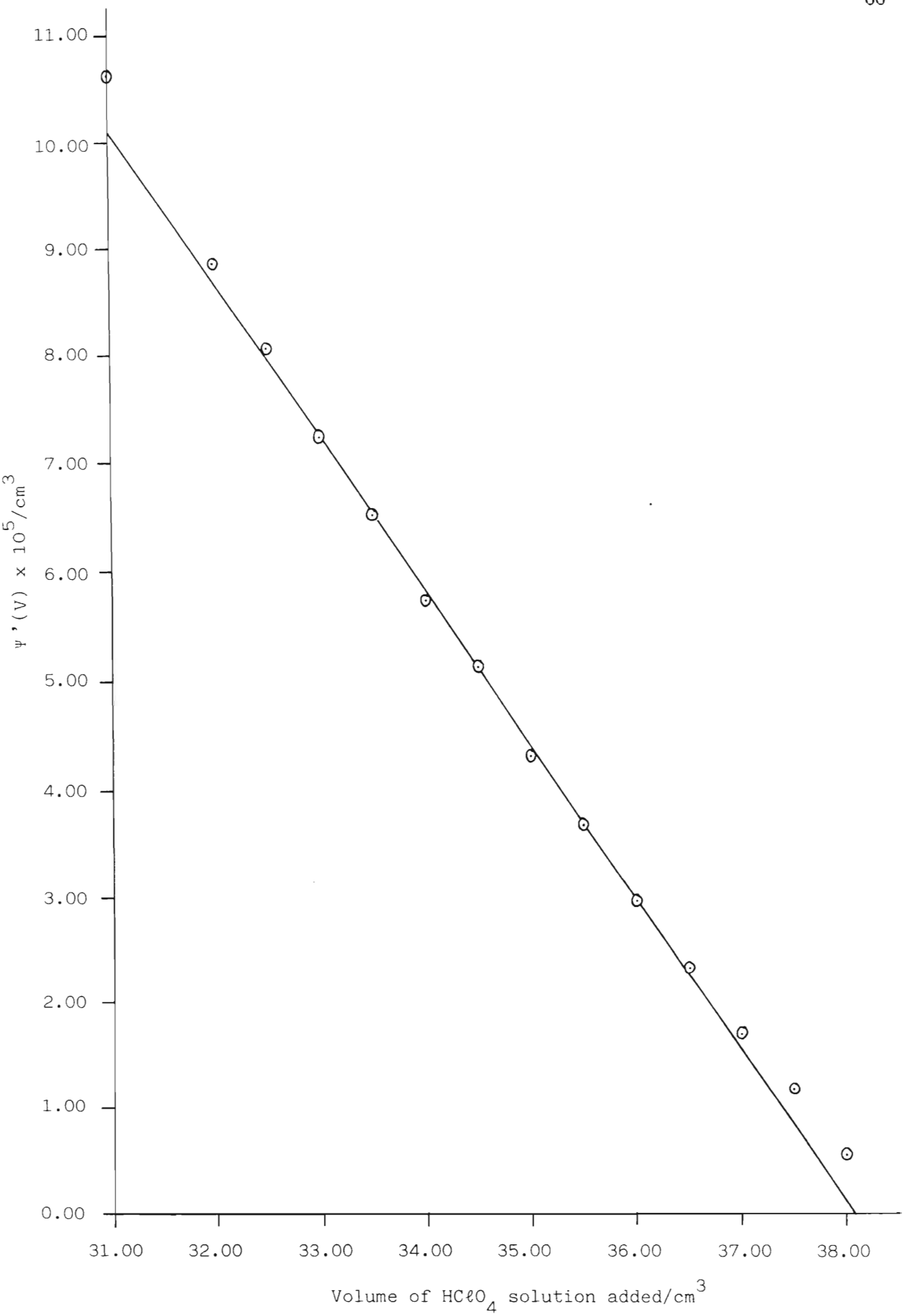

Figure 4.6: Gran plot of the function $\psi'(V)$ for the titration of a weak base (sodium cyanide) with a strong acid.

4.2 COMPUTER METHODS

In this study computer methods were used for the design of experiments, the graphical presentation and analysis of potentiometric data, the calculation of formation constants and for calculation of the composition of equilibrium mixtures (speciation calculations). The computer programs used are described below.

4.2.1 Use of the program HALTAFALL

In this study the computer program HALTAFALL (73) was used to aid the design of experiments (see Chapter 6). HALTAFALL was used to simulate titrations in a single phase by calculating the equilibrium concentrations of all known and/or assumed species in equilibrium mixtures, from the overall concentrations of all the components and from known or estimated values of formation constants. The speciation information obtained from HALTAFALL, was used to determine the optimum combinations of reagent concentrations required, to give optimum formation of a particular species thought to be formed. In this manner experimental runs were designed (see Chapter 6).

Once stability constants for a particular system were known, HALTAFALL was used to obtain values of $\bar{Z}_M$ (calc) vs log[L], as well as the speciation of the zinc in the form of various complexes within certain concentration ranges. These values were compared with observed values.

The sensitivity and feasibility of any proposed experimental run was tested, using HALTAFALL, by estimating the effect on the measured p[H] of a change of one log unit in a particular stability constant (see Chapter 6). An indication could thereby be obtained of the degree of precision to which the particular stability constant could be determined.

4.2.2 Use of the program MINIQUAD

In the initial stages of this study the computer program MINIQUAD (41) was used for the computation of formation constants of complex species in solution,

from the potentiometric data.

MINIQUAD was superseded by the computer program ESTA (43,44,69, 70), which is described briefly in Section 4.2.3.

4.2.3 Use of the program ESTA

In this study the potentiometric titration data were analysed using the computer program ESTA (43,44,69,70), which was recently described by Murray and May (44,70).

ESTA is a flexible suite of programs which allows calculations concerned with competitive aqueous solution equilibria, to be preformed on potentiometric titration data. ESTA is used to investigate the phenomena associated with chemical interactions in solution and for simulating equilibrium distributions of chemical species in solutions.

In ESTA, the calculations are preformed by two main program modules, namely the simulation module called "ESTA 1" and the optimisation module called "ESTA 2".

ESTA 1, produces results on a point to point basis. ESTA 1 can be used to determine a single value for almost any of the parameters which characterise a titration, by setting up and solving the mass balance equations.

The simulation facilities of ESTA 1 fall into two categories namely speciation calculations and potentiometric titration calculations. The potentiometric titration calculations category includes the simulation of titrations and analyses of data involving use of the formation function, the deprotonation function, the point–by–point estimation of single formation constant values, the calculation of analytical concentrations and the influence of experimental errors in the data.

ESTA 2 is the optimisation module, which enables values of formation constants, vessel and burette concentrations, electrode intercept and slope, and initial vessel volume to be refined by a least squares procedure, for which there is a choice of objective functions, namely EMF residuals or total electrode ion concentration residuals.

The other modules provide convenient means of manipulating data for a variety of purposes.

The ESTA programs are described in detail in the literature by the authors (43,44).

ESTA was used as it represents a significant advance over other optimisation programs, such as MINIQUAD (41) for the following reasons:

(i) ESTA allows a novel approach to be taken to the problem of species or model selection. The presence of various possible major and/or minor species can be tested for, on a titration point by titration point basis, by making use of the BETA task in the simulation module (ESTA 1). The value of a single possible species formation constant is optimised to produce agreement with the observed cell EMF at each titration point. Such calculations may be repeated for any number of postulated or trial species. Likely minor species can then be identified by searching for regions in the titrations where:

(a) a fairly constant value of log β is calculated at a significant number of consecutive titration points, provided that in this range the percentage formation of that complex is rapidly changing, and,

(b) where the postulated species is calculated to be present in significant amounts (between approximately 15 and 85%) and the percentage formation of that complex changes

rapidly.

When a new species is introduced into the model, the optimisation module–ESTA 2– can be used to optimise formation constants for all complexes, both major and minor species, assumed to be present. The entire procedure can then be repeated, starting with the BETA task in ESTA 1, to find the next candidate for inclusion in the model, and ending with an optimisation to incorporate the new member fully into the model. A flow chart showing the sequence of steps involved in model selection is presented in Figure 4.7. The process can continue until the fit between experimental and calculated data (as defined by the value of the objective function or the R–factor) can no longer be improved significantly. In the above situation good agreement between observed and calculated formation function and deprotonation function plots, will also be expected.

(ii) A sophisticated weighting procedure is used to allow for the propagation of random experimental errors, on the objective function used for least squares optimisation. This was felt to be an important consideration in the present study, which involved measurements made on solutions with reagent concentrations in the sub–millimolar region.

(iii) The likely effect of experimental errors on the reliability of the models proposed and the associated formation constants, can be investigated directly using the data simulation capabilities of the program.

(iv) ESTA, unlike MINIQUAD, allows for refinement of titration parameters such as cell calibration constants and reagent concentrations as well as formation constants. This facility must be used with discretion.

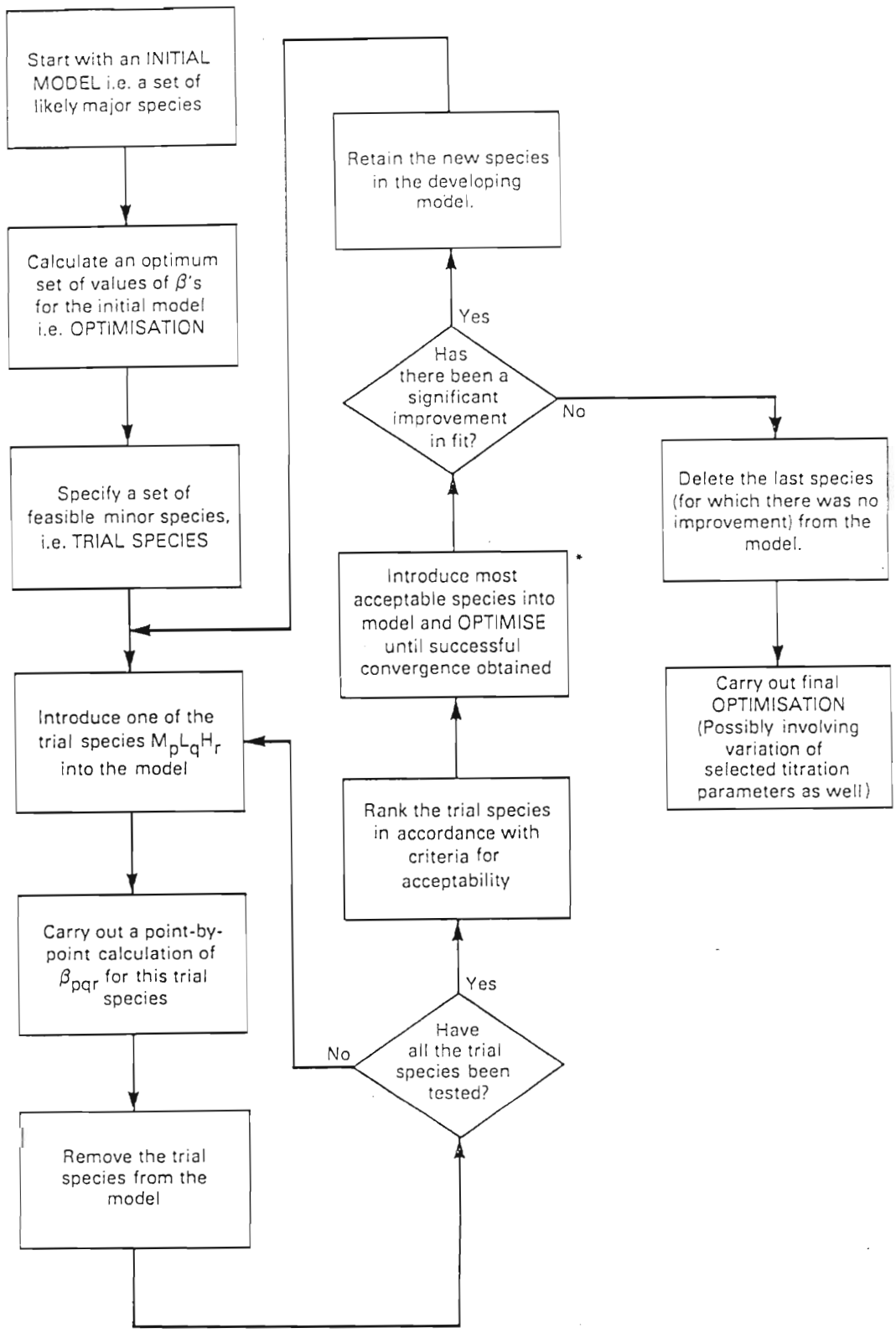

*Occasionally it may be found that the "best" of the trial species is not accepted into the model at the optimisation stage. If so, try the next best trial species etc. until one is accepted (i.e. leads to successful convergence).

Figure 4.7: A flowchart showing the sequence of steps involved in model selection.

(v) The program allows corrections to be made for changes in ionic strength, by using the extended Debye–Hückel expression for calculation of activity coefficients. This feature can be useful for investigations in which for some reason, reagent concentrations become comparable (some 10% or more) to the concentration of background electrolyte.

(vi) The formation constant optimisation is carried out using the optimisation module of the program, which uses numerical methods that are rapid and robust.

Optimisation is carried out with respect to the objective function, U, using task OBJE of the optimisation module. U is given by:

$$U = \frac{1}{N-n_p} \sum_{n=1}^{N} W_n (E_n^{obs} - E_n^{calc})^2 \quad ,$$

where

N = number of experimental points

n_p = number of parameters simultaneously optimised

E_n^{obs} = observed electrode potential at the n^{th} data point

E_n^{calc} = the calculated electrode potential (from the model) at the n^{th} data point

W_n = the weighting factor, obtained from the formula

$$W_n = \left[\left[\frac{\delta(E_n^{obs} - E_n^{calc})}{\delta V} \right]^2 \sigma^2_V + \left[\frac{\delta(E_n^{obs} - E_n^{calc})}{\delta E_n^{obs}} \right]^2 \sigma^2_E \right]^{-1} \quad ,$$

where σ_V and σ_E represent the estimated random errors in the titre volumes and electrode potentials, chosen as 0.01 cm^3 and 0.1 mV respectively. The derivatives are evaluated analytically.

(vii) ESTA has excellent graphical capabilities which facilitate production of plots of observed and calculated formation and deprotonation functions.

CHAPTER FIVE

CELL CALIBRATION

In this study, the glass electrode potentiometric method was employed to measure protonation and metal–ligand formation constants. In the glass electrode potentiometric method, hydrogen ion concentrations are determined experimentally, in order to provide information about other chemical species, which occur in the test solution. It is therefore very important that the glass electrode system is calibrated correctly and accurately, as this will affect the determination of the hydrogen ion concentration.

Despite, or perhaps as a result of the accuracy required in measuring the hydrogen ion concentrations, considerable differences exist in the way in which glass electrode systems are calibrated (74). Many investigators still employ buffer solutions of specific pH values for cell calibration in the determination of formation constants. This method is unsatisfactory in metal–ligand equilibrium studies owing to,

(i) the difficulties involved in relating pH values to hydrogen ion activities (74),

(ii) the fact that the formation constants then obtained involve a mixture of concentrations and activities (75), and

(iii) the value of the junction potential term E_j, see equation (5.5), in the calibrating buffer solutions may differ appreciably from the value appropriate to the test solutions (76).

A cell calibration technique employed by many researchers who employ potentiometric methods to measure formation constants, is to use solutions of known hydrogen ion concentrations (74,77). This is often done by titrating strong acid solutions with strong alkali solutions and plotting the cell equilibrium EMF at each titration point against the corresponding values of $\log_{10}[H^+]$, where $[H^+]$ denotes the free hydrogen ion concentration. The procedure aims to obtain a linear calibration

curve for the electrode system. Variation to this method exists, in which the ligand rather than the hydroxide ion is used as the base (72,74), this method could be described as the strong acid–weak base calibration method.

Some rather sophisticated methods have been developed that allow for the values of the ligand pK_a to be refined simultaneously with refinement to the glass electrode parameters (74).

5.1 THE EMF OF CELLS HAVING A GLASS–INDICATING ELECTRODE

The electrochemical cell used in this study consisted of a test solution surrounding a glass electrode and in electrical contact with a reference electrode through a salt bridge. The cell can be represented as follows:

$$(-)\ \mathrm{RE} \;\Big|\; \underset{p}{\mathrm{SB}} \;\Big|\; \underset{\ell}{\text{test solution}} \;\Big|\; \text{glass electrode}\ (+) \quad ,$$

where

RE = reference electrode
= $Ag/AgC\ell/0.01$ mol dm^{-3} $C\ell^-$, 0.09 mol dm^{-3} $C\ell O_4^-$, 0.10 mol dm^{-3} Na^+.

SB = salt bridge = 0.10 mol dm^{-3} $NaC\ell O_4$.

ℓ represents the liquid junction at the interface between the salt bridge and the test solution.

p represents the liquid junction at the interface between the salt bridge and the reference electrode.

The equilibrium EMF of electrochemical cells involving electrochemical species in solution, is primarily a function of the activities of the electrochemical species and therefore also of the activity coefficients and concentrations of these species. When the composition of the equilibrium solution is varied, the EMF of the cell varies.

In the cell used in this study there are four contributions to the measurable potential difference between the glass electrode and reference electrode. One arises from the reference electrode. The potential of the reference electrode is independent of the composition of the test solution and so may be represented as a fixed potential, E_{ref}. The glass indicating electrode contributes to the measurable potential difference between the glass electrode and the reference electrode. E_g represents the potential of the glass indicating electrode. The potential differences generated across the boundaries p and ℓ will depend on the activities of all the chemical species on either side of them. These boundary potentials are represented by E_p and E_ℓ. E_p is unaffected by changes in the test solution and should remain constant. The measured EMF of the cell is given by the equation:

$$E_{cell} = E_{ref} + E_p + E_\ell + E_g \quad . \tag{5.1}$$

Equation (5.1) can be simplified to give (79);

$$E_{cell} = E_{ref} + E_j + E_g \quad , \tag{5.2}$$

where, E_j is the sum of the junction potentials generated across the liquid boundaries between the reference electrode and salt bridge solutions and the salt bridge and test solutions.

The potential difference across a junction, J, is given by (80):

$$E_J = \frac{-RT}{F} \int_1^2 \sum_i \frac{T_i}{z_i} \, d \ln c_i \gamma_i \quad , \tag{5.3}$$

where,

R represents the gas constant.

T represents the absolute temperature.

F represents Faraday's constant.

z_i represents the charge number of the i^{th} ionic species.

T_i represents the transport number of the ion i.

c_i represents the concentration of ions i in mol dm^{-3}.

γ_i represents the concentration scale activity coefficient of ion i.

1 and 2 represent the bulk solutions between which the boundary is formed.

Glass electrodes, in general, are found experimentally to exhibit a Nernstian or near Nernstian response over a range of concentrations, provided that the solutions are buffered with respect to the concentration or activity of hydrogen ions (77). Therefore equation (5.2) may be written as:

$$E_{cell} = E_{ref} + E_g^0 + \frac{RT}{F} \ln a_H + E_j \quad , \tag{5.4}$$

where

E_g^0 is the glass electrode potential at unit activity of hydrogen ions.

a_H represents the hydrogen ion activity.

As long as ionic strength of the test solution remains constant, thereby holding activity coefficients fairly constant, the activity of free hydrogen ions, a_H, should be proportional to concentration. Thus by collecting together all the constants, equation (5.4) may be written as (61,74,77–81):

$$E_{cell} = E_{cell}^{0\prime} + k \log[H^+] + E_j \quad , \tag{5.5}$$

where

E_{cell} represents the cell potential for a cell containing a glass indicating electrode.

$E_{cell}^{0\prime}$ represents a constant, which depends *inter–alia* on the activity coefficient of the ions present, which are presumed to be constant at constant ionic strength. It is usually determined *in–situ* during each titration in acid solution.

E_j represents the sum of the liquid junction potentials generated across the junction separating the reference electrode filling solution from the salt bridge, and the junction separating the salt bridge from the test solution. The former junction potential

should remain constant during the course of a titration, whereas the latter contribution may well change as the composition of the test solution changes during the titration. In order to keep E_j more or less constant through a titration, the concentration of the inert background electrolyte must be much higher than the concentrations of reagent ions, particularly ions of high mobility such as H^+ and OH^-. In practice, this places limitations on the degree to which one may approach the two extremes of the pH scale while still maintaining linearity of the E_{cell} *vs* $\log[H^+]$ plot.

k represents a constant (termed the "electrode calibration slope") which generally has a value close to (but usually somewhat lower than) that expected from the Nernstian term, i.e. 2.3026 RT/F.

$[H^+]$ represents the concentration of free (uncomplexed) hydrogen ions in solution.

The form of equation (5.5) is the form that is appropriate to use of the glass electrode as a concentration probe (as distinct from an activity probe).

The liquid junction potentials in the cell should be kept as constant as possible during the course of a titration and preferably also as small as possible. These conditions can be achieved by making up all solutions used in the experiment to the same ionic strength, by using the same inert background electrolyte. The concentration of the inert background electrolyte must be much higher than the concentrations of the reagent ions, particularly ions of high mobility, such as H^+ and OH^- ions, so that E_J remains more or less constant, even though the concentrations of the reagent ions may change during the titration. This ensures that the solutions on both sides of the junction have the same ionic strength, thus keeping E_J as small as possible and also keep E_J as constant as possible because as the experiment proceeds, the ionic composition of the solutions change negligibly by comparison.

The quantity of inert background electrolyte required to make up a solution to the required ionic strength can be obtained with the aid of the following equation:

$$I = \tfrac{1}{2} \sum_i c_i z_i^2 \quad , \tag{5.6}$$

where

I represents the ionic strength of a solution.

i represents the i^{th} ionic species.

c_i represents the concentration of the i^{th} species in moℓ dm^{-3}.

z_i represents the charge number of the i^{th} ionic species.

When E_j is held constant, it can be incorporated with $E^{0'}_{cell}$, so that equation (5.5) can be rewritten as (74):

$$E_{cell} = E^0_{cell} + k \log[H^+] \quad . \tag{5.7}$$

If the two solutions on either side of the junction contain appreciably different concentrations of ions, particularly ions of high mobility, it may not be possible to incorporate the junction potential term into the constant E^0_{cell} as indicated above. In such situations the value of E_j is best determined experimentally as a function of the composition of the solution (78).

A limitation to the usefulness of equation (5.5) rests in the fact that reliable cell EMF's can only be measured in cells of this kind when the solution is reasonably well buffered with respect to hydrogen ions or hydroxide ions – either as a result of concentration buffering or the existence of equilibria in solution which can readily generate or absorb these species. Thus, for example, it has been noted (74,82) that a linear E_{cell} *vs* $\log[H^+]$ response can only be obtained in the narrow ranges $2.3 < p[H] < 2.9$ and $10.8 < p[H] < 11.8$, where p[H] represents $-\log[H^+]$, when solutions of strong acid and strong alkali are used as calibrants. The ligand itself can be used together with strong acid as a calibrant (72,74), in which case calibration points can be obtained at values of p[H] in the vicinity of the value/s of the pK_a of

the ligand. In metal–ligand–hydrogen ion systems the solution p[H] may lie well outside the range over which calibration points are obtainable. It is virtually universally assumed by workers in this field that calibration equations of type shown in equation (5.5) can be used in circumstances of this kind to interpolate/extrapolate into such regions. It is the view of the author that for applications in which precision of measurement is critical

(i) the cell should be calibrated *in situ* at the beginning of each potentiometric titration in order to avoid undue disturbance of the liquid junctions during electrode transfer, cell rinsing etc.

(ii) calibration procedures involving use of strong acid calibrants only, together with an assumption of Nernstian electrode response, are unacceptable.

(iii) strong acid–strong base calibration, with determination of the electrode calibration slope k is acceptable provided measurements are made within or between the p[H] ranges in which the response is shown to be linear. In the non–linear region of p[H] $\leq$ 2.3 or p[H] $\geq$ 11.8, the dependence of E_j on $[H^+]$ must be determined experimentally.

(iv) calibration procedures involving strong acid, strong base and ligand solution (a weak base, usually) are probably the best, at least in principle. In practice such procedures can be extremely time–consuming. Considering the unpredictable time–dependence of $E^{0\prime}_{cell}$, very lengthy titrations are to be avoided if possible. Some workers (83) deal with the problem of time–consuming calibration procedures by carrying out a full cell calibration only occasionally, and carrying out a one point check on a daily basis to monitor daily changes in $E^{0\prime}_{cell}$. Naturally, by this procedure, *in situ* calibrations are not possible.

Irrespective of what reagents are used or p[H] ranges covered in the calibration step, cell calibration generally requires evaluation of various adjustable parameters appearing in, or implicit in, the electrode equation. These can include

some or all of the following quantities:–

(i) the calibration "intercept" $E^{0\prime}_{cell}$,

(ii) the calibration slope k,

(iii) any parameter required to describe the dependence of E_j on $[H^+]$, e.g. ionic conductances of species in the test and bridge solutions if the Henderson equation is used (84) or a simplified form of that equation,

(iv) the value of the ionic product of water K_w, which is used to calculate values of $[H^+]$ from analytical values of $[OH^-]$ when excess sodium hydroxide is used as a calibrant,

(v) Some authors (70) advocate the introduction of additional terms in the electrode equation to take account of changing concentrations of interfering ions in solution. This involves the introduction of ion–selectivity coefficients as additional parameters,

(vi) In some highly sophisticated calibration procedures reported recently (74,85) the concentrations of some or all of the reagents used in the calibration experiment can be optimised (varied slightly) to produce an improvement of fit to the electrode equation. Interestingly, the above authors seem to insist that the electrode slope k must be set at the Nernstian value. In practice however, the electrode slope k and the ionic product of water K_w and to a lesser extent the concentration of the calibrant solutions used, are strongly correlated so that deviations of the slope k from the Nernstian value can be neatly incorporated into the optimised values of K_w and the reagent concentrations. The actual values produced by this technique for quantities like K_w should be treated with some circumspection.

5.2 METHOD OF CALCULATING THE FREE HYDROGEN ION CONCENTRATION

In potentiometric titration studies using glass electrodes, the value of the free hydrogen ion concentration, $[H^+]$, is very important for calculation purposes. The value of $[H^+]$ in a strong acid–strong base titration is affected by the concentrations of the acid and hydroxide solutions used and any impurities present

in these solutions, which will interfere with the acid–hydroxide equilibrium at a given titration point. Dissolved carbonate in the hydroxide solution is an example of an impurity, which will affect the value of $[H^+]$. In this study, despite the many precautions taken, (see Section 2.1.2 and 3.1), the sodium hydroxide solutions used were found to contain varying amounts of dissolved carbonate impurity (at the 1% – 5% level). Owing to the protonation equilibria

$$H^+ + CO_3^{2-} \rightleftharpoons HCO_3^-$$
$$H^+ + HCO_3^- \rightleftharpoons H_2CO_3 \rightleftharpoons H_2O + CO_2$$

the presence of carbonate impurities will affect the calculated value of $[H^+]$ during strong acid–strong base titrations. Since the total carbonate concentration can be estimated by Gran plots of the data obtained in the calibration titrations (59–61,63), it is possible to correct for the effect of carbonate on the calculated value of $[H^+]$.

Since the reaction vessel was well flushed with N_2 during the calibration titration it was assumed that

(i) at p[H] values less than 10, all CO_3^{2-} in the system is flushed out of the system by virtue of the equilibria

$$CO_3^{2-} + H_2O \rightleftharpoons 2OH^- + CO_2\uparrow \qquad (5.8)$$

or

$$CO_3^{2-} + 2H^+ \rightleftharpoons H_2O + CO_2\uparrow \qquad (5.9)$$

being driven essentially completely to the right within the time scale of the measurements (72), with consequent generation of two moles of OH^- or removal of two moles of H^+ per mole of CO_3^{2-} originally present,

(ii) at p[H] values of greater than 10, the remaining CO_3^{2-} (in the instance of titration of acid with alkali), or the CO_3^{2-} originally present (in the instance of

titration of alkali with acid) is involved in the equilibrium

$$CO_3^{2-} + H_2O \rightleftharpoons HCO_3^- + OH^- \qquad (5.10)$$

the effect of which can be calculated from a knowledge of the corresponding equilibrium constant.

The selection of p[H] = 10 as the cut–off point in this procedure is a practical if somewhat arbitrary measure (72) and is subject to an uncertainty of ~ 0.5 pH unit. The error incurred as a result of this uncertainty is however second order and negligible in these experiments. In retrospect, it is perhaps advisable not to flush the solution continuously with N_2 when sodium hydroxide is used as titrant or titrate, and pH values of 10 or higher are involved!

The value of $[H^+]$ for various points during a strong acid–strong base titration were calculated in the following manner:

(i) When a solution containing background electrolyte and acid is titrated with a sodium hydroxide solution containing some dissolved carbonate, CO_3^{2-}, the initial data points are below a p[H] value of 10. As mentioned above, below a p[H] value of 10 and in the presence of an N_2 gas stream, all the carbonate added to the titrate will be converted to carbon dioxide, CO_2 (see equation (5.8) and (5.9)). The equilibria are driven to the right by constant removal of CO_2 in the N_2 gas stream. This means that for every CO_3^{2-} ion present, two H^+ ions would be used to form a water molecule, so the value of $[H^+]$ would be decreased by the presence of CO_3^{2-} ions in the hydroxide titrant. Therefore below a p[H] value of 10, twice the carbonate concentration, $[CO_3^{2-}]$, has to be deducted from the total hydrogen ion concentration, H_T, to obtain the true value of $[H^+]$. In this study, when carbonate was present in the hydroxide titrant and the p[H] value was below 10, $[H^+]$ was calculated using the

following equation:

$$[H^+] = \frac{V_A[H^+]_A - V_B[OH^-]_B - 2(V_B[CO_3^{2-}]_B)}{V_T} \qquad (5.11)$$

$$= \frac{V_A[H^+]_A - V_B[BASE]_B}{V_T} \quad , \qquad (5.12)$$

where

V_A = Volume of acid titrate.

$[H^+]_A$ = Initial concentration of acid in the titrate.

V_B = Volume of titrant added.

$[OH^-]_B$ = Concentration of hydroxide ion in titrant.

$[CO_3^{2-}]_B$ =Concentration of carbonate ion in titrant.

V_T = Total volume in reaction vessel.

$[BASE]_B$ = Total concentration of base in the titrant obtained from the Gran plot method.

$= [OH^-]_B + 2[CO_3^{2-}]_B$.

When a solution containing background electrolyte and acid is titrated with a hydroxide solution containing some dissolved carbonate, and sufficient titrant has been added to reach a p[H] value of 10, the carbonate added subsequently will remain in solution. In this study at p[H] values equal to 10 and above, the values of $[H^+]$ were calculated using the computer program HALTAFALL (73), so that the effect of the carbonate was accounted for. The computer program data file was set up by treating the titrant volume that gave a p[H] value of 10, as the beginning point of a titration, such that at this point $V_{TITRANT} = 0$, $[CO_3^{2-}]_{TITRATE} = 0$ and $[OH^-]_{TITRATE} = \frac{V_A[H^+] - V_X[BASE]_B}{V_{TX}}$,

where

V_X = Volume of titrant added to reaction solution to get a p[H] value equal to 10.

V_{TX} = Total volume in reaction vessel at the point where the p[H] = 10.

Treating the data in the p[H] region of 10 and above as a separate titration when using HALTAFALL, instead of combining it with the acid data points allows the CO_3^{2-} added to the titrate in the p[H] region below 10 to be totally lost from the system, and not to be considered in the calculation of $[H^+]$ for points above a p[H] value of 10.

(ii) When a solution containing background electrolyte and hydroxide which contains dissolved CO_3^{2-} is titrated with an acid solution, the initial points will be above a p[H] value of 10. In this study the computer program HALTAFALL was used to calculate the value of $[H^+]$ for points equal to or above a p[H] value of 10, so that the effect of the presence of dissolved CO_3^{2-} could be accounted for.

At p[H] values of less than 10, when sufficient hydrogen ions are present, all the carbonate present in the reaction solution would be converted to CO_2 gas and removed from the system in the N_2 gas stream. The value of $[H^+]$ for points below a p[H] value of 10 was calculated using equation (5.11).

Using the methods described in this section to obtain values of $[H^+]$ at each titration point in the cell calibration procedure, the effect of CO_3^{2-} present in the hydroxide solutions was corrected for.

5.3 CHECK FOR LINEARITY OF ELECTRODE RESPONSE

A number of experiments were carried out at a temperature of 25.0^0C and an ionic strength of 0.10 moℓ dm^{-3} in order to check for linearity of electrode response, i.e. to check that E_{cell} varies linearly with p[H], in accordance with

equation (5.7). This is tantamount to determining the range/s of p[H] values in which the junction potential term E_j is effectively a constant, and the solutions are sufficiently concentration buffered to produce reliable cell EMF readings (see Section 5.1). The experiments described in this section also gave an indication of the order of concentrations of acid and hydroxide solutions that could be used for cell calibration purposes.

The ionic strength of all solutions used in these experiments were made up to 0.10 moℓ dm^{-3} by the use of $NaCl\ell O_4$ as inert background electrolyte.

The experiments, in this section, were carried out in two ways:

(i) A known volume of $NaCl\ell O_4$, (0.10 moℓ dm^{-3}), was titrated with volume increments of $HCl\ell O_4$ solutions of known hydrogen ion concentrations. A sequence of $HCl\ell O_4$ titrant solutions of increasing $HCl\ell O_4$ concentration was used. The concentration of the titrant ranged from about 1.0 x 10^{-3} moℓ dm^{-3} to about 7.5 x 10^{-2} moℓ dm^{-3}. In these runs the cell EMF was recorded using two glass electrodes, a RADIOMETER G202B, (low sodium ion error electrode), and a RADIOMETER G202C electrode. Representative data are given in Table 5.1

(ii) A solution made up of a known volume of $NaCl\ell O_4$ (0.10 moℓ dm^{-3}) and a known volume of $HCl\ell O_4$ of known hydrogen ion concentration, was titrated with volume increments of sodium hydroxide solutions. A sequence of NaOH titrant solutions of decreasing hydroxide ion concentration was used. The hydroxide ion concentration of the titrant solutions ranged from about 1.0 x 10^{-2} moℓ dm^{-3} to about 1.0 x 10^{-3} moℓ dm^{-3}. The concentrations of the hydroxide solutions was determined by Gran's method, (see Section 4.1.3). A RADIOMETER G202B electrode

TABLE 5.1 Data obtained from the titration of $NaC\ell O_4$ (0.10 mol ℓ dm^{-3}) with acid solutions. (I = 0.10 mol ℓ dm^{-3}).

Conc. of hydrogen ions in the titrate, $[H^+]_o$, and titrant, $[H^+]_T$ and initial volume, V_o	Volume of titrant solution added. V/cm^3	p[H]	E_{cell}/mV (G202B)	(G202C)
$[H^+]_o$ = 0 mol ℓ dm^{-3}	2.00	4.41	−22.4	−4.4
	3.00	4.25	−4.9	+12.7
$[H^+]_T$ = 1.002 x 10^{-3} mol ℓ dm^{-3}	4.00	4.13	+4.3	+22.8
	5.00	4.04	+11.4	+29.8
V_o = 50.00 cm^3	6.00	3.97	+16.8	+35.1
	8.00	3.86	+24.8	+43.0
	9.00	3.82	+27.9	+46.0
	10.00	3.78	+30.6	+48.6
$[H^+]_o$ = 1.669 x 10^{-4} mol ℓ dm^{-3}	2.00	3.29	+61.4	+79.2
	4.00	3.08	+74.3	+92.0
$[H^+]_T$ = 1.075 x 10^{-2} mol ℓ dm^{-3}	5.00	3.01	+78.7	+96.4
	6.00	2.95	+82.4	+100.0
V_o = 60.00 cm^3	8.00	2.85	+88.1	+105.6
	9.00	2.81	+90.4	+107.9
	10.00	2.78	+92.5	+109.9
$[H^+]_o$ = 1.678 x 10^{-3} mol ℓ dm^{-3}	2.00	2.43	+111.9	+129.2
	4.00	2.25	+121.6	+138.8
$[H^+]_T$ = 7.522 x 10^{-2} mol ℓ dm^{-3}	5.00	2.18	+125.0	+142.2
	6.00	2.13	+127.9	+145.0
V_o = 70.00 cm^3	8.00	2.04	+132.3	+149.5
	9.00	2.00	+134.2	+151.2
	10.00	1.96	+135.7	+152.7

* Conc. = Concentration.

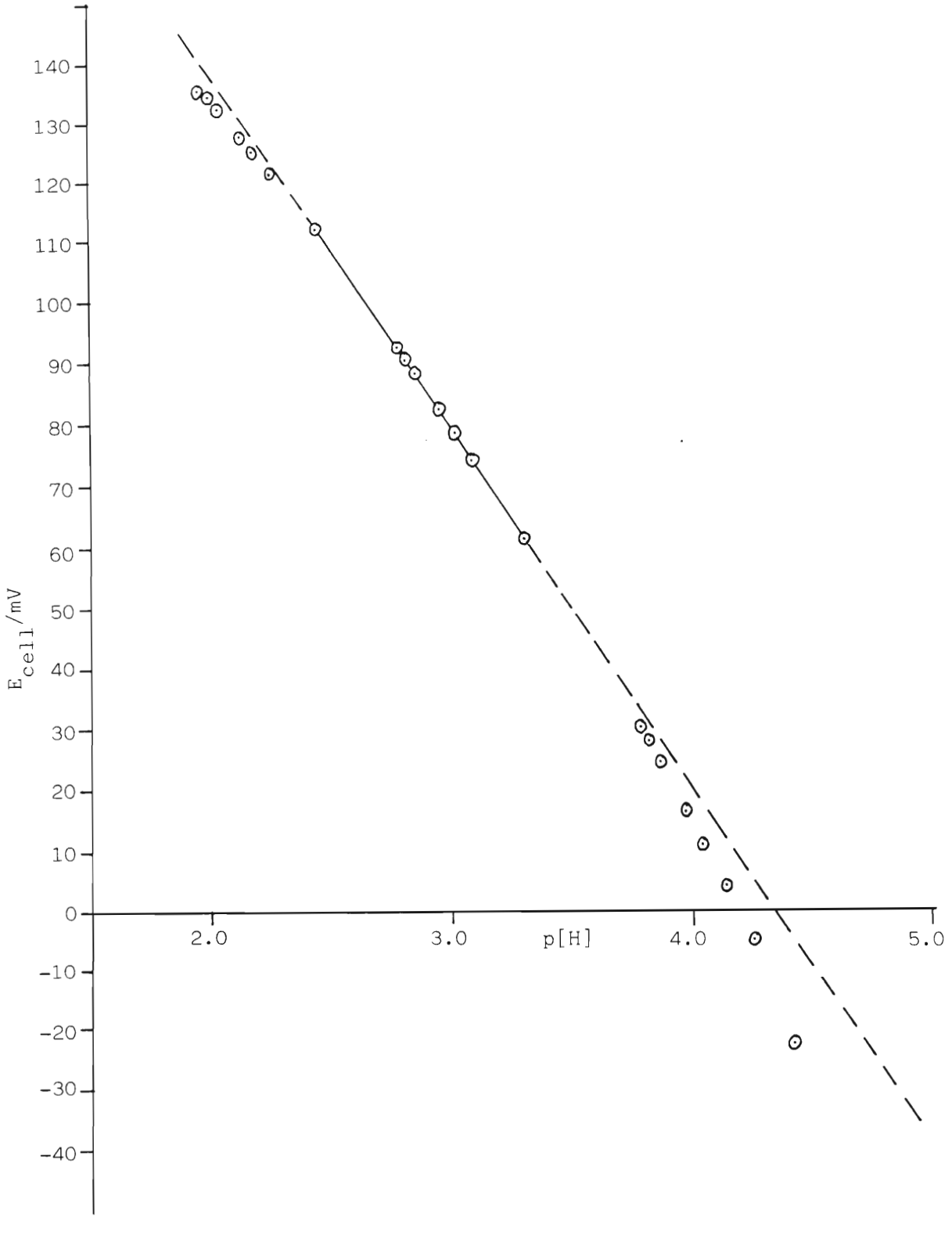

Figure 5.1: Plot of cell EMF as a function of p[H] obtained when a solution of background electrolyte is titrated with acid solutions.

was used in this series of experiments. Representative data are given in Table 5.2.

Plots of E_{cell} against p[H], for the two kinds of titrations described are shown in Figures 5.1 and Figure 5.2 respectively. Only one set of data from each method was plotted for the sake of clarity.

From the results given in Table 5.1 and shown in Figure 5.1 it is concluded, that when a glass electrode is calibrated by titrating a $NaC\ell O_4$ (0.10 moℓ dm^{-3}) solution with acid solutions of increasing concentrations, as in this study, a linear E_{cell} against p[H] response is obtained in the region

$$2.4 \leq p[H] \leq 3.5 \quad .$$

Below this p[H] range, deviations can be attributed to changing values of E_j which are no longer negligible. Above this range, deviations can be attributed to inadequate concentration buffering in solutions that are very dilute in hydrogen ions (74,82).

The results in Table 5.2 and shown in Figure 5.2 confirm the results obtained by method (i). Additionally the results show that when a dilute acid solution, i.e. 3.0×10^{-4} moℓ dm^{-3} $HC\ell O_4$, is titrated with a dilute hydroxide solution, of about 1.0×10^{-3} moℓ dm^{-3}, the p[H] range can be extended to 4.0, in the low p[H] range. In the alkaline region the corresponding range appears to be $10.0 < p[H] < 11.5$.

The results of these experiments indicate that in order to obtain linear E_{cell} against p[H] responses in the strong acid–strong base calibration procedure, the concentration of the titrate and titrant solutions should be in the order of 1.0×10^{-2} moℓ dm^{-3}, before introduction into the reaction vessel.

Other authors (74,82) have found that the linear response occurs in the p[H] ranges of 2.3 to 2.9 and 10.8 to 11.8.

TABLE 5.2 Data obtained from the titration of a solution of background electrolyte and acid with hydroxide solutions. ($I = 0.10$ mol dm^{-3}).

Concentration of reactants in the titrate $[\ ]_o$, and titrant, $[\ ]_T$, and initial volume, V_o	Volume of titrant solution added V/cm^3	p[H]	E_{cell}/mV
$[H^+]_o = 1.689 \times 10^{-3}$ mol dm^{-3}	0.00	2.77	+91.5
	1.00	2.82	+89.0
$[OH^-]_T = 1.009 \times 10^{-2}$ mol dm^{-3}	2.00	2.87	+86.3
	3.00	2.92	+83.4
$V_o = 70.00$ cm^3	4.00	2.98	+80.1
	5.00	3.04	+76.3
	6.00	3.12	+72.0
	7.00	3.21	+66.9
	8.00	3.32	+60.6
	9.00	3.46	+52.3
$[H^+]_o = 3.463 \times 10^{-4}$ mol dm^{-3}	1.00	3.48	+51.1
	2.00	3.50	+49.9
$[OH^-]_T = 1.008 \times 10^{-3}$ mol dm^{-3}	4.00	3.55	+47.2
	6.00	3.60	+44.3
$V_o = 79.00$ cm^3	8.00	3.65	+41.2
	10.00	3.71	+37.8
	12.00	3.78	+34.0
	14.00	3.85	+29.8
	16.00	3.93	+25.0
	18.00	4.02	+19.3
	20.00	4.14	+12.3
	22.00	4.29	+ 3.2
	24.00	4.51	− 9.5
	26.00	4.96	−36.3

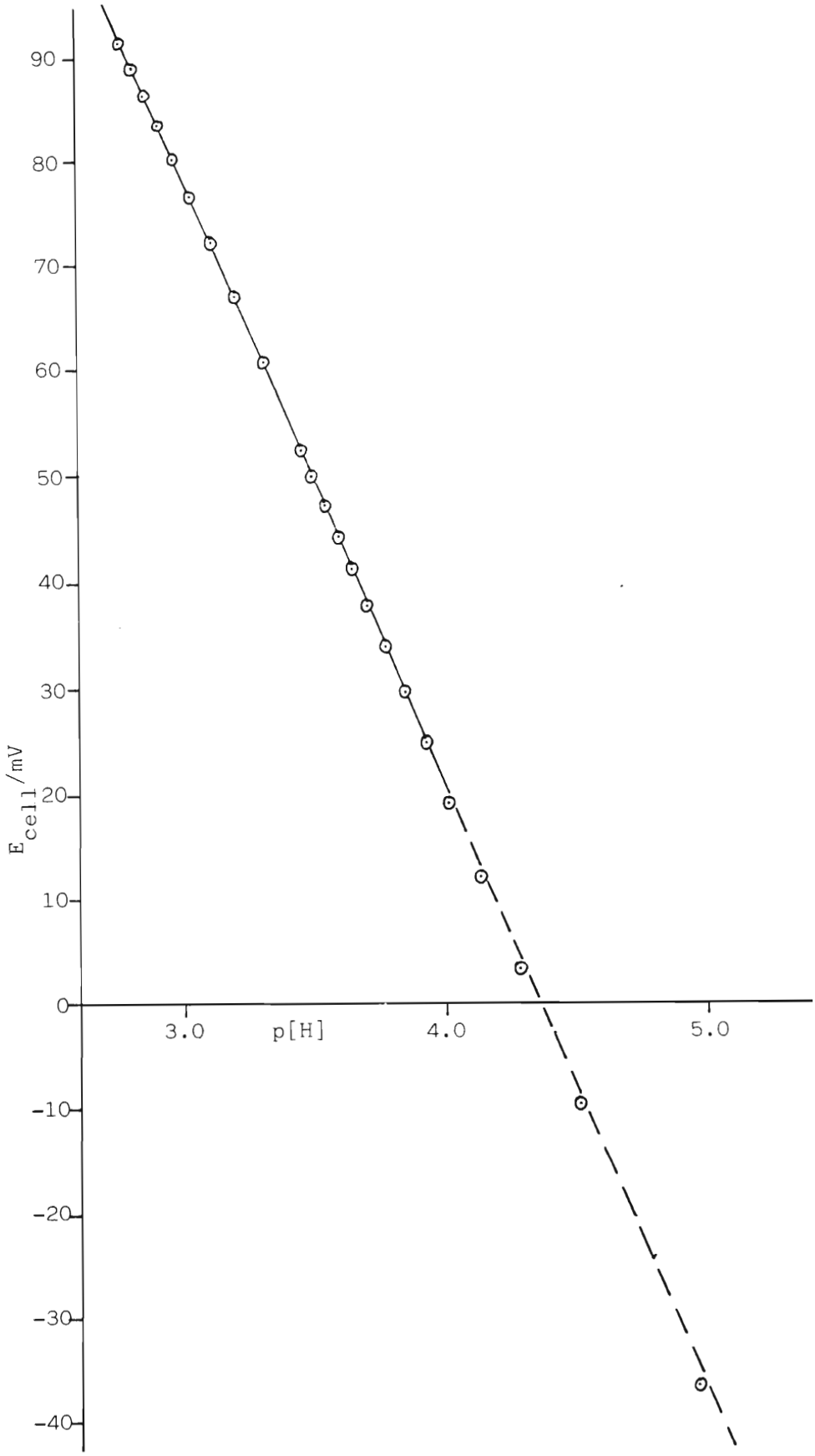

Figure 5.2: Plot of cell EMF as a function of p[H] obtained when a solution of background electrolyte and acid is titrated with hydroxide solutions.

5.4 METHODS OF CELL CALIBRATION USED IN THIS STUDY

In this study the glass electrodes were calibrated, *in situ*, at the beginning of each experimental titration. This was necessary as it is known that the standard potential of the glass electrode membrane varies from day to day and that it is difficult to reproduce liquid junction potentials with adequate precision (74).

In this study all the glass electrodes used were designated by a letter, so that the electrode used in an experiment could be identified. All solutions in this study were made up to an ionic strength of 0.10 mol dm^{-3} by using $NaClO_4$ as background electrolyte. Hydroxide and dissolved carbonate concentrations were determined *in situ* using Gran's method (see Section 4.1.3). All experiments were carried out at a temperature of 25.0^{0}C.

Two approaches were used to calibrate the glass electrodes in this study. The methods used were:

(i) The first method entailed titrating a solution containing background electrolyte and a strong base (approx 1 x 10^{-2} mol dm^{-3}) with a standardised solution of a strong acid (approx. 1 x 10^{-2} mol dm^{-3}). Depending on the solution p[H] value required at the end of the calibration stage of the experiment, the order of the titration was reversed, such that a solution containing background electrolyte and strong acid was titrated with a solution of a strong base. NaOH was used as the base and $HClO_4$ was used as the acid. In some titrations the concentration of the acid used was approximately 1 x 10^{-3} mol dm^{-3}.

The equilibrium cell EMF was recorded after addition of each increment of titrant. Equilibrium cell EMF values were recorded in both the high and low p[H] regions.

(ii) In the second method a similar procedure was adopted, except that more dilute acid solutions (approx. 1.0 x 10^{-3} mol dm^{-3}) were titrated with more dilute hydroxide solutions (approx. 1.0 x 10^{-3} mol dm^{-3}), to calibrate the glass electrodes.

Initially, the second method was used, because of the fear of generating large volumes of HCN(g), when NaCN was added to the reaction vessel, after the calibration procedure was completed.

The Gran plot method of equivalence point determination (see Section 4.1.3) was used to determine the concentration of the NaOH solution and that of any carbonate contamination present in it. The value of $[H^+]$, thus p[H] at each point during the titration was calculated as described in Section 5.2

The data from the two calibration methods were treated differently, as a consequence of the findings described in Section 5.3.

In the first calibration method, in which relatively concentrated acid and hydroxide solution were used, the equilibrium cell EMF, E_{cell}, values were plotted against the corresponding p[H] values, in both high and low p[H] regions, taking into account the findings described in Sections 5.2 and 5.3. A typical plot of E_{cell} against p[H], for the calibration of a glass electrode using perchloric acid and sodium hydroxide solutions, is shown in Figure 5.3. Representative data for the plot is given in Table 5.3. The values of the constants E^0_{cell} and k, required for equation (5.7) were obtained by doing a "least–squares" best fit calculation on the points lying on the linear part of the E_{cell} versus p[H] curve. Constant k was given by the gradient of the line and constant E^0_{cell} by the intercept of the line at p[H] = 0. For the data given in Table 5.3 and plotted in Figure 5.3, E^0_{cell} = 251.78 mV and k = 57.58 mV.

The above calibration method has the advantage that a wide range of p[H] values is spanned, i.e. the calibration procedure includes points both in the high and low p[H] regions, and E^0_{cell} and k can be obtained with greater accuracy than just using points from the low p[H] region.

For the second calibration method in which relatively dilute acid solutions were titrated with dilute hydroxide solutions, all data outside the p[H] region of 2.8 to 4.0 was discarded as they were found to lie outside the linear region (see Section 5.3). The value of the constant k was determined for each electrode by

TABLE 5.3 Data obtained when a cell containing a glass electrode is calibrated by titrating a solution containing background electrolyte and acid with a hydroxide solution. ($I = 0.10$ mol dm^{-3}).

Concentration of reactants in the titrate, $[\ ]_o$, and titrant, $[\ ]_T$, and initial volume, V_o	Volume of titrant solution added V/cm^3	p[H]	E_{cell}/mV
	0.00	2.88	+ 86.0
$[H^+]_o = 1.320 \times 10^{-3}$ mol dm^{-3}	2.00	3.03	+ 77.4
	3.00	3.12	+ 72.0
$[OH^-]_T = 9.990 \times 10^{-3}$ mol dm^{-3}	4.00	3.24	+ 65.4
	4.50	3.31	+ 61.3
$V_o = 57.00\ cm^3$	5.00	3.39	+ 56.6
	5.50	3.49	+ 50.9
	6.00	3.62	+ 43.6
	9.00	10.13	− 331.5
	9.50	10.25	− 338.4
	10.00	10.35	− 344.2
	11.00	10.49	− 352.2
	12.00	10.59	− 358.0
	13.00	10.67	− 362.6

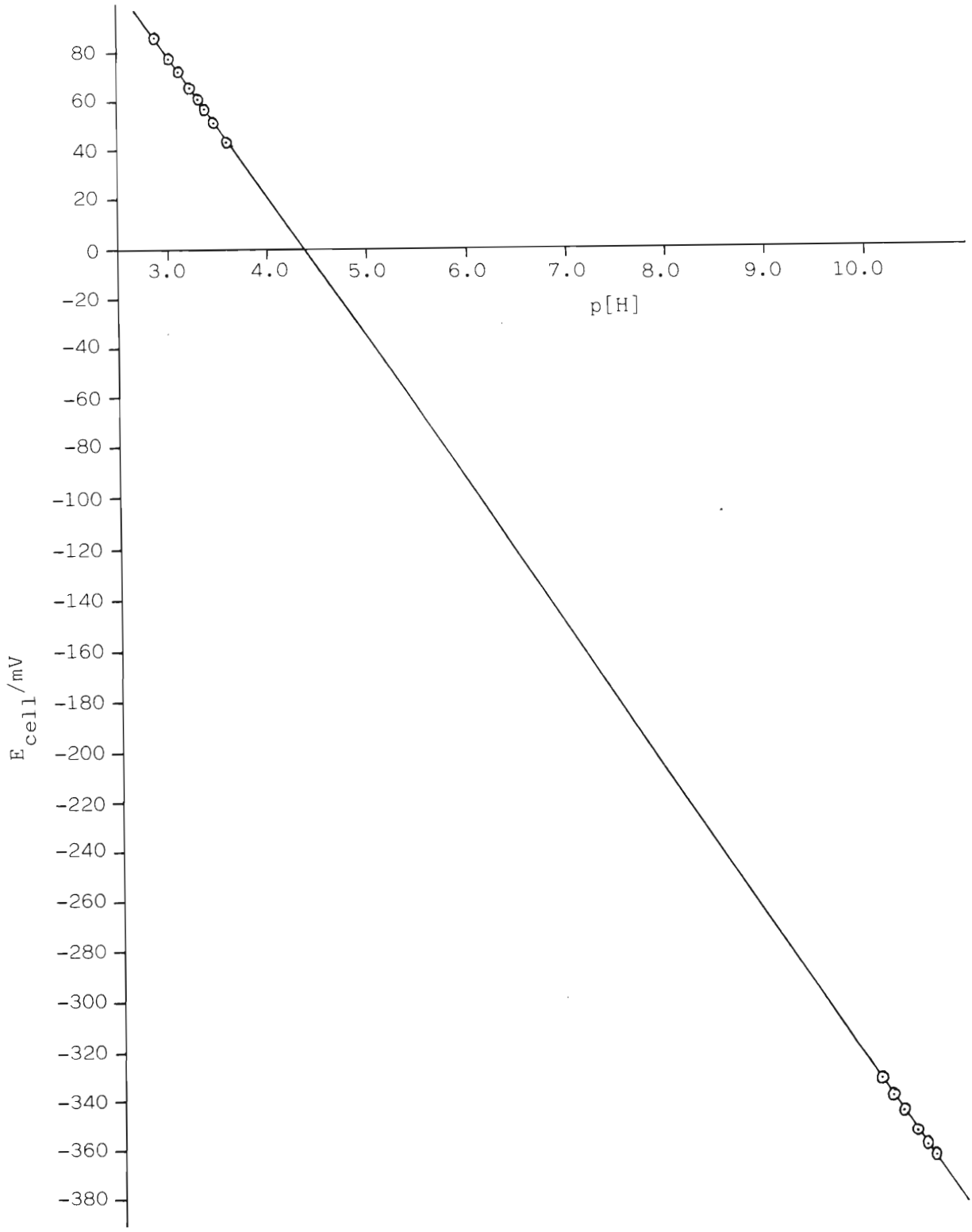

Figure 5.3: Plot of cell EMF as a function of p[H] when a cell containing a glass electrode is calibrated by titrating a solution of background electrolyte and strong acid with a strong base solution.

taking the mean of all k values obtained for that electrode, when it was calibrated using more concentrated acid and hydroxide solutions. The value of E^0_{cell} was obtained by solving equation (5.7) for E^0_{cell}, for each calibration data point in the p[H] range 2.8 to 4.0, making use of the value of k obtained as detailed above. The E^0_{cell} value for a particular calibration run was obtained by taking the mean of the E^0_{cell} values obtained for the data points in the p[H] range 2.8 to 4.0 for that particular run.

The methods used in this study for the determination of the calibration constants k and E^0_{cell} are felt by the author to be more accurate and justifiable than some methods that have been used in the glass electrode potentiometric field. The methods in question involve the assumption that glass electrodes behave in a Nernstian fashion and thus involve the assumption that k has a value of 59.16 mV at 25^0C. The value of E^0_{cell} is then obtained using a few points in the acid region.

5.5 CRITERIA FOR ATTAINMENT OF EQUILIBRIUM

The potentiometric titration method for determination of formation constants requires that electrochemical equilibrium be attained at each point during the titration. Thus, sufficient time must be allowed for:–

(i) the glass electrode to attain its equilibrium potential at any particular solution p[H],
(ii) chemical equilibrium to be attained in the test solution.

A criterion for equilibrium adopted in this study was that the cell EMF should remain constant (to ± 0.1 mV) for a minimum period of 5 minutes. To meet this condition, "equilibration" times varied from about 6 minutes per titration point at low p[H] values (p[H] = 6 or below) to about 90 minutes per point at high p[H] values (p[H] = 8 to 11). The latter period seemed rather long and suggests that chemical equilibrium may be approached slowly at high p[H] values – although glass electrodes are known to require long equilibration times at high p[H].

As a further test for attainment of equilibrium, the direction of the titration was occasionally reversed, i.e. after the total required volume of a sodium hydroxide titrant had been added, an acid titrant would then be used to lower the p[H] once again, in a step–wise fashion with cell EMF readings being taken at a number of intermediate points. If equilibrium had been attained at each titration point then calculated values of the formation function $\bar{Z}_H$ or $\bar{Z}_M$ (defined in Section 4.1.1) should have the same value for both "forward" and "reverse" titrations at any particular value of p[H] or log A respectively (also defined in Section 4.1.1). This test for attainment of equilibrium is valid provided that no polynuclear or hydrolysed complex species are formed.

CHAPTER SIX

SELECTION OF EXPERIMENTAL CONDITIONS

When investigating hydrogen ion–ligand, metal–ligand or metal–ligand–hydroxide ion systems, data should be collected over as wide a concentration range as possible, especially if, as in this potentiometric investigation, the concentration of only one of the reacting species, namely the free hydrogen ion, $[H^+]$, is measured.

When determining the concentration ranges to be covered in a medium of ionic strength 0.10 moℓ dm^{-3}, the following two factors were considered:

(i) If possible, each of the species likely to be formed should predominate at some stage during the potentiometric titration.

(ii) In the p[H] range covered, where $p[H] = -\log[H^+]$, the measured p[H] must be a sensitive function of the stability constants to be determined.

6.1 DETERMINATION OF THE PROTONATION CONSTANT FOR THE CYANIDE ION

The p[H] of the solution is a reasonably sensitive function of the protonation constant, pK_a, of a ligand when the p[H] lies in the region:

$$pK_a - 1 < p[H] < pK_a + 1 \quad .$$

From the reported pK_a values for cyanide (see Table 1.3), it can be assumed that the important p[H] region for the cyanide ion is between 8.0 and 10.5.

This investigation involved working over a wide p[H] range, particularly at high p[H] levels. It was decided, for safety reasons, not to work below a p[H] of 6, as this would lead to the generation of large quantities of hydrogen cyanide vapour, which would also introduce an error in the calculated concentration values for the hydrogen cyanide in solution, even when working in a sealed system.

Experiments were carried out using a DRAGËR gas detector and hydrogen cyanide–detecting tubes to estimate the hydrogen cyanide content of the vapour space above the test solution in the cell, at various p[H] levels. These showed that with the nitrogen flow turned off and at a p[H] of 6.7, approximately 0.14% of the total amount of hydrogen cyanide present was in the vapour phase. This percentage increased rapidly as the p[H] decreased.

It was decided to titrate an acid solution into a solution of cyanide, (CN^-), ligand having an initial p[H] value of approximately 9.6. The ligand solution was added to the cell after the calibration procedure had been completed.

Simulated titration runs in which reagent concentrations were varied, were carried out using HALTAFALL (73), in order to select reagent concentrations for experimental titrations. The following stability constants, obtained from the literature (86) and valid at 25^0C and I = 0.1 moℓ dm^{-3} were used as estimates in HALTAFALL.

$$\beta_{011} = 1.0233 \times 10^9$$
$$K_w = 1.6596 \times 10^{-14}$$

Table 6.1, below indicates the reagent concentrations used in HALTAFALL to calculate two sets of species distributions.

TABLE 6.1 Reagent concentrations used in HALTAFALL for simulated titrations involving the protonation of cyanide

Calculation No.	Conc. of cyanide in titrate /moℓ dm^{-3}	Hydrogen ion conc. in titrate /moℓ dm^{-3}	Conc. of cyanide in titrant /moℓ dm^{-3}	Hydrogen ion conc. in titrant /moℓ dm^{-3}
1	2.7×10^{-3}	6.7×10^{-4}	0.0	1.0×10^{-2}
2	2.5×10^{-3}	5.9×10^{-4}	0.0	1.0×10^{-2}

Conc. = Concentration.

The upper limit to the concentration of the acid solution that could be used in the titrations, was determined by the need to avoid large changes in the ionic strength during a titration.

The aim of these simulated titrations, using HALTAFALL, was also to determine whether the measured p[H] would be a sensitive function of the stability constant to be determined.

The formation curve for the hydrogen cyanide complex obtained from calculation No. 1 is shown in Figure 6.1. The sensitivity of the measured p[H] to changes in the hydrogen cyanide stability constant was tested by changing the logarithm of the constant, up and down by one log unit. HALTAFALL was used to obtain the p[H] change resulting from the change in the constant. The calculated p[H] values were plotted against the volume of titrant added. The plot for calculation 1 is shown in Figure 6.2. Since the digital voltmeter that was to be used was precise to ± 0.1 mV and 6 mV corresponds to a change of 0.1 of a p[H] unit, Figure 6.2 indicates that there should be no difficulty in determining the pK_a of cyanide, under the simulated conditions. This kind of calculation can of course only be usefully carried out if fairly good estimates for the desired stability constants are available.

6.2 DETERMINATION OF STABILITY CONSTANTS FOR THE FORMATION OF COMPLEXES OF Zn^{2+} WITH THE LIGAND CN^- AT LOW p[H]

When determining the stability constants for complex formation of Zn^{2+} and CN^-, it is possible to work over a fairly large pH range, because the Zn^{2+} does not hydrolyse readily (87–94). The hydrolysis reaction of Zn^{2+} can be represented by:

$$Zn^{2+} + nH_2O = Zn(OH)_n^{(2-n)+} + nH^+ \quad . \qquad (6.1)$$

This means that if hydrolysis occurs, a lower p[H] reading will be

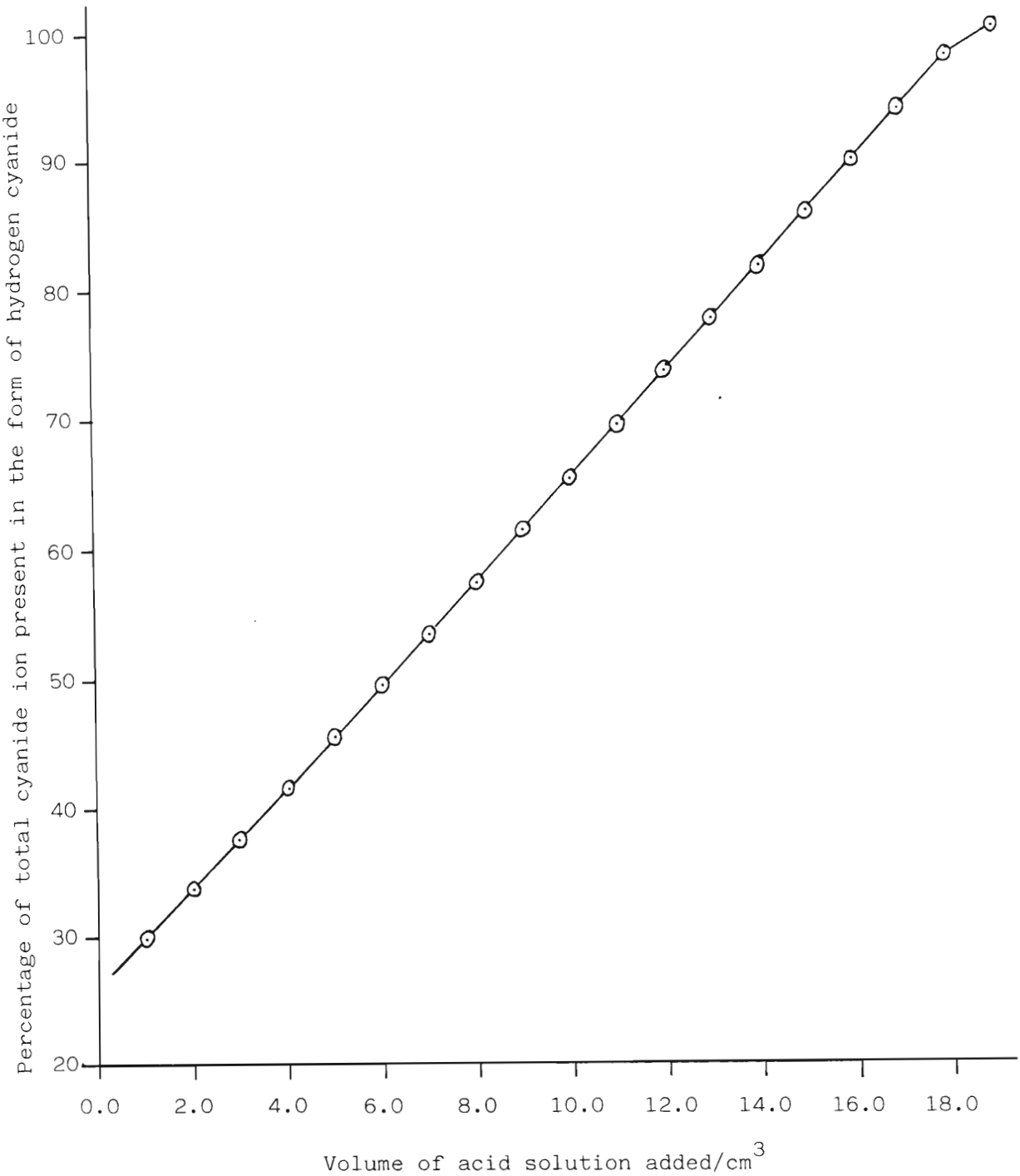

Figure 6.1 Plot illustrating the percentage of total cyanide ion present in the form of hydrogen cyanide, from calculation No. 1, at various volumes of acid solution added.

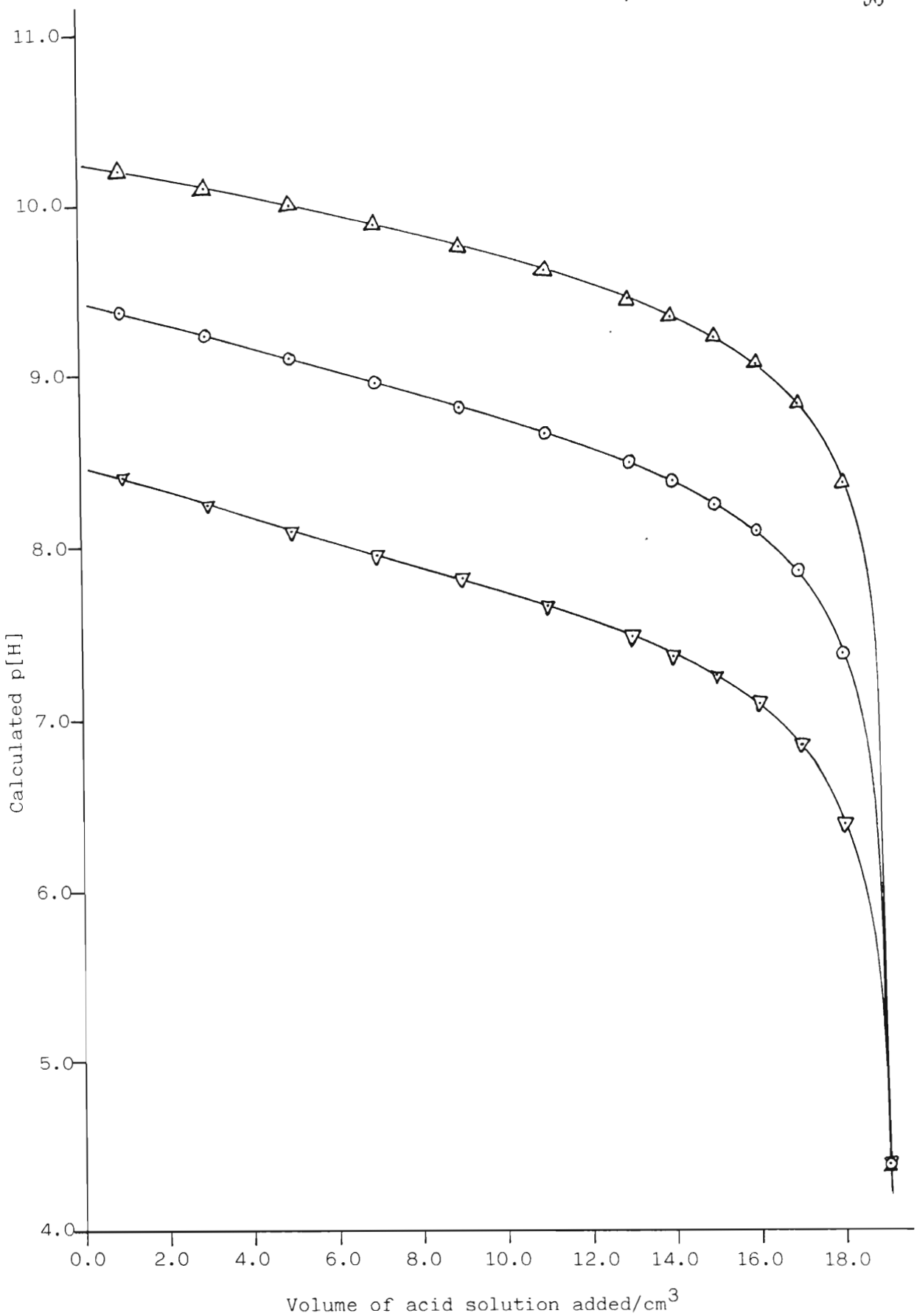

Figure 6.2: Solution p[H] calculated on the basis of various values of pK_a for cyanide in calculation No. 1. The points △ and ▽ indicate an increase and decrease of one log unit in log β_{011} respectively.

obtained than would have been the case in the absence of hydrolysis. A lower p[H] reading will also be recorded if any of the zinc cyanide complexes hydrolyse to form ternary complexes.

The proposed titrations to determine or check reported values (see Table 1.1) of the stability constants for the reactions of Zn^{2+} with CN^-, at various metal to ligand ratios, were based on work carried out by Persson (21). These titrations were carried out by titrating the zinc cyanide solution with acid solutions. Some of the initial experiments in this study were designed to maintain the total metal and total ligand concentrations constant throughout the runs, in order to facilitate a decision as to the presence or absence of polynuclear or ternary complexes. This was accomplished by the simultaneous addition of more than one titrant solution during a given titration.

Species distributions for the proposed Zn^{2+}/CN^- titrations were calculated using HALTAFALL, on the basis of the following constants (21);

$$\beta_{110} = 2.20 \times 10^{5}$$
$$\beta_{120} = 1.06 \times 10^{11}$$
$$\beta_{130} = 4.80 \times 10^{16}$$
$$\beta_{140} = 3.70 \times 10^{21}$$

and the solubility product, K_{so}, for $Zn(CN)_2$

$$K_{so}\ Zn(CN)_2 = 4.20 \times 10^{-16}\ (95)$$

All these constants were valid at 25^0C and I = 3.0 mol dm^{-3}. No β values were available for all four species at an ionic strength of 0.1 mol dm^{-3} at 25^0C.

The Zn^{2+} hydrolysis constants (86) and the K_{so} for $Zn(OH)_2$ (95) were also included in the HALTAFALL calculations, in order to ascertain whether any of the zinc hydroxide complexes would be formed in appreciable concentrations.

HALTAFALL calculations for the proposed titrations showed that the measured p[H] was sensitive to changes in the $Zn(CN)_n^{(2-n)+}$, (n = 1 to 4), stability constants, (see Figure 6.3), and so the glass electrode could be used in determining these stability constants.

Species distribution calculations for the proposed titrations using HALTAFALL, showed that the complexes should be formed in significant amounts. Figure 6.4 shows the species distribution plot for one of the proposed titrations.

The HALTAFALL calculations confirmed that for the p[H] range encountered in the proposed titrations, hydrolysis of Zn^{2+} should be insignificant.

6.3 DETERMINATION OF STABILITY CONSTANTS FOR THE FORMATION OF TERNARY COMPLEXES OF Zn^{2+} WITH LIGANDS CN^- AND OH^- AT HIGH p[H]

One of the aims of this investigation was to detect the formation of ternary complexes of the form $Zn(CN)_q(OH)_r$ if these are formed in solution. A potential problem arises from the fact that both the cyanide and hydroxide ions are quite strongly basic. The experimental method can only succeed if ligand replacement reactions such as

$$Zn(CN)_4^{2-} + OH^- \rightleftharpoons Zn(CN)_3(OH)^{2-} + CN^-$$

leads to a change in the p[H] of the solution that is large enough to be measured precisely with the procedure used. It is essential to know, at the outset, whether the proposed titrations can achieve the desired aim.

One way of assessing the viability of experiments such as these, is to estimate a realistic value for the logarithm of the formation constant log β of a ternary complex such as $Zn(CN)_3(OH)^{2-}$, and to calculate expected solution p[H] (or cell EMF) as a function of volume of titrant added. The estimated value of log β can then be changed by 1 log unit and the calculation repeated. The concentrations of

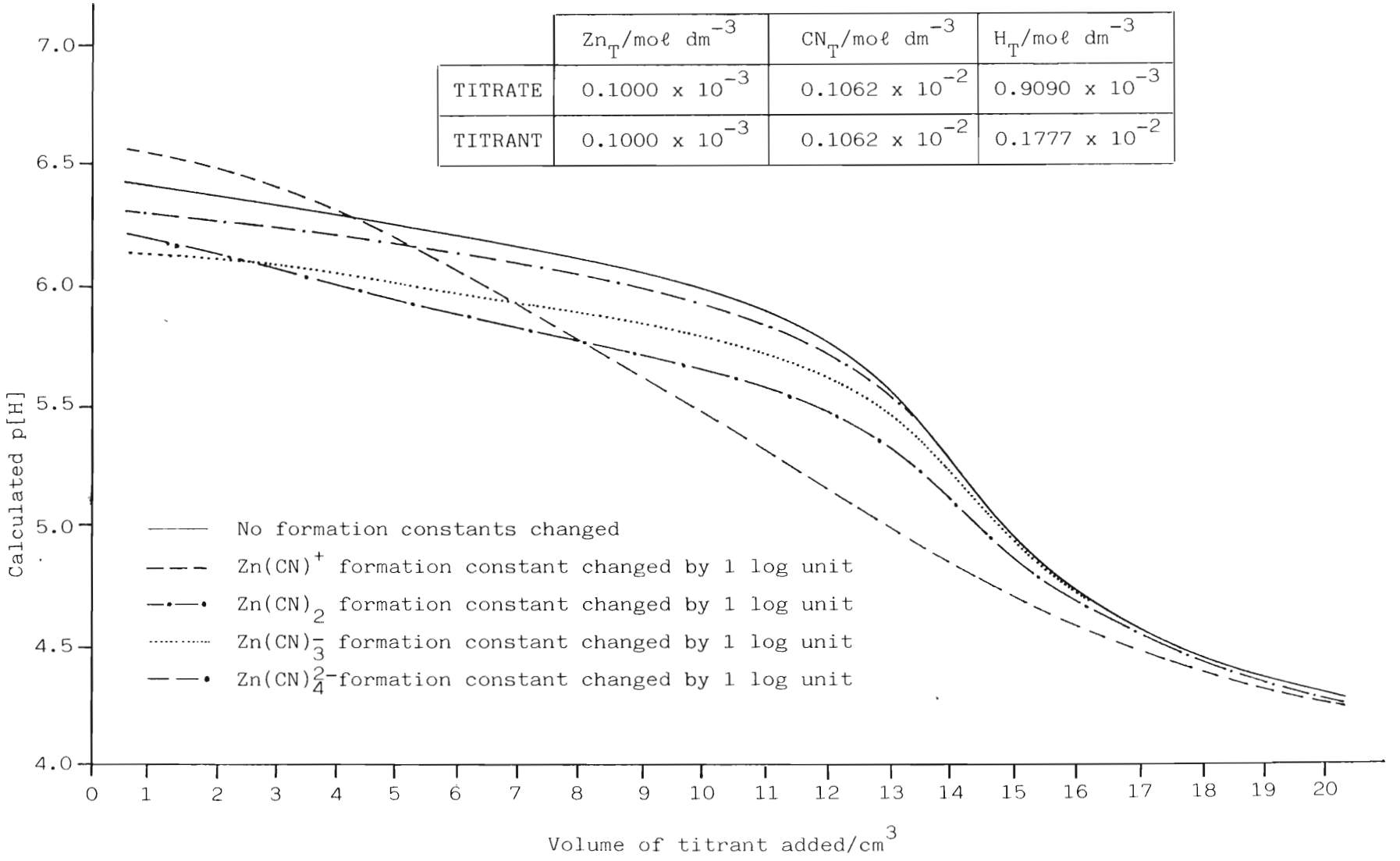

Figure 6.3: A plot of simulated potentiometric titration data in which is shown the effect of a 1 log unit change in the value of selected formation constants for various binary Zn-CN species on the observed cell EMF.

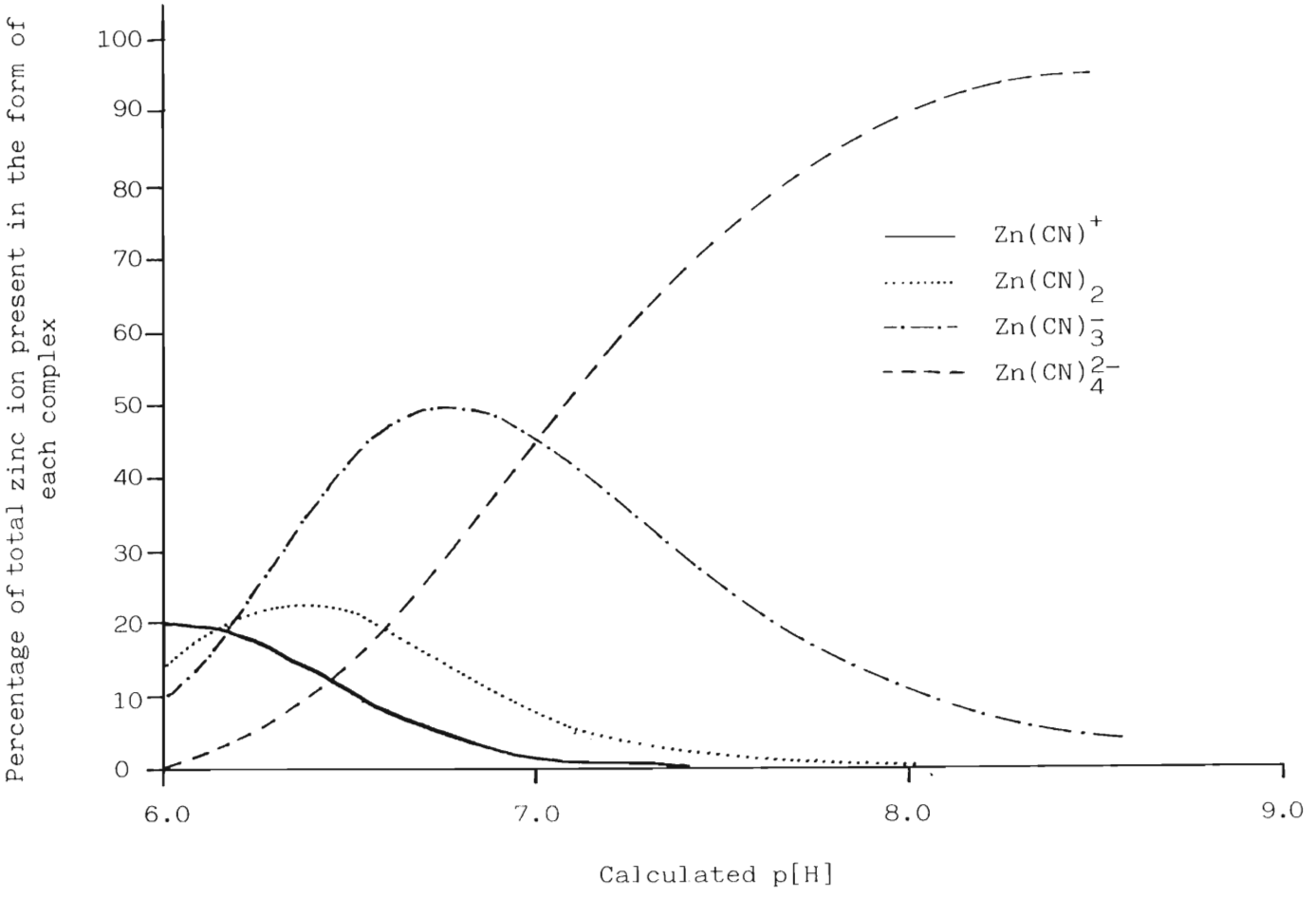

Figure 6.4: Speciation of $Zn(CN)_n^{(2-n)+}$, (n = 1 to 4), complexes as a function of calculated p[H], using simulated potentiometric titration data.

reagents used and the p[H] range covered must be such that the p[H] values predicted in these two titrations differ appreciably from one another.

These experimental runs involved titrating the zinc/cyanide solution in the cell with hydroxide instead of acid (see Section 6.2).

Before HALTAFALL could be used to calculate the species distribution for the proposed $Zn^{2+}/CN^{-}/OH^{-}$ titrations, it was necessary to estimate stability constant values for possible $Zn(CN)_q(OH)_r$ complexes, which could form at high p[H] values. There are a large number of methods of estimating stability constants (96–103). The estimation method used in this study was a statistical method proposed by V.S. Sharma and J. Schubert (96).

The estimated values for constants obtained by this method are given in Table 6.2.

TABLE 6.2 Stability constant values for mixed ligand complexes estimated using the statistical method proposed by V.S. Sharma and J. Schubert

$\log \beta_{14\text{-}1}$	22.6
$\log \beta_{13\text{-}2}$	21.2
$\log \beta_{13\text{-}1}$	19.6

The values obtained by the Sharma and Schubert method were used in conjunction with stability constants used in Section 6.2 to calculate the species distribution and sensitivity of the measured p[H] to changes in the stability constants for the relevant species.

A result for a typical simulated titration calculated by means of the HALTAFALL program is shown in Figure 6.5 It can be seen that an increase of 1 log unit in $\log \beta_{13\text{-}1}$ results in a predicted EMF decrease of approximately 0.15 p[H] units (or approximately 9 mV) over the titration. This is an acceptable, but by no means high, sensitivity of measured cell EMF on the value of $\log \beta_{13\text{-}1}$ – particularly

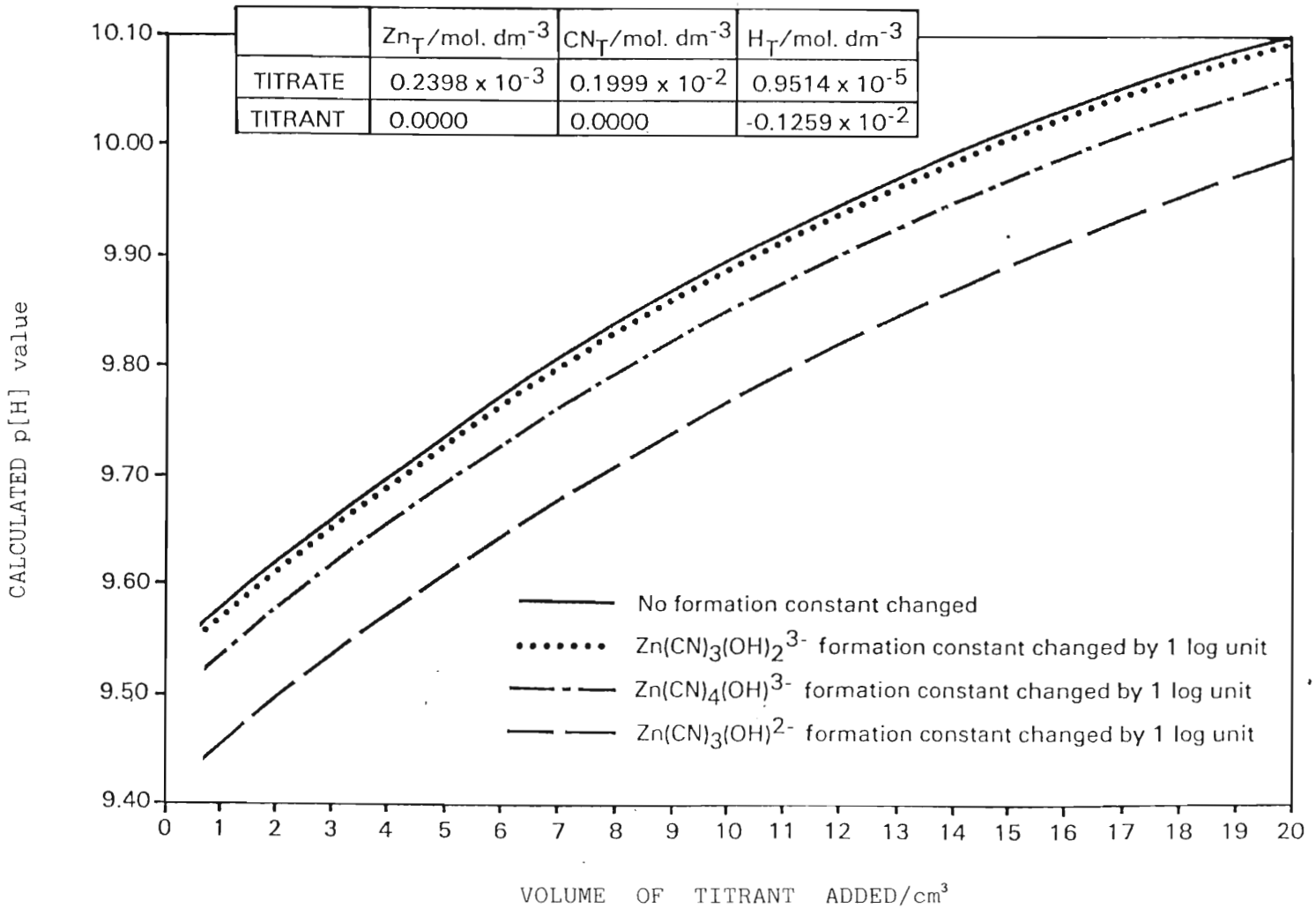

Figure 6.5: A plot of simulated potentiometric titration data in which is shown the effect of a 1 log unit change in the value of selected formation constants for various mixed ligand species on the observed cell EMF.

when it is borne in mind that it is possible that log $\beta_{13\text{-}1}$ may be correlated with another formation constant, say log β_{140}, that may be determined simultaneously. No allowance has been made in Figure 6.5 for correlation effects. The indications from Figure 6.5 are that, subject of course to the correctness of the estimates made, the proposed titration would not be useful for determining log $\beta_{13\text{-}2}$, either because the complex $Zn(CN)_3(OH)_2^{3-}$ does not form to any significant extent or because the solution p[H] is insensitive to formation of this species from other species in solution. Finally, it is clear that particular care should be taken to reduce experimental error (particularly errors of a systematic nature) as far as possible, if erroneous results or worse still "computer complexes" are to be avoided. Accordingly, care was taken to calibrate the glass electrodes correctly and accurately (see Section 5.4). Even so, the author feels that, owing to unavoidable diurnal variations in E^0_{cell} and the long duration of the titrations (up to 18 hours per titration), the reliability of E^0_{cell} values cannot be much better than $\pm$ 2 mV.

CHAPTER SEVEN

EXPERIMENTAL PROCEDURE AND DATA

This chapter describes the procedures and reports the experimental data for the potentiometric titrations, which were carried out in this study, for the determination of the protonation constant of cyanide and for the determination of the formation constants of the complexes formed by zinc and cyanide ions in aqueous solutions at moderately high p[H] values.

This study involved a series of potentiometric titrations which were carried out at a constant temperature of 25.0 ± 0.05^{0}C and employed $NaC\ell O_4$ as background electrolyte to adjust the ionic strength to 0.10 moℓ dm^{-3}.

The potentiometric apparatus was allowed to come to equilibrium over a period of approximately 2 hours after the first addition of calibrating titrant solution. After each subsequent addition of titrant solution, sufficient time was allowed to ensure that the system had come to equilibrium (see Section 5.5).

The solutions used in the titrations were prepared from stock solutions, the preparation of which are described in Chapter 2. The NaCN solutions were prepared freshly for each titration as described in Section 2.4. The hydroxide containing solutions were in some instances found to be contaminated with small quantities of carbonate impurity. The composition and concentrations of the components of the hydroxide containing solutions were determined *in situ*, using the Gran method (see Section 4.1.3).

The first step of every titration carried out in this study involved the *in situ* calibration of the cell, as described in Chapter 5. Values of the cell calibration constants E^0_{cell} and k varied appreciably from day to day. However, the calibration equation (5.7) was found to reproduce the calibration data to a precision typically of the order of 0.6 mV. It is therefore clear that although the cell EMF was measured to approximately 0.1 mV, the accuracy of the measurements is limited by the

accuracy of the calibration procedure and is probably around 0.5 to 1.0 mV.

The contents of the reaction vessel were flushed with nitrogen gas during the calibration step only. No flushing was carried out after addition of cyanide to avoid loss of volatile HCN from the system. The system was, however, kept sealed in the reaction vessel after flushing was discontinued.

The data from approximately half of the total number of titrations carried out in this study were rejected, on the grounds that the cell calibration method used in the early phase of the study involved use of dilute solutions of strong acid and produced data in the non–linear response region (see Section 5.3) of the glass electrode, and therefore, in retrospect was considered to be inadequate.

The titration procedures used in this study and the experimental data found to be useful for the purpose of this study are reported below.

The values quoted in Tables 7.1, 7.2 and 7.3, for E^0_{cell}, slope (k) and concentrations are the values used in the computations and are not to be taken as significant to the number of digits quoted.

7.1 DETERMINATION OF THE PROTONATION CONSTANT OF CYANIDE

The titration procedure and the experimental data for the determination of the protonation constant of cyanide are described in the following two sections.

7.1.1 Titration procedure

In this study, three potentiometric titrations were carried out in order to determine the protonation constant of cyanide at 25.0^{0}C and an ionic strength of 0.10 moℓ dm^{-3}.

The first step of every titration, was the *in situ* calibration of the cell. The cell calibration constants E^0_{cell} and slope (k) were calculated from the

calibration step data, as described in Section 5.4. The ligand protonation step was then carried out.

The cell calibration step was carried out by incrementally titrating an $HC\ell O_4$ solution of approximately 1.0 x 10^{-2} moℓ dm^{-3}, into a solution comprising 50.0 cm^3 $NaC\ell O_4$ (0.10 moℓ dm^{-3}) and a known volume of a hydroxide containing solution of approximately 1.0 x 10^{-2} moℓ dm^{-3}.

The ligand protonation titration, for the determination of the protonation constant for cyanide, was carried out by adding a known volume of a NaCN solution, of approximately 1.0 x 10^{-2} moℓ dm^{-3}, to the solution remaining in the reaction vessel, after completion of the calibration stage of the experiment. Following the addition of NaCN solution, the solution in the reaction vessel was titrated with an $HC\ell O_4$ solution of approximately 1.0 x 10^{-2} moℓ dm^{-3}. In titration number 3, the direction of titration was reversed by switching to a hydroxide titrant after completion of the titration with acid. The reversal of the titration direction was done in order to test for attainment of electrochemical equilibrium.

Below is a summary of the titration procedure used in this study for the determination of the protonation constant for cyanide:

CELL CALIBRATION STEP	50.0 cm^3 $NaC\ell O_4$ (0.10 moℓ dm^{-3}) 10.0 cm^3 NaOH (approx. 1.0 x 10^{-2} moℓ dm^{-3}) TITRATE WITH: AND TAKE CELL EMF READINGS 16.0 cm^3 $HC\ell O_4$ (approx. 1.0 x 10^{-2} moℓ dm^{-3}) N_2 GAS FLUSH: SWITCH OFF
PROTONATION CONSTANT DETERMINATION STEP	25.0 cm^3 NaCN (approx. 9.9 x 10^{-3} moℓ dm^{-3}) TITRATE WITH: AND TAKE CELL EMF READINGS 18.0 cm^3 $HC\ell O_4$ (approx. 1.0 x 10^{-2} moℓ dm^{-3}) TITRATE WITH: AND TAKE CELL EMF READINGS 10.0 cm^3 NaOH (approx. 1.0 x 10^{-2} moℓ dm^{-3}) [Reverse Titration]

[ ] : instructions.

The results obtained from the titrations were used to calculate the cyanide protonation constant using techniques described in Chapter 4.

7.1.2 Experimental data

The potentiometric titration data collected from the titrations described in Section 7.1.1 are presented in Table 7.1.

In Table 7.1, the description of each potentiometric titration performed in this section begins with the values for the cell calibration constants, E^0_{cell} and slope (k), obtained from the cell calibration stage of the titration, and the initial volume, V_o, of the titrate solution at the beginning of the cyanide protonation constant determination stage. Following the above data is a listing of the concentrations of the components in the titrate solution, denoted $[\,]_o$, and the titrant solution, denoted $[\,]_T$. Thus $[H]_o$ or $[H]_T$ refer to the total excess hydrogen ion concentration in the titrate and titrant respectively. A negative value of $[H]_o$ and $[H]_T$ represents excess hydroxide ion.

The concentration of the background electrolyte and ionic charges have been omitted for simplicity.

The description of the solutions is followed by a listing of the volume and cell EMF data and some derived quantities, such as $\bar{Z}_H$(obs) and p[H], for each point in the titration under discussion. The data for each titration point are presented as follows:

$$V_T,\ E_{cell},\ \bar{Z}_H(obs),\ p[H];\quad ,$$

where the titrant volume, V_T, and the cell EMF value, E_{cell}, are given in units of cm^3 and mV respectively. Data for the various points are separated by semi–colons.

TABLE 7.1 Experimental Data and Derived Quantities from Titrations for the Determination of the Protonation Constant for Cyanide, at 25.0°C and an Ionic Strength of 0.10 mol dm^{-3}.

Run 1:

E^0_{cell} = 254.3801 mV; Slope = 58.0844; V_o = 101.00 cm^3;
$[H]_o$ = 5.7721 x 10^{-4} mol dm^{-3}, $[CN]_o$ = 2.4545 x 10^{-3} mol dm^{-3},
$[H]_T$ = 9.9996 x 10^{-3} mol dm^{-3}, $[CN]_T$ = 0.0000 mol dm^{-3}.

0.00,	−301.70, 0.26, 9.574;	1.00,	−296.00, 0.30, 9.476;
3.00,	−287.30, 0.37, 9.326;	4.00,	−283.20, 0.41, 9.255;
6.00,	−275.30, 0.49, 9.119;	8.00,	−267.30, 0.56, 8.981;
10.00,	−258.90, 0.64, 8.837;	12.00,	−249.70, 0.72, 8.678;
14.00,	−238.20, 0.80, 8.480;	16.00,	−222.10, 0.88, 8.203;
18.00,	−187.50, 0.96, 7.608.		

Run 2:

E^0_{cell} = 253.1447 mV; Slope = 57.9327; V_o = 101.00 cm^3;
$[H]_o$ = 5.6968 x 10^{-4} mol dm^{-3}, $[CN]_o$ = 2.4545 x 10^{-3} mol dm^{-3},
$[H]_T$ = 9.9996 x 10^{-3} mol dm^{-3}, $[CN]_T$ = 0.0000 mol dm^{-3}.

0.00,	−301.50, 0.26, 9.574;	2.00,	−292.10, 0.33, 9.412;
4.00,	−283.70, 0.41, 9.267;	6.00,	−275.90, 0.48, 9.132;
8.00,	−267.90, 0.56, 8.994;	10.00,	−259.60, 0.64, 8.851;
12.00,	−250.40, 0.72, 8.692;	14.00,	−239.20, 0.80, 8.499;
16.00,	−223.40, 0.88, 8.226;	18.00,	− 190.80, 0.96, 7.663.

Run 3:

E^0_{cell} = 253.6948 mV; Slope = 58.0815; V_o = 89.00 cm^3;
$[H]_o$ = 6.6121 x 10^{-4} mol dm^{-3}, $[CN]_o$ = 2.8551 x 10^{-3} mol dm^{-3},
$[H]_T$ = 9.9996 x 10^{-3} mol dm^{-3}, $[CN]_T$ = 0.0000 mol dm^{-3}.

0.00,	−302.00, 0.25, 9.568;	2.00,	−292.40, 0.29, 9.402;
4.00,	−283.90, 0.40, 9.256;	6.00,	−276.10, 0.48, 9.122;
8.00,	−268.30, 0.55, 8.987;	10.00,	−260.20, 0.63, 8.848;
12.00,	−251.10, 0.71, 8.691;	14.00,	−240.00, 0.78, 8.500;
16.00,	−225.20, 0.86, 8.245;	18.00,	−196.10, 0.94, 7.744.

E^0_{cell} = 253.6948 mV; Slope = 58.0815; V_o = 107.00 cm^3;
$[H]_o$ = 2.2322 x 10^{-3} mol dm^{-3}, $[CN]_o$ = 2.3748 x 10^{-3} mol dm^{-3},
$[H]_T$ = −1.0160 x 10^{-2} mol dm^{-3}, $[CN]_T$ = 0.0000 mol dm^{-3}.

2.00,	−224.40, 0.86, 8.232;	4.00,	−239.90, 0.78, 8.498;
6.00,	−251.20, 0.70, 8.693;	9.00,	−264.70, 0.59, 8.925;
10.00,	−268.60, 0.55, 8.993;	12.10,	−276.60, 0.47, 9.130;
13.00,	−279.90, 0.43, 9.187;	15.00,	−284.50, 0.35, 9.266.

7.2 DETERMINATION OF FORMATION CONSTANTS FOR COMPLEXES FORMED BY ZINC AND CYANIDE IONS AT MODERATELY HIGH p[H] VALUES

The titrations described in this section were carried out to determine the formation constants for complexes formed by zinc and cyanide ions in aqueous solutions at moderately high p[H] values, a temperature of 25.0^0C and an ionic strength of 0.10 moℓ dm^{-3}.

The titration procedures and experimental data for twelve potentiometric titrations, carried out at various ligand: metal ratios and at various total (analytical) metal ion concentrations, are reported.

Table 7.2, shows the values of Zn_T and CN_T in the solution in the cell just prior to the acid or alkali titrant being added in order to strip ligand off from/add ligand onto the metal ion, these are termed initial values of Zn_T and CN_T. Table 7.2 also shows the ligand to metal ratios (expressed as the quotient CN_T/Zn_T), as well as the p[H] range covered, for the twelve potentiometric titrations considered in this part of the study.

Titration procedures and experimental data are reported separately (see Section 7.2.1 and 7.2.2).

7.2.1 Titration procedures

The titrations carried out in this section can be divided into two groups, namely,

(i) runs at intermediate p[H] values (3.5 – 10.0) and
(ii) runs at high p[H] values (9.3 – 11.2).

The grouping depends on the titrant initially used to strip the ligand from the metal ion.

TABLE 7.2. Initial values of Zn_T and CN_T, the ligand:metal quotient and p[H] ranges covered for titrations considered in this study.

Titration No. *	Zn_T/mol dm^{-3}	CN_T/mol dm^{-3}	CN_T/Zn_T	p[H] range
1B	2.9917×10^{-4}	2.9036×10^{-3}	9.7	9.0 → 7.5 → 9.1
1C	2.9917×10^{-4}	2.9036×10^{-3}	9.7	9.0 → 7.5 → 9.1
2B	1.0063×10^{-4}	1.6397×10^{-3}	16.3	8.6 → 4.8 → 7.9
3B	1.0063×10^{-4}	1.1082×10^{-3}	11.0	6.9 → 6.3
4B	7.1414×10^{-4}	4.2809×10^{-3}	6.0	9.8 → 7.2
5B	4.3409×10^{-4}	1.9126×10^{-3}	4.4	9.3 → 6.9
6B	2.5789×10^{-4}	5.1969×10^{-3}	20.2	10.0 → 4.0 → 6.1
7E	2.6636×10^{-4}	3.9965×10^{-3}	15.0	10.0 → 3.6
8B	2.5795×10^{-4}	1.1612×10^{-3}	4.5	9.4 → 9.8
9E	2.7131×10^{-4}	2.7177×10^{-3}	10.0	10.5 → 11.2 → 9.8
10E	2.8494×10^{-4}	2.8486×10^{-3}	10.0	10.7 → 11.3 → 9.4
11E	2.5795×10^{-4}	1.0518×10^{-2}	40.8	10.6 → 11.2

* The letters given with the run identifiers refer to the specific glass electrodes used (i.e. electrodes B, C and E).

The initial step of each titration was the *in situ* calibration of the cell (see Section 5.4), from which values for the cell calibration constants E^0_{cell} and k were obtained.

The cell calibration was carried out by one of two methods, either a solution of $HC\ell O_4$ of known concentration was titrated into a solution comprising 50.0 cm^3 $NaC\ell O_4$ (0.10 $mo\ell\ dm^{-3}$) and a known volume of a hydroxide solution of known concentration, or a hydroxide solution of known concentration was titrated into a solution comprising 50.0 cm^3 $NaC\ell O_4$ (0.10 $mo\ell\ dm^{-3}$) and a known volume of a $HC\ell O_4$ solution of known concentration. The calibration method used, was determined by the p[H] value required at the end of the cell calibration step.

Each titration in this section of the study is identified by a combination of a number and a letter. The numerical component identifies the titration, while the letter indicates the particular glass electrode used. Thus 4B indicates titration No. 4 in this series, carried out using glass electrode B (see Table 7.2).

The titration procedures used in the two groups of titrations are described below:

(i) <u>Runs at intermediate p[H] values (3.5 – 10.0):</u>

The titrations in this group were denoted 1B, 1C, 2B, 3B, 4B, 5B, 6B and 7E. Titration No. 1 in this series was monitored using two glass electrodes simultaneously, i.e. electrodes B and C.

In this group of titrations, $HC\ell O_4$ was used as titrant to strip the ligand from the metal ion. For titrations 1B, 1C, 2B and 6B the titrations were carried out in two stages, with hydroxide added as titrant after completion of titration with acid. This reversal of the titration direction was done in order to test for attainment of electrochemical equilibrium (see Section 5.5).

The titrations were carried out in two ways:

(a) The first titration method, which was used for titrations 1B, 1C, 2B and 3B, consisted of using a titrant which was a mixture of $Zn(C\ell O_4)_2$, NaCN and $HC\ell O_4$. The titrant solutions were added from three separate burettes, i.e. one for each solution. The titrant solution for the titration direction reversal was a mixture of $Zn(C\ell O_4)_2$, NaCN and a hydroxide solution. Each titrant solution was once again added from a separate burette. A summary of the procedure for the type of titrations described above is given below:

$50.0\ cm^3\ NaC\ell O_4\ (0.10\ mo\ell\ dm^{-3})$
$6.0\ cm^3\ NaOH$
TITRATE WITH: AND RECORD CELL EMFS
$13.0\ cm^3\ HC\ell O_4$
N_2 GAS FLUSH: SWITCH OFF
$5.0\ cm^3\ Zn(C\ell O_4)_2$ (approx. $4.7 \times 10^{-3}\ mo\ell\ dm^{-3}$)
$5.0\ cm^3$ NaCN (approx. $4.6 \times 10^{-2}\ mo\ell\ dm^{-3}$)
TITRATE WITH: AND RECORD CELL EMFS
$10.0\ cm^3\ Zn(C\ell O_4)_2$ (approx. $8.9 \times 10^{-4}\ mo\ell\ dm^{-3}$)
$10.0\ cm^3$ NaCN (approx. $8.7 \times 10^{-3}\ mo\ell\ dm^{-3}$)
$10.0\ cm^3\ HC\ell O_4$ (approx $1.0 \times 10^{-2}\ mo\ell\ dm^{-3}$)
TITRATE WITH: AND RECORD CELL EMFS
$10.0\ cm^3\ Zn(C\ell O_4)_2$ (approx. $8.9 \times 10^{-4}\ mo\ell\ dm^{-3}$)
$10.0\ cm^3$ NaCN (approx. $8.7 \times 10^{-3}\ mo\ell\ dm^{-3}$)
$10.0\ cm^3$ NaOH (approx. $1.0 \times 10^{-2}\ mo\ell\ dm^{-3}$)

(b) The second titration method, which was used for titrations 4B, 5B, 6B and 7E, involved the use of only $HC\ell O_4$ as the titrant. The direction of the titration 6B was reversed after the acid addition, by using a hydroxide titrant. A summary of the procedure for the type of titration

described above is shown below:

50.0 cm^3 $NaC\ell O_4$ (0.10 $mo\ell\ dm^{-3}$)
10.0 cm^3 $HC\ell O_4$
TITRATE WITH: AND RECORD CELL EMFS
15.0 cm^3 NaOH
N_2 GAS FLUSH: SWITCH OFF
10.0 cm^3 $Zn(C\ell O_4)_2$ (approx. 2.4×10^{-3} $mo\ell\ dm^{-3}$)
10.0 cm^3 NaCN (approx. 4.9×10^{-2} $mo\ell\ dm^{-3}$)
TITRATE WITH: AND RECORD CELL EMFS
12.0 cm^3 $HC\ell O_4$ (approx. 1.0×10^{-2} $mo\ell\ dm^{-3}$)
TITRATE WITH: AND RECORD CELL EMFS
10.0 cm^3 NaOH (approx. 1.0×10^{-2} $mo\ell\ dm^{-3}$)

The experimental data for titrations 1B, 1C, 2B, 3B, 4B, 5B, 6B and 7E are given in Section 7.2.2.

(ii) Runs at high p[H] values (9.3 – 11.2)

The titrations in this group were denoted 8B, 9E, 10E and 11E. These titrations involved the use of an excess of hydroxide over any acid that may have been present at the end of cell calibration and resulted in attainment of p[H] values as high as 11.3 (see Table 7.2).

The cell calibration for the titrations, in this group, was carried out by titrating the solution in the reaction vessel, which consisted of 50.0 cm^3 $NaC\ell O_4$ (0.10 $mo\ell\ dm^{-3}$) and a known volume of $HC\ell O_4$ of known concentration, with a hydroxide solution of known concentration.

Following the calibration step known volumes of $Zn(C\ell O_4)_2$ and NaCN of known concentrations were added to the reaction vessel. The solution in the reaction vessel was titrated with a hydroxide solution.

For titrations 9E and 10E, the direction of the titration was subsequently reversed by addition of $HC\ell O_4$.

A summary of the procedure for the type of titrations carried out in this section is given below:

50.0 cm^3 $NaC\ell O_4$ (0.10 $mo\ell\ dm^{-3}$)
7.0 cm^3 $HC\ell O_4$
TITRATE WITH: AND RECORD CELL EMFS
12.0 cm^3 NaOH
N_2 GAS FLUSH: SWITCH OFF
5.0 cm^3 $Zn(C\ell O_4)_2$ (approx. 4.6 x 10^{-3} $mo\ell\ dm^{-3}$)
10.0 cm^3 NaCN (approx. 2.3 x 10^{-2} $mo\ell\ dm^{-3}$)
TITRATE WITH: AND RECORD CELL EMFS
18.0 cm^3 NaOH (approx. 1.0 x 10^{-2} $mo\ell\ dm^{-3}$)
TITRATE WITH: AND RECORD CELL EMFS
10.0 cm^3 $HC\ell O_4$ (approx. 1.0 x 10^{-2} $mo\ell\ dm^{-3}$)

The experimental data for titrations 8B, 9E, 10E and 11E are given in Section 7.2.2.

7.2.2 Experimental data

The cell calibration constants, E^0_{cell}, the slope (k) and the initial volume (V_o) are presented for each titration in Table 7.3, together with the solution concentrations. The volume and cell potential data are listed for each point in the titration under discussion. In Table 7.3 subscripts (o) refers to the titrate and (T) refers to the titrant. [H] refers to the total excess hydrogen ion concentration in solution. A total excess hydroxide ion concentration, in solution, is indicated by a negative value of [H].

The hydroxide solutions used in this study were often contaminated by carbonate ions, thus $[CO_3]_o$ refers to the total excess carbonate ion concentration in

solution and $[CO_3]_T$ to the total carbonate ion concentration contained in the hydroxide titrant solution.

The concentrations of the background electrolyte and ionic charges are omitted for simplicity.

The data for each titration point for runs 1B, 1C, 2B and 3B are presented as follows:

$$V_T(\text{zinc}),\ V_T(\text{cyanide}),\ V_T(\text{acid/hydroxide}),\ E_{cell}\ ,\ .$$

The zinc, cyanide and acid titrant solutions were added from three separate burettes (see Section 7.2.1).

The data for each titration point for the remaining experimental runs are presented as follows:

$$V_T(\text{acid/hydroxide}),\ E_{cell}\ ;\ .$$

The titrant value, V_T, and cell EMF value, E_{cell}, are given in units of cm^3 and mV respectively. Data for the various points are separated by semi–colons.

TABLE 7.3 Experimental Data from Titrations for the Determination of Formation Constants for Complexes formed by Zinc and Cyanide Ions at 25.0°C, an Ionic Strength of 0.10 mol dm^{-3} and Moderately High p[H] Values.

Run 1B:

E^0_{cell} = 251.0853 mV; Slope = 58.1010; V_o = 79.70 cm^3;
$[Zn]_o$ = 2.9917 x 10^{-4} mol dm^{-3}, $[CN]_o$ = 2.9036 x 10^{-3} mol dm^{-3},
$[H]_o$ = 9.1700 x 10^{-4} mol dm^{-3}, $[CO_3]_o$ = 0.0000 mol dm^{-3},
$[Zn]_T$ = 8.9915 x 10^{-4} mol dm^{-3}, $[CN]_T$ = 8.7402 x 10^{-3} mol dm^{-3},
$[H]_T$ = 1.3079 x 10^{-2} mol dm^{-3}, $[CO_3]_T$ = 0.0000 mol dm^{-3}.

0.00,	0.00,	0.00,	−274.20;
1.00,	1.00,	1.00,	−266.80;
2.00,	2.00,	2.00,	−259.30;
3.00,	3.00,	3.00,	−251.90;
4.00,	4.00,	4.00,	−244.20;
6.00,	6.00,	6.00,	−227.30;
8.00,	8.00,	8.00,	−207.80;
10.00,	10.00,	10.00,	−184.90.

E^0_{cell} = 251.0853 mV; Slope = 58.1010; V_o = 109.70 cm^3;
$[Zn]_o$ = 2.9932 x 10^{-4} mol dm^{-3}, $[CN]_o$ = 2.9063 x 10^{-3} mol dm^{-3},
$[H]_o$ = 1.8585 x 10^{-3} mol dm^{-3}, $[CO_3]_o$ = 0.0000 mol dm^{-3},
$[Zn]_T$ = 8.9915 x 10^{-4} mol dm^{-3}, $[CN]_T$ = 8.7402 x 10^{-3} mol dm^{-3},
$[H]_T$ = −1.8254 x 10^{-2} mol dm^{-3}, $[CO_3]_T$ = 3.0800 x 10^{-4} mol dm^{-3}.

2.00,	2.00,	2.00,	−222.30;
4.00,	4.00,	4.00,	−244.60;
6.00,	6.00,	6.00,	−258.70;
8.00,	8.00,	8.00,	−270.00;
10.00,	10.00,	10.00,	−279.80.

Run 1C:

E^0_{cell} = 264.6729 mV; Slope = 58.8629; V_o = 79.70 cm^3;
$[Zn]_o$ = 2.9917 x 10^{-4} mol dm^{-3}, $[CN]_o$ = 2.9036 x 10^{-3} mol dm^{-3},
$[H]_o$ = 9.1700 x 10^{-4} mol dm^{-3}, $[CO_3]_o$ = 0.0000 mol dm^{-3},
$[Zn]_T$ = 8.9915 x 10^{-4} mol dm^{-3}, $[CN]_T$ = 8.7402 x 10^{-3} mol dm^{-3},
$[H]_T$ = 1.3079 x 10^{-2} mol dm^{-3}, $[CO_3]_T$ = 0.0000 mol dm^{-3}.

0.00,	0.00,	0.00,	–264.80;
1.00,	1.00,	1.00,	–257.60;
2.00,	2.00,	2.00,	–249.90;
3.00,	3.00,	3.00,	–242.30;
4.00,	4.00,	4.00,	–234.70;
6.00,	6.00,	6.00,	–217.70;
8.00,	8.00,	8.00,	–198.20;
10.00,	10.00,	10.00,	–174.80.

E^0_{cell} = 264.6729 mV; Slope = 58.8629; V_o = 109.70 cm^3;
$[Zn]_o$ = 2.9932 x 10^{-4} mol dm^{-3}, $[CN]_o$ = 2.9063 x 10^{-3} mol dm^{-3},
$[H]_o$ = 1.8585 x 10^{-3} mol dm^{-3}, $[CO_3]_o$ = 0.0000 mol dm^{-3},
$[Zn]_T$ = 8.9915 x 10^{-4} mol dm^{-3}, $[CN]_T$ = 8.7402 x 10^{-3} mol dm^{-3},
$[H]_T$ = –1.8254 x 10^{-2} mol dm^{-3}, $[CO_3]_T$ = 3.0800 x 10^{-4} mol dm^{-3}.

2.00,	2.00,	2.00,	–212.30;
4.00,	4.00,	4.00,	–235.10;
6.00,	6.00,	6.00,	–249.40;
8.00,	8.00,	8.00,	–261.10;
10.00,	10.00,	10.00,	–270.90.

Run 2B:

E^0_{cell} = 249.3130 mV; Slope = 57.8828; V_o = 79.00 cm^3;
$[Zn]_o$ = 1.0063 x 10^{-4} mol dm^{-3}, $[CN]_o$ = 1.6397 x 10^{-3} mol dm^{-3},
$[H]_o$ = 9.3949 x 10^{-4} mol dm^{-3}, $[CO_3]_o$ = 0.0000 mol dm^{-3},
$[Zn]_T$ = 3.0239 x 10^{-4} mol dm^{-3}, $[CN]_T$ = 4.9196 x 10^{-3} mol dm^{-3},
$[H]_T$ = 1.0069 x 10^{-2} mol dm^{-3}, $[CO_3]_T$ = 0.0000 mol dm^{-3}.

0.00,	0.00,	0.00,	−250.00;
1.00,	1.00,	1.00,	−237.90;
2.00,	2.00,	2.00,	−223.80;
4.00,	4.00,	4.00,	−181.20;
5.00,	5.00,	5.00,	−157.80;
6.00,	6.00,	6.00,	−141.30;
7.00,	7.00,	7.00,	−130.20;
8.00,	8.00,	8.00,	−120.90;
9.00,	9.00,	9.00,	−110.00;
11.00,	11.00,	11.00,	−26.30.

E^0_{cell} = 249.3130 mV; Slope = 57.8828; V_o = 112.00 cm^3;
$[Zn]_o$ = 1.0068 x 10^{-4} mol dm^{-3}, $[CN]_o$ = 1.6397 x 10^{-3} mol dm^{-3},
$[H]_o$ = 1.6516 x 10^{-3} mol dm^{-3}, $[CO_3]_o$ = 0.0000 mol dm^{-3},
$[Zn]_T$ = 3.0239 x 10^{-4} mol dm^{-3}, $[CN]_T$ = 4.9196 x 10^{-3} mol dm^{-3},
$[H]_T$ = −1.8433 x 10^{-2} mol dm^{-3}, $[CO_3]_T$ = 3.1500 x 10^{-4} mol dm^{-3}.

1.00,	1.00,	1.00,	−118.20;
2.00,	2.00,	2.00,	−140.00;
4.00,	4.00,	4.00,	−208.00.

Run 3B:

E^0_{cell} = 246.9066 mV; Slope = 57.9040; V_o = 79.00 cm^3;
$[Zn]_o$ = 1.0063 x 10^{-4} mol dm^{-3}, $[CN]_o$ = 1.1082 x 10^{-3} mol dm^{-3},
$[H]_o$ = 9.0701 x 10^{-4} mol dm^{-3}, $[CO_3]_o$ = 0.0000 mol dm^{-3},
$[Zn]_T$ = 3.0190 x 10^{-4} mol dm^{-3}, $[CN]_T$ = 3.3242 x 10^{-3} mol dm^{-3},
$[H]_T$ = 5.3380 x 10^{-3} mol dm^{-3}, $[CO_3]_T$ = 0.0000 mol dm^{-3}.

0.00,	0.00,	0.00,	−154.90;
0.50,	0.50,	0.50,	−150.20;
1.00,	1.00,	1.00,	−146.20;
1.50,	1.50,	1.50,	−142.70;
2.50,	2.50,	2.50,	−136.60;
3.50,	3.50,	3.50,	−131.10;
4.00,	4.00,	4.00,	−128.10;
5.00,	5.00,	5.00,	−122.40;
5.50,	5.50,	5.50,	−119.00.

Run 4B:

E^0_{cell} = 242.0386 mV; Slope = 57.9623; V_o = 105.00 cm^3;
$[Zn]_o$ = 7.1414 x 10^{-4} mol dm^{-3}, $[CN]_o$ = 4.2809 x 10^{-3} mol dm^{-3},
$[H]_o$ = 6.1229 x 10^{-5} mol dm^{-3}, $[CO_3]_o$ = 1.7048 x 10^{-6} mol dm^{-3},
$[Zn]_T$ = 0.0000 mol dm^{-3}, $[CN]_T$ = 0.0000 mol dm^{-3},
$[H]_T$ = 5.3720 x 10^{-3} mol dm^{-3}, $[CO_3]_T$ = 0.0000 mol dm^{-3}.

0.00,	−324.20;
3.00,	−311.60;
6.00,	−300.40;
8.00,	−293.60;
10.00,	−287.20;
12.00,	−280.90;
14.00,	−274.70;
16.00,	−268.50;
18.00,	−262.40;
20.00,	−255.90;
23.00,	−245.40;
27.00,	−229.80;
30.00,	−217.10;
32.00,	−208.50;
34.00,	−199.50;
38.00,	−181.20;
40.00.	−172.90.

Run 5B:

E^0_{cell} = 242.5999 mV; Slope = 57.9623; V_o = 105.00 cm^3;

$[Zn]_o$ = 4.3409 x 10^{-4} mol dm^{-3}, $[CN]_o$ = 1.9126 x 10^{-3} mol dm^{-3},

$[H]_o$ = –2.5238 x 10^{-6} mol dm^{-3}, $[CO_3]_o$ = 3.4571 x 10^{-6} mol dm^{-3},

$[Zn]_T$ = 0.0000 mol dm^{-3}, $[CN]_T$ = 0.0000 mol dm^{-3},

$[H]_T$ = 5.2650 x 10^{-3} mol dm^{-3}, $[CO_3]_T$ = 0.0000 mol dm^{-3}.

0.00,	–298.80;
2.00,	–279.10;
4.00,	–260.10;
6.00,	–242.10;
8.00,	–224.80;
12.00,	–193.20;
14.00,	–180.90;
16.00,	–171.30;
18.00,	–163.50;
19.00,	–160.00;
20.00,	–156.90.

Run 6B:

E^0_{cell} = 234.8509 mV; Slope = 57.9623; V_o = 95.02 cm^3;

$[Zn]_o$ = 2.5789 x 10^{-4} mol dm^{-3}, $[CN]_o$ = 5.1969 x 10^{-3} mol dm^{-3},

$[H]_o$ = –2.7247 x 10^{-5} mol dm^{-3}, $[CO_3]_o$ = 5.4725 x 10^{-6} mol dm^{-3},

$[Zn]_T$ = 0.0000 mol dm^{-3}, $[CN]_T$ = 0.0000 mol dm^{-3},

$[H]_T$ = 4.2984 x 10^{-2} mol dm^{-3}, $[CO_3]_T$ = 0.0000 mol dm^{-3}.

0.00,	–349.20;
1.00,	–329.30;
2.00,	–313.90;
3.00,	–301.60;
4.00,	–290.90;
5.00,	–280.50;
6.00,	–269.50;
7.00,	–256.70;
8.00,	–239.10;
9.00,	–206.10;
10.00,	–140.30;
11.00,	–105.50;
12.00,	5.50.

E^0_{cell} = 234.8509 mV; Slope = 57.9623; V_o = 107.02 cm^3;

$[Zn]_o$ = 2.2898 x 10^{-4} mol dm^{-3}, $[CN]_o$ = 4.6142 x 10^{-3} mol dm^{-3},

$[H]_o$ = 4.7955 x 10^{-3} mol dm^{-3}, $[CO_3]_o$ = 4.8589 x 10^{-6} mol dm^{-3},

$[Zn]_T$ = 0.0000 mol dm^{-3}, $[CN]_T$ = 0.0000 mol dm^{-3},

$[H]_T$ = −2.1930 x 10^{-3} mol dm^{-3}, $[CO_3]_T$ = 1.7700 x 10^{-4} mol dm^{-3}.

40.00, −113.20;
43.50, −116.10.

Run 7B:

E^0_{cell} = 239.2838 mV; Slope = 56.5366; V_o = 92.00 cm^3;

$[Zn]_o$ = 2.6636 x 10^{-4} mol dm^{-3}, $[CN]_o$ = 3.9965 x 10^{-3} mol dm^{-3},

$[H]_o$ = −1.1609 x 10^{-5} mol dm^{-3}, $[CO_3]_o$ = 2.3043 x 10^{-6} mol dm^{-3},

$[Zn]_T$ = 0.0000 mol dm^{-3}, $[CN]_T$ = 0.0000 mol dm^{-3},

$[H]_T$ = 4.2984 x 10^{-2} mol dm^{-3}, $[CO_3]_T$ = 0.0000 mol dm^{-3}.

0.00, −328.10;
1.00, −304.00;
1.50, −294.10;
2.00, −285.60;
2.50, −277.70;
3.00, −270.20;
3.50, −262.60;
4.00, −254.50;
4.50, −245.50;
5.00, −234.50;
5.50, −220.00;
6.00, −198.10;
6.50, −163.80;
7.00, −129.30;
7.50, −110.30;
8.00, −94.30;
8.50, −68.00;
9.00, 38.40.

Run 8B:

E^0_{cell} = 240.3246 mV; Slope = 57.9623; V_o = 95.00 cm^3;

$[Zn]_o$ = 2.5795 x 10^{-4} mol dm^{-3}, $[CN]_o$ = 1.1612 x 10^{-3} mol dm^{-3},

$[H]_o$ = –3.6105 x 10^{-6} mol dm^{-3}, $[CO_3]_o$ = 8.0000 x 10^{-7} mol dm^{-3},

$[Zn]_T$ = 0.0000 mol dm^{-3}, $[CN]_T$ = 0.0000 mol dm^{-3},

$[H]_T$ = –2.4720 x 10^{-3} mol dm^{-3}, $[CO_3]_T$ = 3.0000 x 10^{-5} mol dm^{-3}.

0.00,	–302.80;
2.00,	–306.10;
4.00,	–309.10;
7.00,	–313.60;
10.00,	–317.50;
13.00,	–320.80;
17.00,	–325.30;
21.00,	–329.00.

Run 9E:

E^0_{cell} = 245.6221 mV; Slope = 56.2840; V_o = 84.00 cm^3;

$[Zn]_o$ = 2.7131 x 10^{-4} mol dm^{-3}, $[CN]_o$ = 2.7177 x 10^{-3} mol dm^{-3},

$[H]_o$ = –5.9146 x 10^{-4} mol dm^{-3}, $[CO_3]_o$ = 7.8810 x 10^{-6} mol dm^{-3},

$[Zn]_T$ = 0.0000 mol dm^{-3}, $[CN]_T$ = 0.0000 mol dm^{-3},

$[H]_T$ = –2.1430 x 10^{-2} mol dm^{-3}, $[CO_3]_T$ = 2.6600 x 10^{-4} mol dm^{-3}.

0.00,	–345.30;
3.00,	–358.80;
6.00,	–367.50;
9.00,	–373.50;
12.00,	–377.90;
15.00,	–381.40;
18.00,	–384.30.

E^0_{cell} = 245.6221 mV; Slope = 56.2840; V_o = 102.00 cm^3;

$[Zn]_o$ = 2.2343 x 10^{-4} mol dm^{-3}, $[CN]_o$ = 2.2381 x 10^{-3} mol dm^{-3},

$[H]_o$ = –2.3780 x 10^{-3} mol dm^{-3}, $[CO_3]_o$ = 2.9961 x 10^{-5} mol dm^{-3},

$[Zn]_T$ = 0.0000 mol dm^{-3}, $[CN]_T$ = 0.0000 mol dm^{-3},

$[H]_T$ = 1.0746 x 10^{-2} mol dm^{-3}, $[CO_3]_T$ = 0.0000 mol dm^{-3}.

4.00, –376.80;
8.00, –367.40;
10.00, –361.60;
12.00, –354.40;
14.00, –345.40;
16.00, –334.20;
18.00, –320.50;
20.00, –306.50.

Run 10E:

E^0_{cell} = 241.0142 mV; Slope = 55.6981; V_o = 86.00 cm^3;

$[Zn]_o$ = 2.8494 x 10^{-4} mol dm^{-3}, $[CN]_o$ = 2.8486 x 10^{-3} mol dm^{-3},

$[H]_o$ = –9.2571 x 10^{-4} mol dm^{-3}, $[CO_3]_o$ = 2.6651 x 10^{-5} mol dm^{-3},

$[Zn]_T$ = 0.0000 mol dm^{-3}, $[CN]_T$ = 0.0000 mol dm^{-3},

$[H]_T$ = –2.2364 x 10^{-2} mol dm^{-3}, $[CO_3]_T$ = 6.3100 x 10^{-4} mol dm^{-3}.

0.00, –354.60;
3.00, –364.60;
6.00, –371.50;
9.00, –376.40;
12.00, –380.30;
15.00, –383.50;
18.00, –385.90.

E^0_{cell} = 241.0142 mV; Slope = 55.6981; V_o = 104.00 cm^3;

$[Zn]_o$ = 2.3563 x 10^{-4} mol dm^{-3}, $[CN]_o$ = 2.3556 x 10^{-3} mol dm^{-3},

$[H]_o$ = –2.7008 x 10^{-3} mol dm^{-3}, $[CO_3]_o$ = 7.6587 x 10^{-5} mol dm^{-3},

$[Zn]_T$ = 0.0000 mol dm^{-3}, $[CN]_T$ = 0.0000 mol dm^{-3},

$[H]_T$ = 1.0746 x 10^{-2} mol dm^{-3}, $[CO_3]_T$ = 0.0000 mol dm^{-3}.

2.00,	–382.50;
4.00,	–378.70;
6.00,	–374.30;
8.00,	–369.50;
10.00,	–364.40;
14.00,	–450.10;
18.00,	–328.80;
20.00,	–315.50;
22.00,	–302.90;
24.00,	–291.10;
26.00,	–279.80.

Run 11E:

E^0_{cell} = 251.7842 mV; Slope = 57.5784; V_o = 95.00 cm^3;

$[Zn]_o$ = 2.5795 x 10^{-4} mol dm^{-3}, $[CN]_o$ = 1.0518 x 10^{-2} mol dm^{-3},

$[H]_o$ = –5.2836 x 10^{-4} mol dm^{-3}, $[CO_3]_o$ = 0.0000 mol dm^{-3},

$[Zn]_T$ = 0.0000 mol dm^{-3}, $[CN]_T$ = 0.0000 mol dm^{-3},

$[H]_T$ = –9.8960 x 10^{-3} mol dm^{-3}, $[CO_3]_T$ = 0.0000 mol dm^{-3}.

0.00,	–359.90;
2.00,	–364.20;
4.00,	–368.00;
7.00,	–373.20;
10.00,	–377.40;
13.00,	–380.80;
16.00,	–383.70;
20.00,	–387.30;
25.00,	–390.50.

CHAPTER EIGHT

RESULTS AND DISCUSSION

In this chapter the results derived from the potentiometric data for the hydrogen ion–cyanide and the zinc–cyanide systems are described and discussed.

As mentioned in Chapter 5, a criterion for attainment of electrochemical equilibrium adopted in this study was that the cell EMF should remain constant (to ± 0.1 mV) for a minimum period of 5 minutes. To meet this condition, "equilibration" times varied from about 6 minutes per titration point at low pH values (pH = 6 or below) to about 90 minutes per point at the highest pH values (≈ 11), encountered in the study of the zinc–cyanide system. The latter period seems rather long and suggests that chemical equilibrium may be approached slowly at high p[H] values – although glass electrodes are known to require long equilibration times at high p[H].

The titrations in which the direction of titration was reversed (see Chapter 7), were used as a further test of attainment of equilibrium. If equilibrium had been attained at each titration point then calculated values of the formation function, $\bar{Z}_H$ or $\bar{Z}_M$, should have the same value for both "forward" and "reverse" titrations at any particular value of p[H] or pA respectively. This test of attainment of equilibrium is valid provided that no polynuclear or hydrolysed complex species are formed.

During this study, solutions containing mixtures of background electrolyte ($NaClO_4$), cyanide and varying quantities of perchloric acid were examined by U.V. spectroscopy. Results of the U.V. spectrophotometric examination indicated that a slow decomposition or possibly oxidation reaction takes place, to produce a species absorbing at λ_{max} = 298 nm. The absorption at λ_{max} = 298 nm was observed to increase slowly with time. It was noticed that the "decomposition" reaction was light sensitive and that the reaction occurred

relatively slowly in solutions containing either completely protonated ligand (HCN) or in solutions containing only the deprotonated form (CN^-). The reaction seemed to proceed faster in buffered solutions containing roughly equal quantities of HCN and CN^-. From the comparative stability of cell EMF values in the solutions studied it was inferred however that the extent of the side reaction observed was fairly minor in nature.

The contents of the reaction vessel were flushed with nitrogen gas during the calibration step only (see Chapter 7). No flushing was carried out after addition of cyanide, to avoid loss of volatile HCN from the system. The system was, however, kept sealed in the reaction vessel after flushing was discontinued.

8.1 THE HYDROGEN ION–CYANIDE SYSTEM

In order to determine the formation constants of complexes formed in the hydrogen ion–cyanide system, in the absence of any metal ions, three titrations were carried out at slightly different initial cyanide ion to hydrogen ion ratios (see Table 8.1). The analytical (total) hydrogen ion, H_T, and cyanide ion, CN_T, concentrations quoted in Table 8.1 are the values used for computations and are not to be taken as significant to the number of digits quoted. In titration 3 the direction of the titration was reversed by switching to a hydroxide titrant after completion of the titration (see Table 7.1).

TABLE 8.1 Initial values of H_T and CN_T, CN_T/H_T quotients and p[H] ranges covered for titrations in the study of the protonation of the cyanide ion.

Titration No.	H_T/mol dm^{-3}	CN_T/mol dm^{-3}	CN_T/H_T	p[H]range	Plotting symbol
1	5.7721×10^{-4}	2.4545×10^{-3}	4.25	9.6 → 7.6	⊙
2	5.6968×10^{-4}	2.4545×10^{-3}	4.31	9.6 → 7.7	⊡
3	6.6121×10^{-4}	2.8551×10^{-3}	4.32	9.6 → 7.7 7.7 → 9.3	▲–forward ▽–reverse

Values of the formation function $\bar{Z}_H$(obs) are plotted as discrete points versus p[H] in Figure 8.1, for data collected from the above titrations in the absence of any metal ions (see Table 7.1). Figure 8.1 also shows the plot of $\bar{Z}_H$(calc) versus p[H], shown as a continuous line. Figure 8.1, shows that the degree of superimposability of the curves for titration 3 (forward) and (reverse) is reasonable, indicating that the system had reached chemical equilibrium.

Since the plot of $\bar{Z}_H$(obs) versus p[H] levels off at a $\bar{Z}_H$(obs) value of just less than one, it was assumed that no protonated species, other than HCN is found in the hydrogen ion–cyanide system studied (66). Although agreement between observed and calculated formation functions is not perfect, it is felt that particularly in view of the sub–millimolar concentration levels studied, the level of agreement between observed and calculated formation functions is acceptable. This result is consistent with the findings of previous studies of the same system (21,27,28,30,86,104).

From the data obtained from these potentiometric titrations and using computer techniques (see Section 4.2) a log $\beta \pm 3\sigma$ value of 9.08 ± 0.01 was obtained for the pK_a of HCN at an ionic strength of 0.10 mol dm^{-3} and a temperature of 25.0^{0}C. The value of pK_w at an ionic strength of 0.10 mol dm^{-3} and a temperature of 25.0^{0}C was taken to be 13.78 (86).

8.2 ZINC–CYANIDE SYSTEM

In the study of the complexes formed by zinc and cyanide ions at moderately high p[H] values, the data from eleven potentiometric titrations were used. The titrations were carried out at various ligand:metal ratios and at various total (analytical) metal, Zn_T, and cyanide, CN_T, ion concentrations (see Table 7.2). In titration 1, two glass electrodes were used, namely B and C. In some titrations mixtures of zinc and cyanide ions were titrated with acid, in others sodium hydroxide titrant was used, and, in a few instances the direction of titration was reversed by switching to a hydroxide titrant on completion of the titration with acid

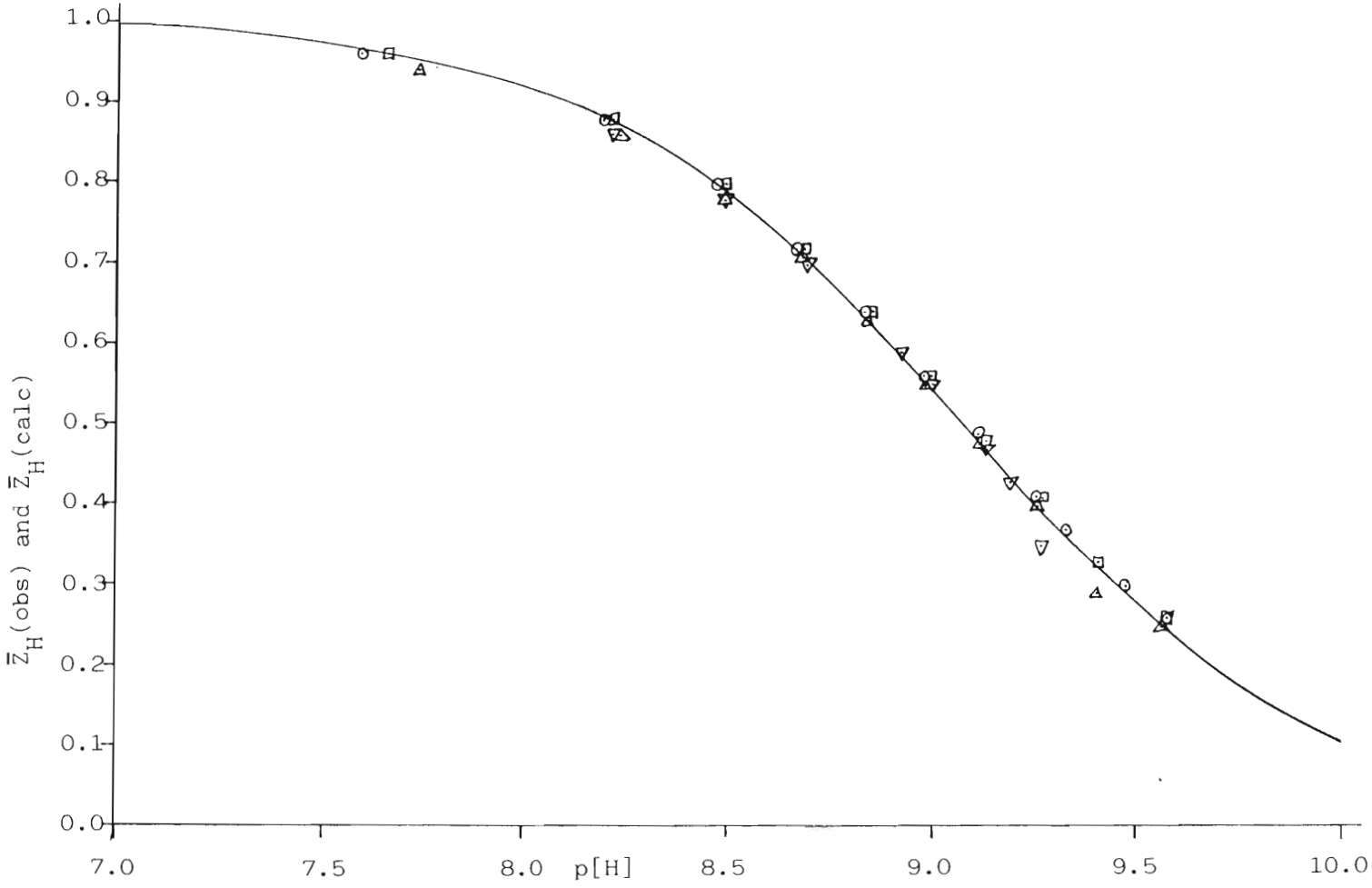

Figure 8.1: The formation functions $\bar{Z}_H$(obs) (discrete points) and $\bar{Z}_H$(calc) (continuous curve) plotted versus p[H] for measurements carried out in the hydrogen-ion cyanide system. Key to the plot symbols used is given in Table 8.1 in the text.

and *vice–versa*. The initial values of Zn_T and CN_T, the ligand to metal ratio (expressed as the quotient CN_T/Zn_T), as well as the p[H] ranges covered, are given in Table 7.2.

Titrations 1B, 1C, 2B, 6B, 9E and 10E involved reversal in the direction of titration. It was found that plots of $\bar{Z}_M$ versus pA for both the forward and reverse branches of titrations 1B, 1C, 2B and 6B were superimposable to within experimental error (see Figure 8.2), indicating that electrochemical equilibrium was attained for p[H] values up to at least 9, and also that significant amounts of hydrolysed complex species are not formed below p[H] = 9 in systems having $CN_T/Zn_T \geq 10$. This is more or less in accord with the conclusions of previous workers, who have rarely made measurements at p[H] values above 8.5.

Titrations 9E, 10E and 11E involved the use of an excess of hydroxide over any acid that may have been present at the end of cell calibration, and resulted in the attainment of p[H] values as high as 11.3. For titrations 9E and 10E, which involved reversals in the direction of titration, values of $\bar{Z}_M$ could not be calculated, so this test for attainment of chemical equilibrium could not be applied.

Plots of $\bar{Q}$(obs) versus p[H] for titrations 9E and 10E are shown in Figure 8.3. Values of $\bar{Q}$(obs) obtained during the first part of the titrations, i.e. during raising of the p[H], are plotted as circles, while values obtained during the second part, i.e. when the p[H] was subsequently lowered, are plotted as triangles. A striking feature of the data from titrations 9E, 10E and 11E was that negative values of the deprotonation function $\bar{Q}$(obs) were obtained at high p[H]. The formation of complexes of the form $Zn(CN)_n$ or $Zn(CN)_n(OH)_m$ should not give rise to negative values of $\bar{Q}$, since the processes

$$Zn^{2+} + nHCN \rightarrow Zn(CN)_n^{(2-n)+} + nH^+$$

$$Zn(CN)_n^{(2-n)+} + mOH^- \rightarrow Zn(CN)_n(OH)_m^{(2-n-m)+}$$

$$Zn(CN)_n^{(2-n)+} + mOH^- \rightarrow ZnCN_{n-m}(OH)_m^{(2-n-m)+} + mCN^-$$

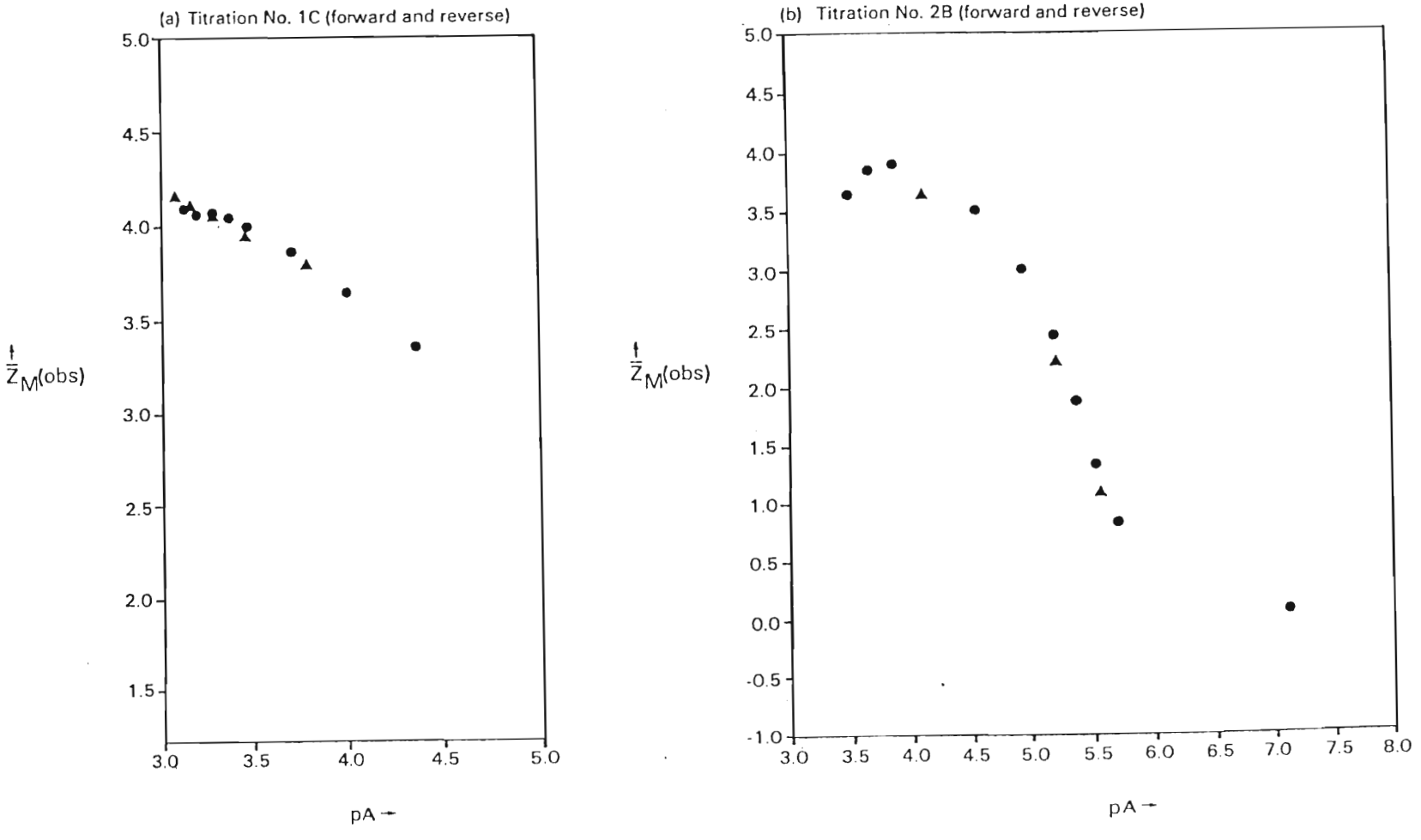

Figure 8.2: The formation function $\bar{Z}_M$(obs) plotted *vs* pA for titrations Nos. 1C and 2B. The titrations were carried out in two parts. Points obtained during initial lowering of p[H] (and therefore also pA) are plotted as dots. Points obtained during subsequent raising of p[H] (and pA) are plotted as triangles. The

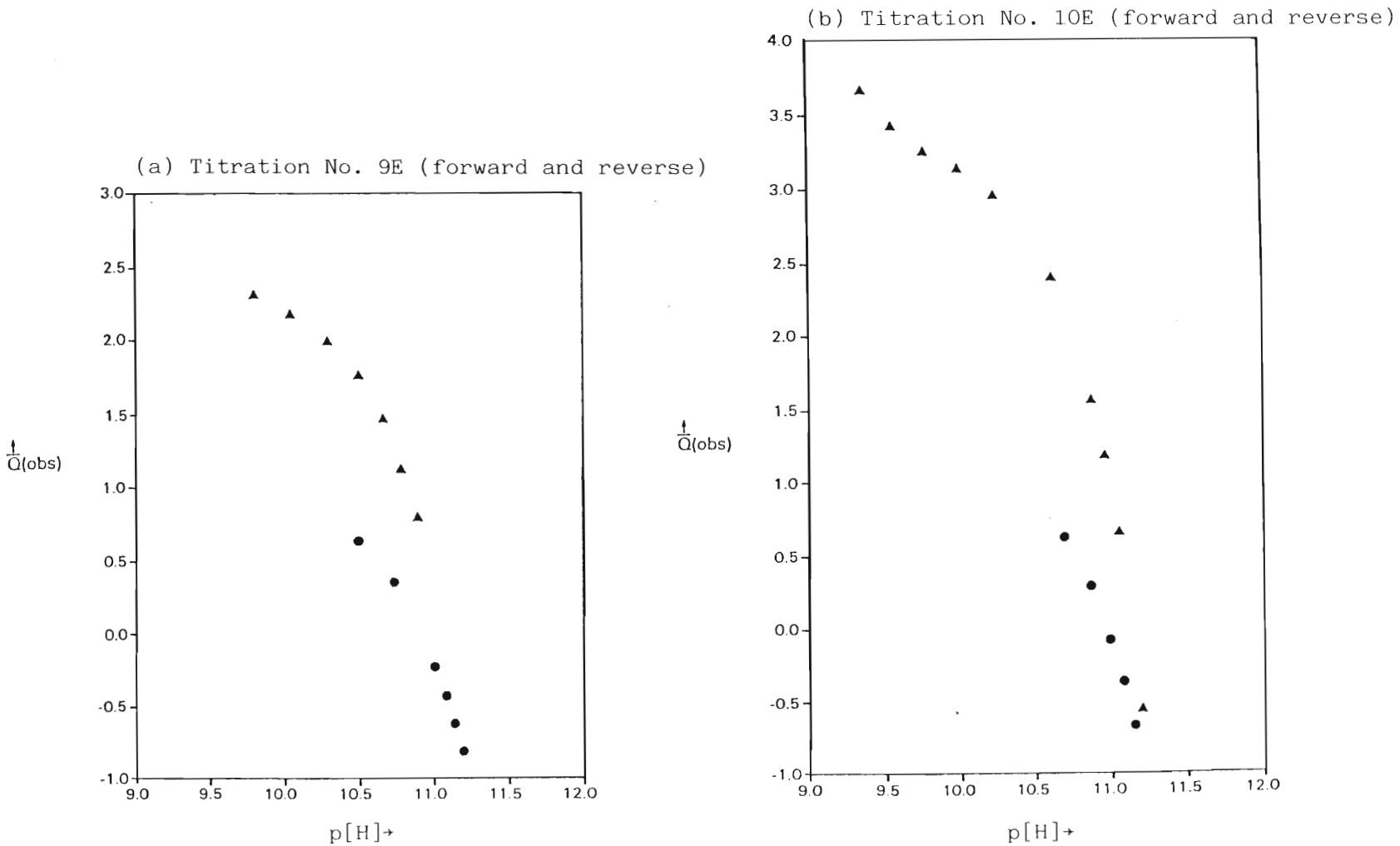

Figure 8.3: The deprotonation function $\bar{Q}$(obs) plotted *vs* p[H] for titrations No. 9E and 10E. The titrations were carried out in two parts. Points obtained during the initial raising of p[H] are plotted as dots. Points obtained during subsequent lowering of p[H] are plotted as triangles. The highest solution p[H] values attained were 11.2 and 11.3 for titrations 9E and 10E respectively.

all either produce H^+ ions or consume OH^- ions – both of which should result in positive values of $\overline{Q}$. Experimentation with the $\overline{Q}$ function however shows that at high p[H] values, i.e. when the concentration of free (uncoordinated) OH^- ions becomes comparable to the concentration of the other species present in the system, $\overline{Q}$ becomes inordinately sensitive to small uncertainties in experimental variables such as the electrode calibration slope k, the value of pK_w taken, or the hydrogen/hydroxide ion concentration. Thus an uncertainty of 0.02 log units in pK_w (or a corresponding small uncertainty in the value of k) leads to uncertainties of approx. 0.5 units in $\overline{Q}$. It is apparent therefore that at high pH values (> 10.5) the $\overline{Q}$ function rapidly becomes very sensitive to small uncertainties in $[H^+]$, and probably also in H_T, and is no longer useful for graphical representation of potentiometric data. The question of whether or not the data may be useful for species selection and computation of formation constants, was investigated by determining the extent to which the calculated p[H] of the solution depends on the formation constants of complex/es of interest (see Section 6.3). For this purpose, values of cumulative formation constants taken from the literature (86,105) were used for the binary Zn^{2+}/CN^- and Zn^{2+}/OH^- complexes. A statistical method proposed by Sharma and Schubert (96) was used to estimate the values of $\log \beta_{14\text{-}1} = 22.6$, $\log \beta_{13\text{-}2} = 21.2$, and $\log \beta_{13\text{-}1} = 19.6$ for the ternary species $Zn(CN)_4(OH)^{3-}$, and $Zn(CN)_3(OH)_2^{3-}$ and $Zn(CN)_3(OH)^{2-}$ respectively. Simulated potentiometric titration data were calculated by means of the HALTAFALL (73) program, using such literature values and estimates for $\log \beta$.

It was found, for example, that at p[H] values above 10.5 and at a ligand to metal ratio of 10:1 the solution p[H] is almost totally insensitive to changes of approx. 1 log unit in the value of the $\log \beta_{13\text{-}1}$ for the complex $Zn(CN)_3(OH)^{2-}$. At a p[H] value of 10, the calculated solution p[H] changes by about 0.06 units (corresponding to a change of cell EMF of about 3.6 mV), an amount which is uncomfortably close to a realistic estimate of the uncertainty in the value of E^0_{cell}. At a ligand to metal ratio of 5:1 the situation is slightly improved, but the sensitivity of measured cell EMF to $\log \beta_{13\text{-}1}$ is still only $\approx$ 2.5 mV, per unit variation in $\log \beta$, at p[H] = 10.5.

The indications therefore are that when the concentration of free (uncomplexed) OH^- ions becomes comparable to the concentration of free CN^- ions, very great precision of electrode calibration is required in order to distinguish between uncoordinated OH^- and CN^- ions. The fact that negative values of $\overline{Q}$ were obtained at high p[H] (see Figure 8.3) is further indication that the precision of the experimental technique was insufficient to allow ligand replacement reactions of the type

$$Zn(CN)_n(OH)_m^{(2-n-m)+} + OH^+ \rightarrow Zn(CN)_{n-1}(OH)_{m+1}^{(2-n-m)+} + CN^-$$

to be followed reliably at p[H] values above 10.

It should also be noted that attainment of electrochemical equilibrium at high p[H] values has not been proven – in spite of the greater than 45 minutes equilibration times allowed.

Consequently, the data collected in titrations 9E, 10E and 11E were not used any further in this work, and subsequent calculations were based on data obtained at p[H] values below 10, i.e. from titrations 1B, 1C, 2B, 3B, 4B, 5B, 6B, 7E and 8B.

For the calculations involved in model selection and determination of formation constants, allowance was made for auxiliary equilibria which may be important in the titrations performed. From the titrations carried out in the absence of metal ions, a value of 9.08 ± 0.01 was obtained for the pK_a of HCN (see Section 8.1). It was assumed that no protonated species other than HCN is formed in such systems. Literature values taken from various data compilations (86,105) for the other constants involved, valid at 25.0^0C and at various ionic strengths, are given in Table 8.2. Where values appropriate to I = 0.1 mol dm^{-3} were not available, these (denoted by an asterisk in the table) were estimated using a method described recently by Linder and Murray (106). For these interpolations, the required values of the ion size parameters å were either obtained from Kielland (107) or estimated as described by Linder and Murray (106).

Table 8.2 Literature values, and values interpolated to I = 0.1 mol dm^{-3} of formation constants used to correct for auxiliary equilibria in the model selection procedure and in calculation of formation constants.

Quantity	I = 0	I = 0.1 mol dm^{-3}	I = 3.0 mol dm^{-3}
pK_w		13.78	
$\log \beta_1^H(HCO_3^-)$		10.00	
$\log K_2^H(H_2CO_3)$		6.16	
$\log \beta_{10\text{-}1}[Zn(OH)^+]$	5.0	4.6*	3.8
$\log \beta_{10\text{-}2}[Zn(OH)_2]$	10.2	9.6*	8.3
$\log \beta_{10\text{-}3}[Zn(OH)_3^-]$	13.9	13.3*	13.7
$\log \beta_{10\text{-}4}[Zn(OH)_4^{2-}]$	15.6	15.2*	18.0
log K[Zn+Zn(OH)]	0.0	0.4*	1.7

* Values estimated as described in the text.

Values of the formation function $\bar{Z}_M$(obs) are plotted versus pA in Figure 8.4 for data collected at p[H] values below 10. For clarity, not all experimental points are shown. The relationship between titration numbers and plotting symbols used in this and subsequent figures is summarised in Table 8.3.

Table 8.3 Plotting symbols used for the various titrations depicted in Figure 8.4, 8.5, 8.7 and 8.8.

Titration	Symbol	Titration	Symbol
1B (forward)	●	4B	▲
1B (reverse)	▲	5B	Δ
1C (forward)	◎	6B (forward)	o
1C (reverse)	x	6B (reverse)	*
2B (forward)	◇	7E	■
2B (reverse)	⊡	8B	ı
3B	□		

Reading from right to left of Figure 8.4, the plot of $\bar{Z}_M$(obs) versus pA after an initial increase begins to level off at $3.5 < \bar{Z}_M(obs) < 4$, followed by a rapid increase with decreasing values of pA. This sudden rapid increase in $\bar{Z}_M$(obs) at low pA values (i.e. high p[H]) is fairly typical for systems in which hydrolysis takes place. It can be easily verified that the $\bar{Z}_M$(obs) versus pA plot is very sensitive to small uncertainties in, particularly, the analytical quantity H_T in this high p[H] region, and also to the value of the pK_a of the ligand, so too much significance should not be accorded to the extreme left hand region of the plot. The plot also shows a "back–fanning" feature to the data from titrations 5B and 8B, in the former instance occurring at pA $\approx$ 3.9, and $\bar{Z}_M$(obs) $\approx$ 4.0. This feature is also fairly characteristic of hydrolysis equilibria. The fact that this "back–fanning" feature occurs early in the plot (reading from left to right) accords with the fact that these two titrations (5B and 8B) were carried out at the lowest ligand–to–metal ratios in this study (see Table 7.2). The lower the ligand to metal ratio the sooner hydrolysis can be expected to occur, when the p[H] of the solution is raised (or the pA lowered). A reasonably complete model of the hydrolytic and other equilibria in a system such as this one should be able to reproduce this "back–fanning" feature at pA $\approx$ 3.9, whereas the portion at the extreme left hand side of the figure is probably too sensitive to small experimental errors for exact reproduction to be feasible.

Another feature of interest in connection with Figure 8.4 is the degree of superimposability of the $\bar{Z}_M$(obs) versus pA curves at varying values of Zn_T. Examination of Table 7.2 shows that the titrations carried out at p[H] values below 10 can be divided into three broad groupings:

(a) Titrations 2B and 3B having $Zn_T \approx 1 \times 10^{-4}$ mol dm^{-3}.

(b) Titrations 1B, 1C, 6B, 7E and 8B having $Zn_T \approx 2.7 \times 10^{-4}$ mol dm^{-3}.

(c) Titrations 4B and 5B having $Zn_T \approx 4 \times 10^{-4}$ mol dm^{-3}.

Thus, Zn_T [group (a)] < Zn_T [group (b)] < Zn_T [group (c)]. There does not appear, in Figure 8.4, to be any discernable systematic separation or grouping of

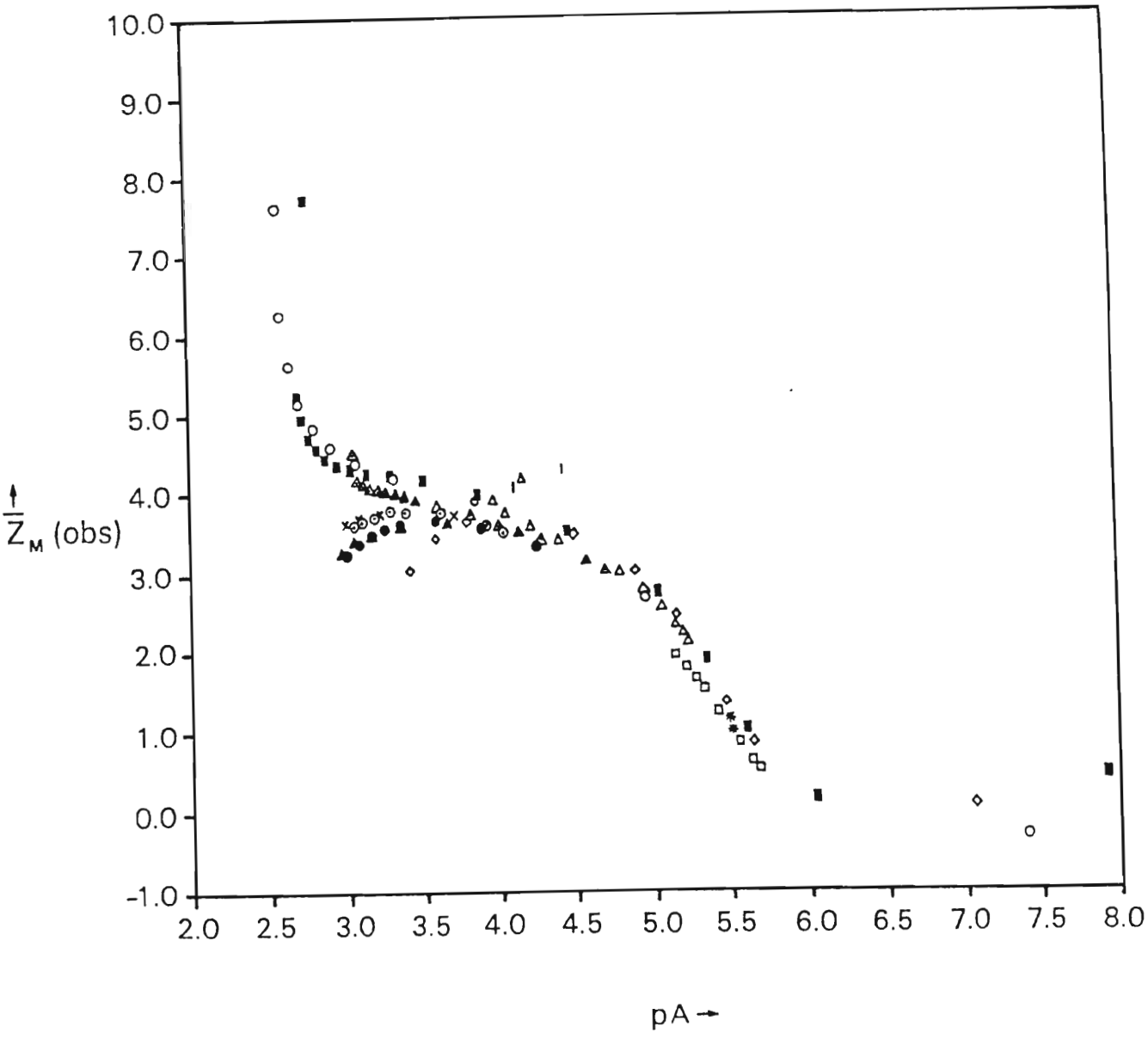

Figure 8.4: The formation function $\bar{Z}_M$(obs) plotted *vs* pA for measurements carried out at p[H] values below 10. Key to the plot symbols used is given in Table 8.3 in the text. A value of pK_a = 9.01 for HCN was used in the calculation of $\bar{Z}_M$(obs).

$\bar{Z}_M$(obs) versus pA curves in terms of the value of Zn_T. The indications therefore are that polynuclear complexes do not form to any significant extent in this ternary system at metal ion concentrations below 7 x 10^{-4} moℓ dm^{-3}.

Values of the deprotonation function $\bar{Q}$(obs) are plotted versus p[H] as discrete points in Figure 8.5, for the titrations carried out below p[H] = 10.0. For clarity, not all experimental points are shown. Also included in Figure 8.5 is a plot of the hydrogen formation function $\bar{Z}_H^*$ (defined in Section 4.1.1) for the ligand–hydrogen ion subsystem. The latter function is shown as a continuous line in the Figure 8.5. In contrast to the situation existing above p[H] = 10.0, virtually all values of $\bar{Q}$(obs) are positive, as expected for a system where complex hydrolysis rather than complex protonation would be expected to occur. Referring back to Figure 8.4, an approach to a plateau is obtained at values of pA ≈ 3.5, corresponding to a value of p[H] ≈ 8.5. From Figure 8.5 it can be seen that at this p[H], $\bar{Q}$(obs) ≈ 3.1 and $\bar{Z}_H^*$ = 0.75. Since only mononuclear complexes ($M_pL_qH_r$) form therefore p = 1. From the relationship given in Section 4.1.1 it follows that

$$r = 0.75q - 3.1 \quad .$$

Accordingly, if q = 3 then r = −1 and if q = 4, r = 0. Thus if a single complex predominates in regions corresponding to the plateau in Figure 8.4, this complex is likely to be either $Zn(CN)_3(OH)^{2-}$ or $Zn(CN)_4^{2-}$. Previous investigations of the zinc–cyanide system (see Table 1.1) have assumed the complex to be $Zn(CN)_4^{2-}$.

Model selection was carried out using a OBJE ⟼ BETA cycling procedure described in Section 4.2.3, by means of which complexes are added one by one to the overall model and the values of all unknown formation constants are optimised after addition of each new complex.

Likely species for incorporation into the model for this system were tested for or ranked by use of the BETA facility for point–by–point calculation of formation constants. The algorithm used in the model selection phase of this study is

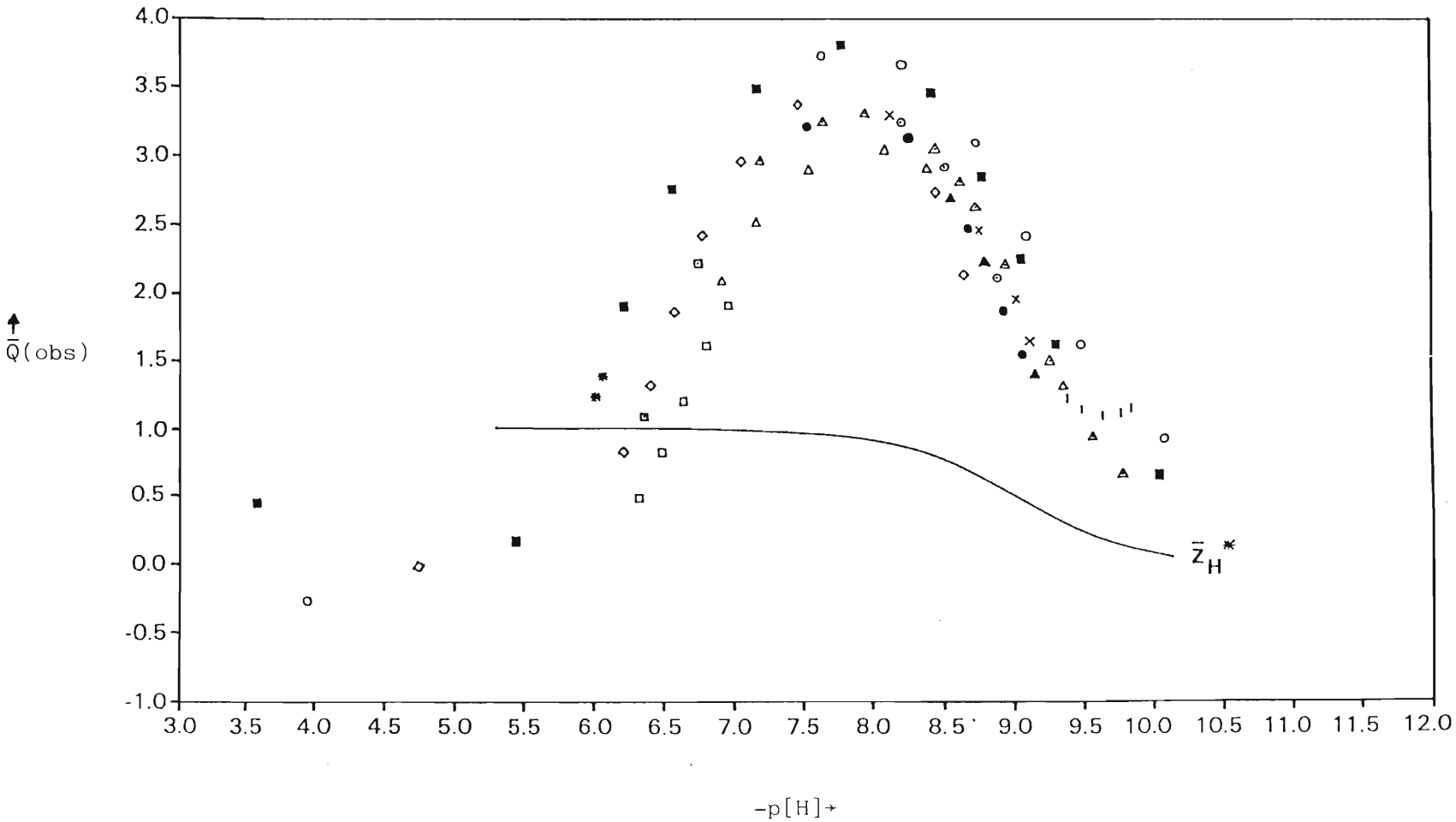

Figure 8.5: The deprotonation function $\bar{Q}$(obs) plotted *vs* p[H] for titrations 1B and C, 2B, 3B, 4B, 5B, 6B, 7E and 8B, i.e. for data collected at p[H] values below 10. Key to the plot symbols used is given in Table 8.3 in the text.

summarized in Figure 4.7, but is duplicated in Figure 8.6 for ease of reference. An essential feature of this algorithm is that the inner of the two nested loops involves only single parameter calculations which are much easier and quicker to carry out than the non–linear multiparameter optimisations involved in the outer (and less frequently traversed) loop. Thus, as many as 10 new trial species can be tested for in about the same time as it takes to carry out a single multi–parameter optimisation involving a single trial species. Our experience with this algorithm is that the time taken to arrive at a satisfactory model for the system is a factor of 5 to 10x less than that required by procedures like PQR analysis (46) which involve numerous multi–parameter optimisations. Time will tell whether the models obtained using this procedure are as "good" as models obtained by PQR analysis, but recent experience in our laboratory involving variations on both approaches have been most encouraging (72,78). The "initial model", which represented the experimenter's guess as to what the major species in the model are likely to be, was taken to be the set of binary species $Zn(CN)_2$, $Zn(CN)_3^-$ and $Zn(CN)_4^{2-}$. The algorithm can then be used to test for the presence or absence of other (presumably minor) species in the system.

In this way, the number of complexes in the model was increased by one each time the outer loop was traversed, and the values of all unknown formation constants were optimised using the OBJE task. A total of 117 data points, grouped into 12 titrations were used in these calculations.

Optimisation was carried out with respect to the objective function OBJE, (see Section 4.2.3), given by

$$\text{OBJE} = U = \frac{1}{N-n_p} \sum_{n=1}^{N} W_n (E_n^{obs} - E_n^{calc})^2 \quad , \tag{8.1}$$

where

N represents the total number of experimental titration points;

n_p represents the number of parameters simultaneously optimised;

E_n^{obs} represents the observed EMF at the n^{th} data point;

E_n^{calc} represents the calculated EMF (for the model) at the n^{th} data point;

W_n represents a weighting factor assigned to the residual at the n^{th} point.

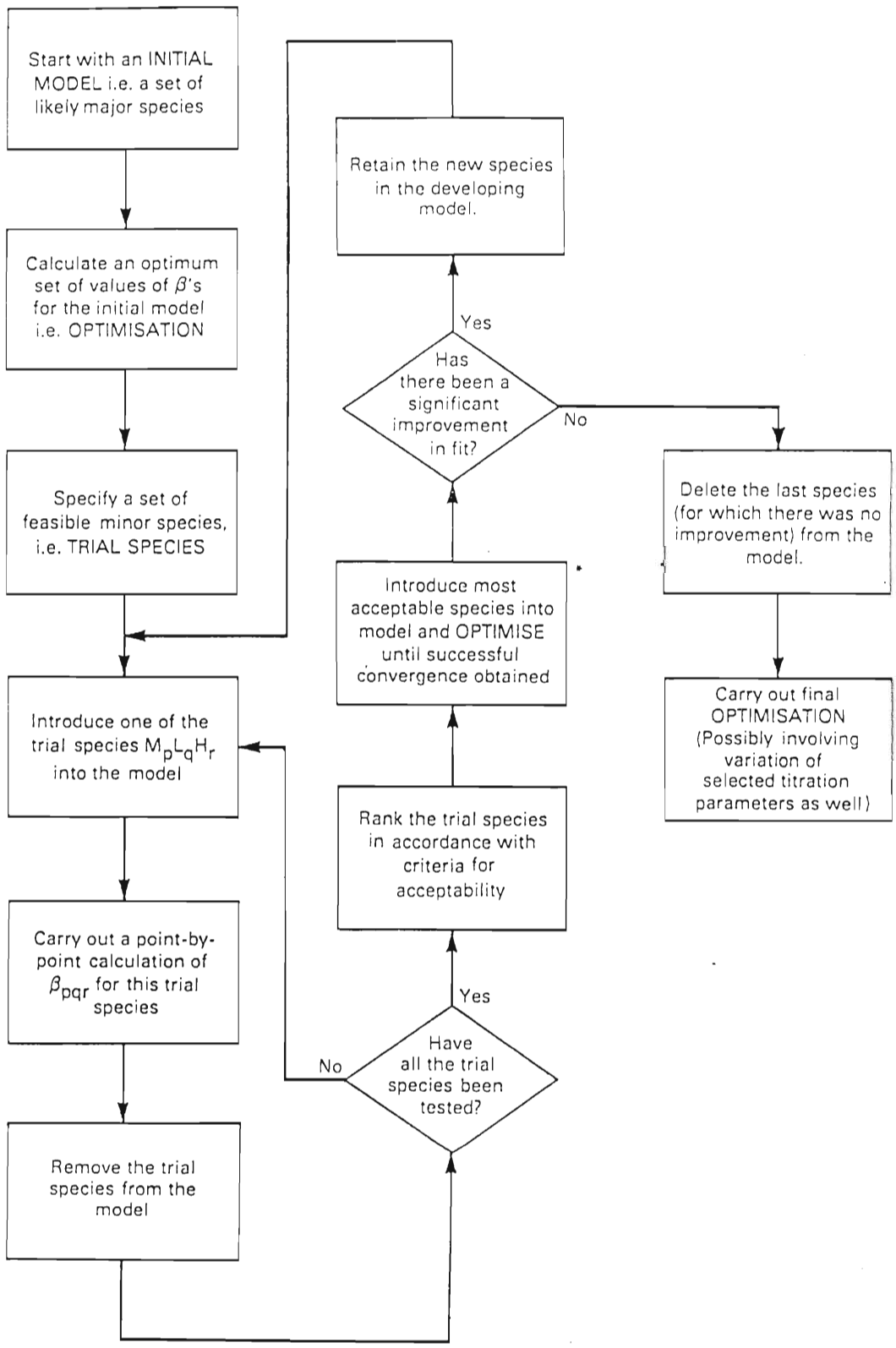

*Occasionally it may be found that the "best" of the trial species is not accepted into the model at the optimisation stage. If so, try the next best trial species etc. until one is accepted (i.e. leads to successful convergence).

Figure 8.6: A flowchart showing the sequence of steps involved in model selection.

The weighting factor W_n, defined as the reciprocal of the variance in the residual $E_n^{obs} - E_n^{calc}$, was calculated by the program ESTA using the error propagation formula

$$W_n = \left[\left[\frac{\delta(E_n^{obs} - E_n^{calc})}{\delta V}\right]^2 \sigma_V^2 + \left[\frac{\delta(E_n^{obs} - E_n^{calc})}{\delta E_n^{obs}}\right]^2 \sigma_E^2\right]^{-1} , \qquad (8.2)$$

where

V represents titre volume,

E represents observed EMF,

and σ_V and σ_E refer to estimated random errors (expressed as standard deviations) in the titre volumes and observed EMF, respectively. In these calculations, the values $\sigma_V = 0.01$ cm^3 and $\sigma_E = 0.1$ mV were used.

The effect of weighting the residuals in the objective function in this way is to sharply reduce the contribution to OBJE of those residuals arising from less reliable readings, taken at or near "end points" or points of inflection in potentiometric titration curves – thus obviating a well recognised hazard encountered when using objective functions based on observed and calculated cell EMF's.

Other choices of objective functions and weighting parameters are possible within the ESTA program and these are discussed in the ESTA Users Manual (44). Extended Debye–Hückel type corrections were applied (44) to correct for ionic strength changes during the titrations, but the effect of these should be minor in view of the submillimolar concentration levels of the reactants.

Results of these calculations are summarised in Table 8.4. Values of the objective function, U, are given in columns 8, 9 and 10 of the table. The formation constants given in column 3 of Table 8.2 were incorporated as fixed values (assumed correct) in all the calculations.

ABLE 8.4 Results of model selection and calculation of formation/hydrolysis constants (expressed as logarithms to base 10).

ycles rough iter op of gorithm	Species and formation/hydrolysis constants [a]						Goodness of fit, U		
	$Zn(CN)_2$	$Zn(CN)_3^-$	$Zn(CN)_4^{2-}$	$Zn(CN)_3(OH)^{2-}$	$Zn(CN)_3(OH)_2^{3-}$	$Zn(CN)_5^{3-}$	117 data points $pK_a = 9.08$	94 data points pK_a optimized	94 data points $pK_a = 9.08$
0	10.94	16.04	20.53	–	–	–	2610	2796	2960
1	10.98	15.53	20.33	3.81 [b]	–	–	720	521	596
2	10.83	16.11	20.41	7.08	–	–	597	416	447
3	10.85	16.10	20.45	6.82	–3.31	–	560	355	401
4	10.80	16.12	20.41	6.61	–3.25	22.93	399	249 [c]	288

For complexes containing the hydroxide ion, e.g. $Zn(CN)_n(OH)_m$, the values given in the table represent $\log \beta_{n,-m} - mpK_w$.

This value refers to the complex $Zn(CN)_2(OH)^-$ which was replaced by $Zn(CN)_3(OH)^{2-}$ at the next cycle.

Simultaneous variation of pK_a (HCN) leads to significant correlation between parameters at cycle 4.

Calculations were performed on two data sets: one comprising all the data obtained for the titrations described in Table 7.2 (117 data points), and the other comprising all the data except those obtained at p[H] values above 6.5 for titrations 6B and 7E (giving a total of 94 data points). The omitted data from the latter two titrations (corresponding to the rapid increase in $\bar{Z}_M$ on the extreme left–hand side in Figure 8.4) are know to be very sensitive to small uncertainties in analytical concentrations. Also, the ligand: metal ratios for these two titrations (20.2 and 15.0 respectively) are both rather high–making the data from these titrations more than usually sensitive to small systematic errors.

Workers in this field sometimes allow the value of pK_w to be refined in calculations of this sort. This often serves the purpose of correcting for deficiencies in the cell calibration procedure, since the value of pK_w and the electrode calibration slope are strongly correlated. This procedure of refining the value of pK_w was not followed in this study.

For the smaller data set, the pK_a of HCN was allowed to vary in one set of calculations (column 9) and was held fixed at the experimentally determined value of 9.08 in the other set (column 10).

It is clear from Table 8.4, that a simple model comprising only the binary species $Zn(CN)_2$, $Zn(CN)_3^-$ and $Zn(CN)_4^{2-}$ fails to account adequately for the present experimental data. The introduction of ternary Zn/CN /OH species produces a marked improvement in fit between observed and calculated cell EMF values. A smaller improvement in fit is obtained on introduction of the five–coordinated species $Zn(CN)_3(OH)_2^{3-}$ and $Zn(CN)_5^{3-}$, but the improvement appears to be significant, particularly when the 94 data point set is considered. It should be noted that, perhaps not surprisingly, a significant degree of correlation (correlation coefficient above 0.90) exists between the values of $\log\beta_{150}$ and $\log\beta_{011}$, $\log\beta_{130}$ and $\log\beta_{140}$, when the pK_a of HCN is treated as an adjustable parameter. However, when the pK_a of HCN is fixed at 9.08, no significantly correlated parameters are found. Attempts to introduce more species into the model were unsuccessful – irrespective

of whether 117 or 94 data points were used in the calculation.

The evidence for inclusion of the five coordinated species $Zn(CN)_3(OH)_2^{3-}$ and $ZN(CN)_5^{3-}$ in the model is not as firm as the evidence for existence of $Zn(CN)_3(OH)^{2-}$. Nevertheless, in the light of other corroborating evidence to be discussed later, the former two complexes are retained in the model.

Final results based on the 94 data point set for the species present in solution and associated formation constants, together with estimated uncertainty limits obtained by multiplying ESTA – calculated standard deviations by 3, are in Table 8.5.

TABLE 8.5 Species present in $Zn^{2+}/CN^-/OH^-(H^+)$ containing solutions at p[H] values below 9.8, together with associated formation constants (expressed as logarithms to base 10).

Species	$\log \beta$ ($\pm 3\sigma$)	
$Zn(CN)_2$	10.8	± 0.1
$Zn(CN)_3^-$	16.12	± 0.06
$Zn(CN)_4^{2-}$	20.41	± 0.07
$Zn(CN)_3(OH)^{2-}$	20.4	± 0.3
$Zn(CN)_3(OH)_2^{3-}$	24.3	± 0.2
$Zn(CN)_5^{3-}$	22.9	± 0.2
HCN	9.08	± 0.01

Plots of $\overline{Z}_M$(obs) (plotted as discrete points) and $\overline{Z}_M$(calc) (plotted as continuous lines), both versus pA, are shown in Figure 8.7. Similarly, plots of $\overline{Q}$(obs) and $\overline{Q}$(calc), both plotted versus p[H], are shown in Figure 8.8. For clarity, not all experimental points are shown in Figures 8.7 and 8.8. Although agreement

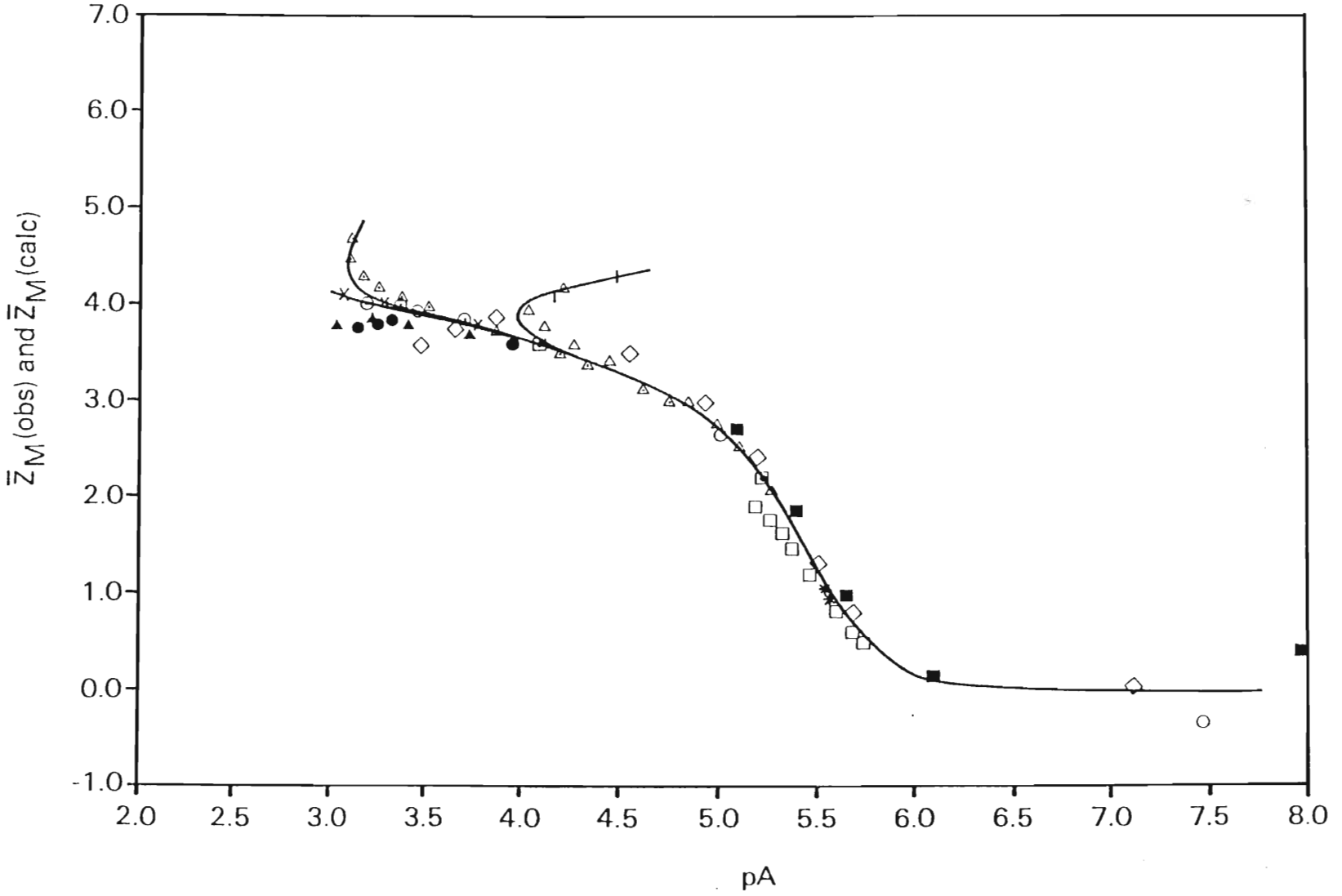

Figure 8.7: The formation function $\bar{Z}_M$(obs) (discrete points) and $\bar{Z}_M$(calc) (continuous curves) plotted *vs* pA. For titrations 6B and 7E only data obtained below p[H] = 6.5 are included. $\bar{Z}_M$(calc) was obtained using the model and

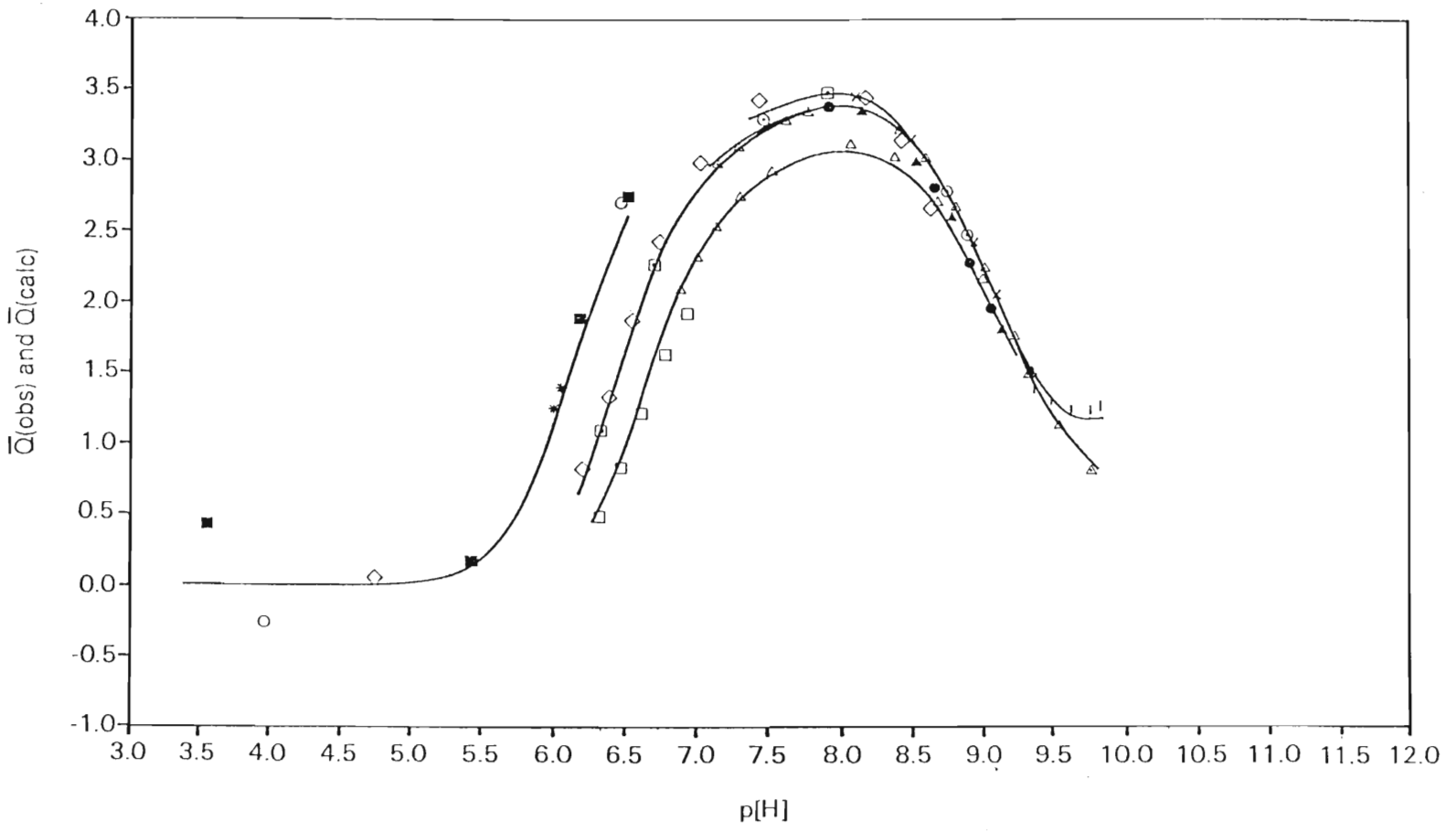

Figure 8.8: The deprotonation function $\bar{Q}$(obs) (discrete points) and $\bar{Q}$(calc) (continuous curves) plotted *vs* p[H]. For titrations 6B and 7E, only data obtained below p[H] = 6.5 are included. $\bar{Q}$(calc) was obtained using the model and formation constants given in Table 8.5 in the text.

between observed and calculated formation functions is not perfect, it is felt that, particularly in view of the sub–millimolar concentration levels studied, the level of agreement between observed and calculated formation functions is acceptable. Features of the formation functions, such as the "back–fanning" displayed by titrations 5B, 8B and 4B in the $\bar{Z}_M$ plot have been reproduced, as well as the relative positions of curves for various titrations on the low p[H] side of the $\bar{Q}$ plot, and the levelling off of the points for titration 8B on the high p[H] side of the $\bar{Q}$ plot.

To provide a visual representation of the speciation of zinc in zinc/cyanide/hydroxide–containing solutions, a plot of the percentage of zinc in the form of each complex is given as a function of p[H] in Figures 8.9 and 8.10 for solutions in which $Zn_T = 3 \times 10^{-4}$ mol dm^{-3}, and $CN_T/Zn_T = 5$ and 10 respectively. At a ligand to metal ratio of 5:1 and p[H] = 9.8 the highest p[H] value considered in this study, the predominating species in solution is $Zn(CN)_4^{2-}$, accounting for 53% of the total zinc in solution, followed by the species $Zn(CN)_3(OH)_2^{3-}$ and $Zn(CN)_3(OH)^{2-}$ in roughly equal amounts of 17% each. The remaining zinc occurs in the complexes $Zn(CN)_3^-$ and $Zn(CN)_5^{3-}$. Thus, at a p[H] of 9.8 and a ligand to metal ratio of 5:1, mixed ligand complex species account for 34% of the total zinc content of the solution. At the same p[H] value, but at a CN_T:Zn_T ratio of 10:1, the binary complexes $Zn(CN)_5^{3-}$ and $Zn(CN)_4^{2-}$ predominate in solution, at the expense largely of the mixed ligand species, which together now account for only about 10% of the total zinc in solution. In both instances, calculations show that binary zinc–hydroxy complexes of the type $Zn_m(OH)_n$ do not from to any appreciable extent under these conditions.

It should be noted that the cyanide concentrations used, as well as the upper limit of p[H] attained in titrations 1B to 8B of Table 7.2, were substantially lower than those used in the electrochemical studies of Nicol *et al.* (1). To provide some basis for comparison however, speciation calculations were carried out for the p[H] range 4 → 12 for a solution in which $Zn_T = 3 \times 10^{-4}$ mol dm^{-3} and $CN_T = 0.01$ mol dm^{-3}, i.e. $CN_T/Zn_T = 33$. The results indicate that at the relatively high cyanide concentration of 0.01 mol dm^{-3} $[Zn(CN)_5^{3-}] >> [Zn(CN)_4^{2-}] >$

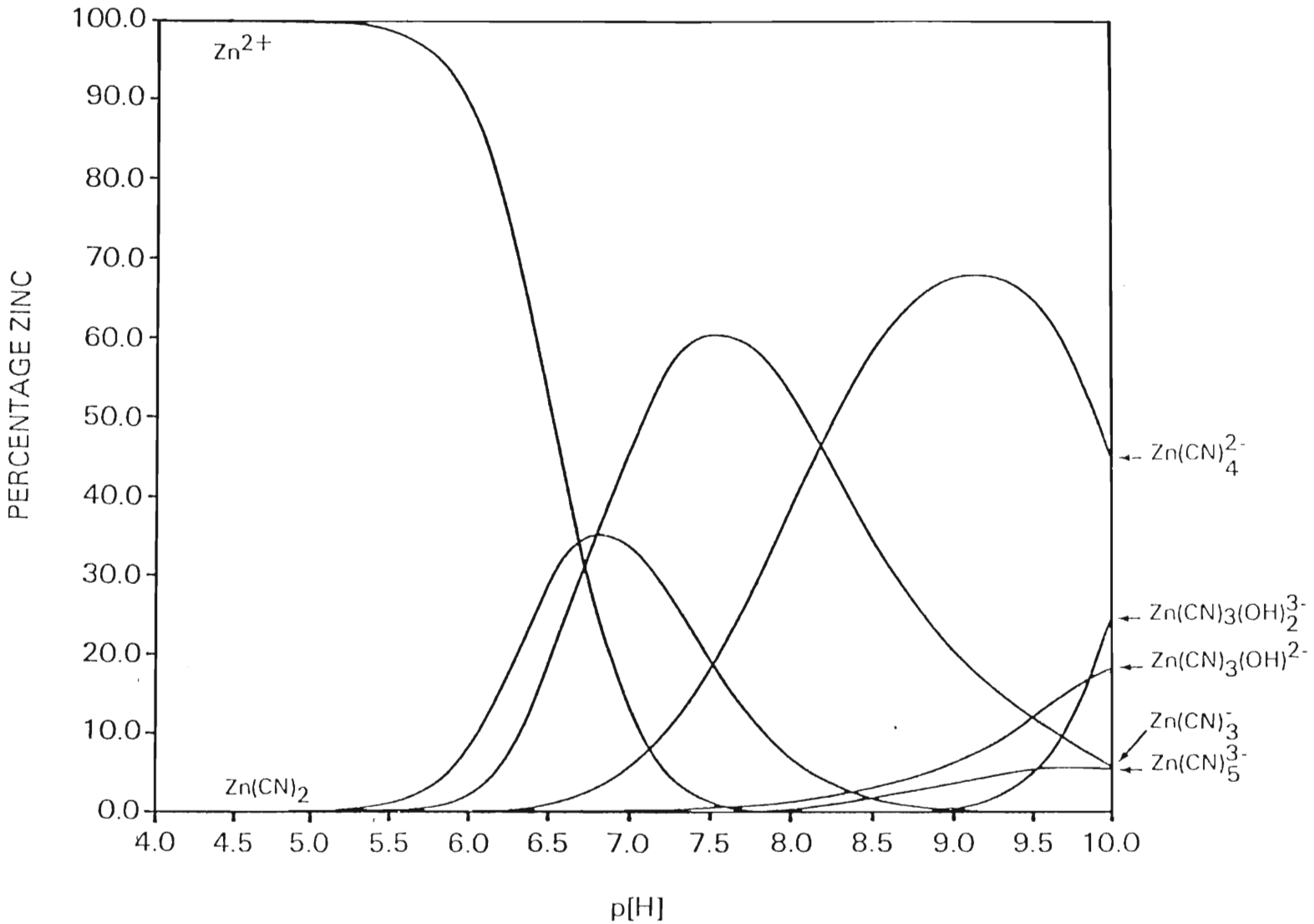

Figure 8.9: Speciation of zinc in Zn-CN-OH solutions as a function of p[H] for $Zn_T = 3 \times 10^{-4}$ mol dm^{-3} and $^{CN}T/Zn_T = 5$. Formation percentages were calculated using formation constants given in Table 8.5 in the text.

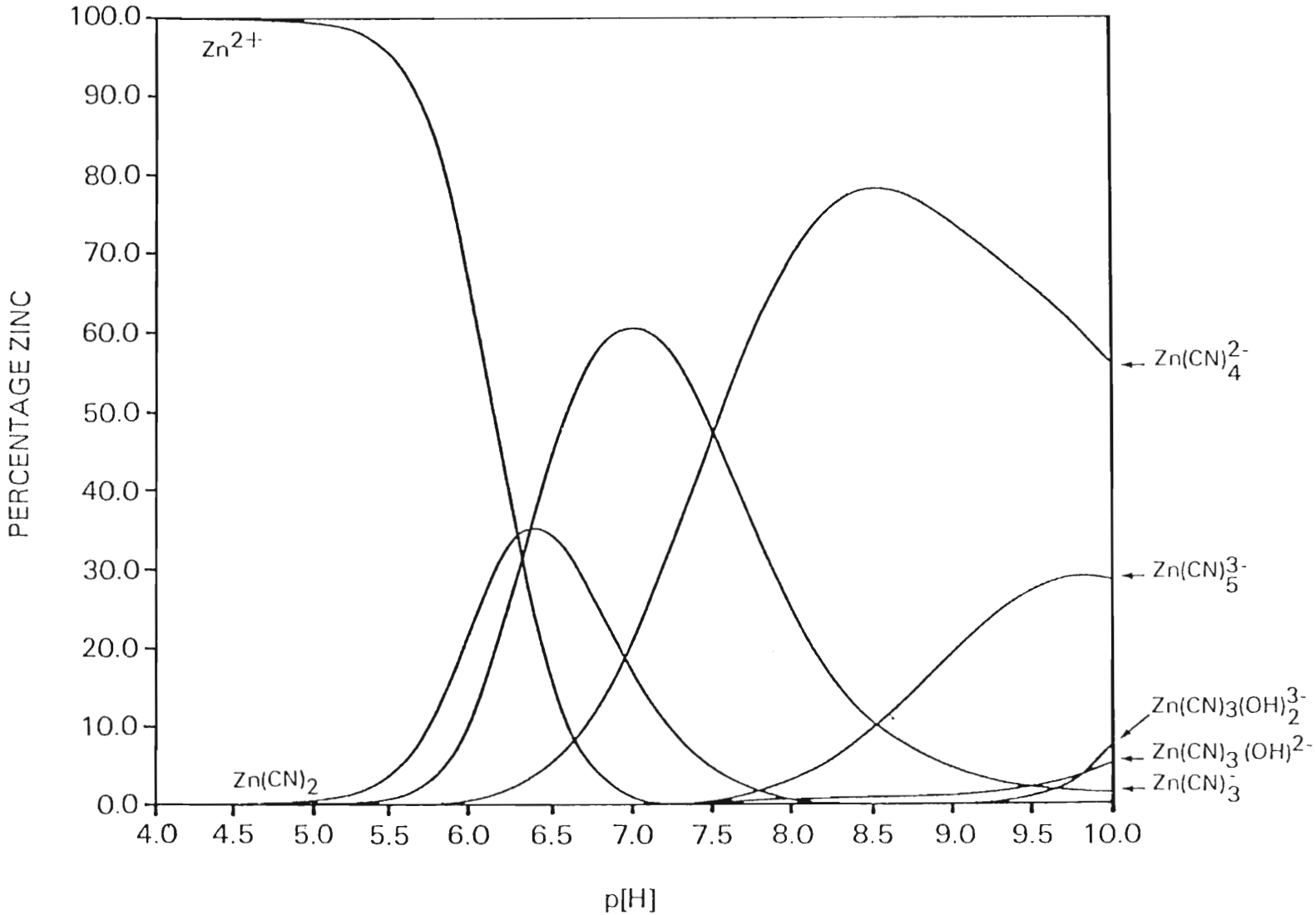

Figure 8.10: Speciation of zinc in Zn-CN-OH solutions as a function of p[H] for Zn_T = 3 x 10^{-4} mol dm^{-3} and $^{CN}T/Zn_T$ = 10. Formation percentages were calculated using formation constants given in Table 8.5 in the text.

$[Zn(CN)_3(OH)_2^{3-}]$ at p[H] values below 11.0. At p[H] values above 11.0 $[Zn(CN)_3(OH)_2^{3-}] > [Zn(CN)_3^{3-}] > [Zn(CN)_4^{2-}] \geq [Zn(CN)_3(OH)^{2-}]$. It is of course entirely possible that other species not detected in this study may appear at p[H] values substantially above 10, and may even predominate at sufficiently high p[H] values. Nevertheless, the relative order of concentrations of the species $Zn(CN)_3^{3-}$, $Zn(CN)_4^{2-}$, $Zn(CN)_3(OH)_2^{3-}$ and $Zn(CN)_3(OH)^{2-}$ given above may still be applicable.

In respect of the existence or otherwise of species of the form $Zn(CN)_n$ with n>4, this study seems to corroborate the conclusion drawn by Pines (8) and Østerud and Prytz (12) on the basis of polarographic evidence, that such species are formed at sufficiently high cyanide concentrations. The latter authors worked at Zn_T concentrations in the range 10^{-4} to 10^{-3} mol dm^{-3} as done in this study, and presumably, at the natural p[H] of solutions formed at various cyanide levels. They reported a polarographic wave, assigned to $Zn(CN)_3^{3-}$, at a CN_T:Zn_T ratio of 8:1 which persisted up to a ligand:metal ratio of 120:1. Speciation calculations carried out using the constants given in Table 8.5, and the program HALTAFALL (73), indicate that $Zn(CN)_3^{3-}$ is formed to an extent of 20% of total zinc in solution (at a natural p[H] of ≈ 9.8) at a ligand:metal ratio of 8:1 – in apparent accord with the observations (and deductions) of Østerud and Prytz.

Other recent studies of the Zn^{2+} + CN^- system involving glass electrode potentiometry, such as those of Martin and Blanc (19) and Persson (21) in which the data were interpreted in terms of complexes $Zn(CN)_2$, $Zn(CN)_3^-$ and $Zn(CN)_4^{2-}$ only (see Table 1.1), were carried out at p[H] values not exceeding ≈ 8.5. Under such conditions one would expect, on the basis of the constants given in Table 8.5, no more than about 2% of the total zinc in solution to be present as the $Zn(CN)_3^{3-}$ complex, and this may explain why these authors did not find it necessary to postulate the existence of this and other ternary complexes.

Although the formation of the mixed ligand species $Zn(CN)_3(OH)^{2-}$ has been established with some confidence in this study, one can be less certain about the five–coordinated species $Zn(CN)_3(OH)_2^{3-}$ and $Zn(CN)_3^{3-}$.

In potentiometric titration studies of this kind, it is generally problematic to decide in an objective manner when to stop introducing new complexes into the model describing the speciation in the system/s studied (108). Thus, the decision to stop at cycle 4 in Table 8.4 was taken in view of the fact that the value of the objective function OBJE for the data set seemed to decrease appreciably up to that point, and that the technique would admit no further complexes in the model. What constitutes a significant improvement in the "goodness of fit" parameter is not easy to determine, and depends, to some degree, on the presence or absence of significant sources of systematic error in the experimental data. Errors of a random nature that affect individual data points are not likely to present difficulties over 94 data points. Errors affecting complete titrations, e.g. errors in cell calibration constants, are more serious, but the number of independent titrations considered in this study is fairly high for studies of this kind (see, for example, references 2, 20 and 22). The most serious systematic errors are those affecting all titrations. Instability of the ligand species towards oxidation and/or non–equilibrium effects at high p[H] values are examples of error sources of this kind. Disappearance of cyanide from the system through oxidation would, if not specifically accounted for, and if accompanied by a reduction in solution p[H], be interpreted as additional complex formation, e.g. would result in values of log β that would be erroneously high or in the postulation of complexes like $Zn(CN)_5^{3-}$ which involve consumption of additional cyanide ions. Accordingly, the possibility cannot be entirely excluded that the last two minor species introduced into the model, i.e. the five coordinate species $Zn(CN)_3(OH)_2^{3-}$ and $Zn(CN)_5^{3-}$, may be "computer complexes", attributable to experimental error of one sort or another. However, due to the large number of precautions taken to avoid errors of the types mentioned above and considering the polarographic evidence of Østerud and Prytz, there are reasonable grounds for believing that such species do form in dilute solutions.

It is of interest that Østerud and Prytz reported at a CN_T:Zn_T ratio of 600:1, (i.e. at a natural pH of $\approx$ 11) the polarographic waves assigned to $Zn(CN)_5^{3-}$ and $Zn(CN)_6^{4-}$ both disappear. This observation may be significant in relation to the observations of Ashurst *et al.* (22), that at free cyanide concentrations (and natural

p[H] values) significantly higher than the highest values used by Østerud and Prytz (12), the free cyanide concentration in solution is consistent with a bound–cyanide:zinc ratio of 4:1. It would seem that although the species $Zn(CN)_5^{3-}$ (and, according to Østerud and Prytz (12), also $Zn(CN)_6^{4-}$) may form in solutions of sufficiently high cyanide concentrations, a point is reached when other reactions are induced which, when sufficiently advanced, (as they presumably may have been in the experiments described by Ashurst *et al.* (22)), the bound cyanide:metal ratio reverts to around 4:1.

The precise nature of the other reactions referred to above, is a matter of speculation at present. Among the possibilities that exist, one may include:

(i) The formation of polymeric species in solution involving cyanide and zinc in the ratio 4:1 with cyanide or hydroxide ions acting as bridging ligands. Polymeric hydroxy species are fairly common in aqueous solutions at high p[H], and some of them, such as those formed by Fe^{3+} and $A\ell^{3+}$ lead to sluggish attainment of equilibrium (109), and others are known to form in a highly irreversible fashion (110).

(ii) The formation of some form of colloidal precipitate involving cyanide and zinc in the ratio 4:1 and possibly also the hydroxide ion. The precipitate would have to be of a colloidal nature since none of the workers on this system (including Ashurst *et al.* who worked on quite concentrated solutions) reported or suspected any precipitate formation.

With regard to the ternary complexes reported in Table 8.5, it is of interest to compare the value of log β = 20.4 for $Zn(CN)_3(OH)^{2-}$ with the corresponding values of log β = 20.41 for $Zn(CN)_4^{2-}$ and log β = 15.2 for $Zn(OH)_4^{2-}$ – all values referred to an ionic strength of 0.10 moℓ dm^{-3}. Other factors being equal, mixed ligand complexes are stabilised in comparison with the corresponding binary complexes involving the same total number of ligands, since there are statistically more ways of making up a mixed ligand complex than the corresponding binary complexes. As discussed by Sharma and Schubert (96) the statistical factor tending

to stabilise the mixed ligand complex $ML_xL'_yL''_z$ ..... can be calculated from

$$S = n!/(x!y!z! .....) \quad ,$$

where n represents the total number of ligands in the complex. If the total number of ligands on the complexes considered is less than the maximum possible coordination number of the metal ion concerned, this should presumably stabilise both the mixed ligand and the corresponding binary complexes to the same extent and therefore produce no nett effect. The logarithm of the formation constant of a mononuclear mixed ligand complex $ML_xL'_y$ can then be estimated by use of the following relation:

$$\log \beta(ML_xL'_y) \simeq \frac{x}{x+y} \log \beta(ML_{x+y}) + \frac{y}{x+y} \log \beta(ML'_{x+y}) + \log S \quad . \qquad (8.3)$$

Application of this relationship leads to a prediction of $\log \beta[Zn(CN)_3(OH)^{2-}] \simeq 19.7$. Comparison with the experimental value of 20.4 ± 0.3 indicates a "ligand enhancement factor" (96), $\Delta \log \beta = 0.7 \pm 0.3$ for this complex, i.e. after correction for statistical effects, this mixed ligand complex shows an enhanced stability of some 0.7 log units.

The existence of a ligand enhancement factor can be rationalised from a consideration of the stepwise formation constants log K for the formation of successive $Zn(CN)_n$ and $Zn(OH)_n$ complexes (see Table 8.6).

It seems clear that the addition of hydroxide ion to Zn(II) inhibits addition of further hydroxide ion to a greater extent than addition of a cyanide ion to Zn(II) inhibits addition of further cyanide ions. This may relate to differences in bonding requirements, charge distribution over the complexes or steric effects involving water molecules of solvation on the complexes. It seems reasonable therefore that a single hydroxide ion should form a more stable complex with $Zn(CN)_3^-$ than would be expected on the basis of its affinity for the species $Zn(OH)_3^-$, as indicated by a fairly large (96) positive ligand enhancement factor. This

TABLE 8.6: Values of the logarithms of cumulative (log β) and stepwise (log K) formation constants for the mononuclear binary complexes of Zn(II) with cyanide and hydroxide ions. (All values given either were determined at, or were corrected to, an ionic strength of 0.1 mol dm^{-3})

Complex	Cumulative log β	Stepwise log K = log β_{1n0} − log $\beta_{1(n-1)0}$
$Zn(CN)_2$	10.8	
		5.32
$Zn(CN)_3^-$	16.12	
		4.29
$Zn(CN)_4^{2-}$	20.41	
		2.49
$Zn(CN)_5^{3-}$	22.9	
$Zn(OH)^+$	4.6	
		5.0
$Zn(OH)_2$	9.6	
		3.7
$Zn(OH)_3^-$	13.3	
		1.9
$Zn(OH)_4^{2-}$	15.2	

observation, together with equation (8.3) may prove useful when estimating formation constants of other mixed ligand complexes like $Zn(CN)_2(OH)^-$, Zn(CN)(OH) etc. any or all of which may form under appropriate experimental conditions, e.g. low cyanide:zinc ratios.

In conclusion, this potentiometric study of the equilibria existing in aqueous zinc–cyanide solutions at 25.0^{0}C, an ionic strength of 0.10 mol dm^{-3}, high

p[H] values, and cyanide:zinc ratios greater than 4:1 has

(i) shown that the ternary complex $Zn(CN)_3(OH)^{2-}$ is formed in significant amounts (5 – 20%) in solutions of p[H] > 8.5;

(ii) provided evidence for the existence in dilute solution of certain five–coordinate complexes such as $Zn(CN)_3(OH)_2^{3-}$ and $Zn(CN)_5^{3-}$ in significant amounts (5 – 25% of total zinc) in solutions of p[H] > 8.5;

(iii) shown that the potentiometric data obtained below p[H] 9.8 are consistent with the formation of the following species together with logarithmic formation constants given in parentheses, $Zn(CN)_2$ (10.8 ± 0.1); $Zn(CN)_3^-$ (16.12 ± 0.06); $Zn(CN)_4^{2-}$ (20.41 ± 0.07); $Zn(CN)_3(OH)^{2-}$ (20.4 ± 0.3); $Zn(CN)_3(OH)_2^{3-}$ (24.3 ± 0.2); $Zn(CN)_5^{3-}$ (22.9 ± 0.2) and HCN (9.08 ± 0.01);

(iv) shown that experimental methods based on measurement of solution p[H] (or a related quantity) alone are unlikely to be of value in the study of $Zn^{2+}/CN^-/OH^-$ equilibria at p[H] values above about 10, unless the real accuracy of these measurements can be improved by an order of magnitude to an uncertainty level of ± 0.003 p[H] units.

REFERENCES

(1) M.J. Nicol, E. Schalch, P. Balestra and H. Hegedus, *J.S. Afr. Inst. Min. Met.*, 79, No. 7, 191 (1979).

(2) G.J. McDougall and R.D. Hancock, *Processing*, 5 (1982).

(3) N. Hedley and H. Tabachnick, "Chemistry of Cyanidation" – American Cyanamid Company (1968), p. 10.

(4) R.L. Paul, *J. Electroanal. Chem.*, 168, 147 (1984).

(5) G.J. McDougall and R.D. Hancock, *Miner. Sci. Eng.*, 12, (2), 85 (1980).

(6) H. Euler, *Ber.*, 36, 2878 (1903).

(7) F. Kunschert, Z. *Anorg. Chem.*, 41, 337 (1904).

(8) I. Pines, *Coll. Czech. Chem. Comm.*, 1, 429 (1929).

(9) K. Masaki, *Bull. Chem. Soc. Japan*, 6, 89 (1931).

(10) H.T.S. Britton and E.N. Dodd, *J. Chem. Soc.*, 1940 (1932).

(11) J. Bjerrum, *Chem. Rev.*, 46, 381 (1950).

(12) T. Østerud and M. Prytz, *Acta Chem. Scand.*, 4, 1250 (1950).

(13) A.I. Stabrovskii, *Zhur. obshchei Khim.*, 21, 1223 (1951); *Zhur. fiz. Khim.*, 26, 949 (1952).

(14) S. Suzuki, *Sci. Reports Res. Inst. Tohoku Univ.* A, 5, 311 (1953).

(15) E. Kordes and F. Langenhoff, Z. *Electrochem.*, 62, 594 (1958).

(16) M.S. Blackie and V. Gold, *J. Chem. Soc.*, 3932 (1959).

(17) R.A. Penneman and L.H. Jones, *J. Inorg. Nucl. Chem.*, 20, 19 (1961).

(18) R.M. Izatt, J.J. Christensen, J.W. Hansen and G.D. Watt, *Inorg. Chem.*, 4, 718 (1965).

(19) R.–P. Martin and M. Blanc, *Bull. Soc. Chim. France*, 1866 (1969).

(20) R.M. Izatt, H.D. Johnston, D.J. Eatough, J.W. Hansen and J.J. Christensen, *Thermochim. Acta*, 2, 77 (1971).

(21) H. Persson, *Acta. Chem. Scand.*, 25, 543 (1971).

(22) K.G. Ashurst, N.P. Finkelstein and L.A. Goold, *J. Chem. Soc.* (A), 1899 (1971).

(23) M. Collier, L. Donneau, M. Fournier and M. Quintin, *J. Chim. Phys.*, 69, 945 (1972).

(24) E. Ferrell, J.M. Ridgion and H.L. Riley, *J. Chem. Soc.*, 1121 (1936).

(25) H.T.S. Britton and R.A. Robinson, *Trans. Faraday. Soc.*, 28, 531 (1932).

(26) G. Anderegg, *Helv. Chim. Acta*, 40, 1022 (1957).

(27) K.P. Ang, *J. Chem. Soc.*, 3822 (1959)

(28) R.M. Izatt, J.J. Christensen, R.T. Pack and R. Bench, *Inorg. Chem.*, 1, 828 (1962).

(29) G. Schwarzenbach and M. Schellenberg, *Helv. Chim. Acta*, 48, 28 (1965).

(30) J.H. Boughton and R.N. Keller, *J. Inorg. Nuclear Chem.*, 28, 2851 (1966).

(31) C. Tsonopoulous, D.M. Coulson and L.B. Inman, *J. Chem. Eng. Data*, 21, 190 (1976).

(32) H.S. Rossotti, *Talanta*, 21, 809 (1974).

(33) F.J.C. Rossotti and H.S. Rossotti, "The Determination of Stability Constants", (McGraw–Hill, New York, 1961).

(34) H.S. Rossotti, "The study of ionic equilibria. An introduction", (Longman, London, 1978).

(35) M.T. Beck, "Chemistry of complex equilibria", (Van Nostrand Reinhold, 1970), p. 27.

(36) M.T. Beck, "Determination of stability constants of metal complexes", in "Essays on Analytical Chemistry in memory of Professor Anders Ringbom", E. Wänninen (ed.), (Pergamon Press, Oxford, 1977), p. 59.

(37) Ref. 34, p. 83.

(38) K.G. Ashurst, N.I.M. Progress Report to April, (1971).

(39) G.N. Lewis and M. Randall, *J. Amer. Chem. Soc.*, 43, 1112 (1921).

(40) P. Debye and E. Hückel, *Phys. Z.*, 24, 185 (1923).

(41) A. Sabatini, A. Vacca and P. Gans, *Talanta*, 21, 53 (1974).

(42) D.J. Leggett, *Talanta*, **24**, 535 (1977).

(43) P.M. May, K. Murray and D.R. Williams, *Talanta*, **32**, 483 (1985).

(44) K. Murray and P.M. May, "ESTA Users' Manual", (UWIST, Cardiff, 1984).

(45) A.I. Vogel, "A textbook of quantitative inorganic analysis, including elementary instrumental analysis", 3rd edition, (Longmans, London, 1961), p. 238.

(46) S. Sjöberg, Ph.D. thesis, University of Umeå, Sweden, (1976).

(47) A.I. Vogel, "Macro and semi–macro quantitative inorganic analysis", 4th edition (Longman, Green and Co. Ltd., 1964), p. 263

(48) Ref. 47, p. 42.

(49) Ref. 47, p. 381.

(50) Ref. 47, p. 353

(51) Ref. 47, p. 327.

(52) Ref. 47, p. 261

(53) Ref. 47, p. 264

(54) Ref. 45, p. 433

(55) Ref. 45, p. 432.

(56) J.D.F. Marsh, W.B.S. Newling and J. Rick, *J. Appl. Chem.*, **2**, 681 (1952).

(57) Ref. 45, p. 271.

(58) Ref. 45, p. 259.

(59) G. Gran, *Acta. Chem. Scand.*, **4**, 559 (1950).

(60) G. Gran, *Analyst*, **77**, 661 (1952).

(61) F.J.C. Rossotti and H. Rossotti, *J. Chem. Ed.*, **42**, 375 (1965).

(62) Ref. 34, p. 80.

(63) M. Mascini, *Ion–Selective Electrode Rev.*, **2**, 17 (1980).

(64) Ref. 34, p. 55.

(65) Ref. 34, p. 24.

(66) Ref. 34, p. 39.

(67) Ref. 34, p. 56.

(68) Ref. 34, p. 125.

(69) K. Murray and P.M. May, Private Communication – UWIST.

(70) K. Murray and P.M. May, "Metal–ligand formation constants by potentiometric titration/computing techniques". A lecture presented at Chelsea College, London. (5th April 1984).

(71) Ref. 34, p. 145.

(72) B.S. Martincigh, Ph.D. thesis, University of Natal, Durban, (1987).

(73) N. Ingri, W. Kakolowicz, L.G. Sillén and B. Warnqvist, *Talanta*, 14, 1261 (1967); 15, XI (1968).

(74) P. May, D.R. Williams, P.W. Linder and R.G. Torrington, *Talanta*, 29, 249 (1982).

(75) Ref. 34, p. 17.

(76) N.R. McQuaker, P.D. Kluckner and D.K. Sandberg, *Environ. Sci. Technol.*, 17, (7), 431 (1983).

(77) Ref. 34, p. 83.

(78) F. Mulla, M.Sc. thesis, University of Natal, Durban, (1981).

(79) G. Biedermann and L.G. Sillén, *Arkiv. Kemi.*, 5, 425 (1953).

(80) Ref. 33, p. 145.

(81) I. Granberg and S. Sjöberg, *Acta. Chem. Scand.*, **A33**, 531 (1979).

(82) A.M. Corrie and D.R. Williams, *Annali di Chimica*, 68, 821 (1978).

(83) P.W. Linder, Private Communication – University of Cape Town (1982).

(84) G.T. Hefter, *Anal. Chem.*, 54, 2518 (1984).

(85) P.W. Linder, R.G. Torrington and D.R. Williams, "Analysis using glass electrodes", (The Open University Press, Milton Keynes, 1984).

(86) R.M. Smith and A.E. Martell, "Critical Stability Constants. Volume 4: Inorganic Complexes", (Plenum Press, New York, 1976).

(87) T. Sekine, *Acta. Chem. Scand.*, 19, 1526 (1965).

(88) D.D. Perrin, *J. Chem. Soc.*, 4500 (1962).

(89) G. Schorsch, *Bull. Soc. Chim. France*, 988 (1965).

(90) L. Pinto, K. Egger and P. Schindler, *Helv. Chim. Acta.*, 47, 425 (1963).

(91) P. Schindler, H. Althaus and W. Feitknecht, *Helv. Chim. Acta.*, 47, 982 (1963).

(92) A.O. Gubeli and J. Ste–Marie, *Canadian J. Chem.*, 46, 1707 (1968).

(93) A.O. Gubeli and J. Ste–Marie, *Canadian J. Chem.*, 45, 827 (1967).

(94) A. Davies and L.A.K. Staveley, *J. Chem. Thermodynamics*, 4, 267 (1972).

(95) P.J. Harris and F. Marsicano, "A preliminary investigation into the mechanism of depression in the flotation of sulphide minerals at the Prieska Copper Mine", National Institute for Metallurgy, Johannesburg. Report Number 1721. June 1975.

(96) V.S. Sharma and J. Schubert, *J. Chem. Edu.*, 46, 506 (1969).

(97) W.E. Bennett, *J. Am. Chem. Soc.*, 79, 1290 (1957).

(98) J.I. Watters and R. De Witt, *J. Am. Chem. Soc.*, 82, 1333 (1960).

(99) Y. Marcus and I. Eliezer, *J. Phys. Chem.*, 66, 1661. (1962).

(100) Y. Marcus and I. Eliezer, *J. Coordin. Chem. Rev.*, 4, 273, (1969).

(101) I. Eliezer, *J. Phys. Chem.*, 68, 2722 (1964).

(102) Ya. D. Fridman, *Russ. J. Inorg. Chem.*, 6, 771 (1966).

(103) Ya. D. Fridman, *Russ. J. Inorg. Chem.*, 11, 59 (1966).

(104) H.T.S. Britton and E.N. Dodd, *J. Chem. Soc.*, 2332 (1931).

(105) A.E. Martell and R.M. Smith, "Critical Stability Constants, Volume 5: First Supplement", (Plenum Press, New York and London, 1982).

(106) P.W. Linder and K. Murray, Talanta, 29, 377 (1982).

(107) J. Kielland, *J. Am. Chem. Soc.*, 59 (2), 1675 (1937).

(108) D.R. Williams, Private Communication, University of Wales Institute of Science and Technology (UWIST) – Cardiff.

(109) D.A. Costanzo, R.E. Biggers and J.T. Bell, *J. Inorg. Nucl. Chem.*, **35**, 609 (1973).

(110) F.A. Cotton and G. Wilkinson, "Advanced Inorganic Chemistry", 2nd edition, (Interscience, 1966) p. 437; p. 858.